INTERNATIONAL CONFERENCE ON

NANOSTRUCTURED BIOCERAMIC MATERIALS

VILNIAUS UNIVERSITETAS • 1579 • UNIVERSITAS VILNENSIS

2020 December 1-3rd | VILNIUS UNIVERITY | VILNIUS

Vilnius University Press

WELCOME

The aim of the conference is to overview and share information about the latest achievements in bioceramic nanotechnologies with the scientific community. Over the duration of the conference, scientists from the fields of chemistry, physics, technology, medicine and implantology will be able to acquaint themselves with synthesis methods, unique properties, and applications of bioceramic nanomaterials.

TABLE OF CONTENTS

The book was compiled by:

Aivaras Kareiva (ORCID 0000-0002-9375-7226)
Greta Inkrataitė (ORCID 0000-0001-7173-7454)
Liudas Daumantas (ORCID 0000-0002-2649-4286)

ISBN 978-609-07-0557-5 (digital PDF)

Organizing and scientific committees

Scientific conference committee:

Prof. habil. dr. Aivaras Kareiva, Faculty of Chemistry and Geosciences, Vilnius university – Chairman

Prof. (HP) dr. Aldona Beganskienė, Lithuania

Prof. habil. dr. Rimantas Ramanauskas, Lithuania

Prof. dr. Vytautė Pečiulienė, Lithuania

Prof. dr. Vygandas Rutkūnas, Lithuania

Organizing committee:

Prof. habil. dr. Aivaras Kareiva – Chairman

Dr. Živilė Stankevičiūtė

PhD student Greta Inkrataitė

PhD student Justinas Januškevičius

PhD student Liudas Daumantas

PhD student Andrius Pakalniškis

Vilnius University

Conference Program

1st December

Online Conference in MS „Teams“

Time	Presenter	Institution	Title of the Lecture
9:00 – 9:05	**Welcome from the Dean of the Faculty of Chemistry and Geosciences Prof. Dr. Aldona Beganskienė**		
9:05 – 9:15	**Welcome from the President of Lithuanian Science Academy Prof. Dr. Jūras Banys**		
9:15 – 9:30	**Welcome from Research Pro-Rector of Vilnius University Prof. Dr. Edita Sužiedėlienė**		
9:30 – 9:40	**Welcome from Vice Dean of the Faculty of Medicine Prof. Dr. Vytautas Kasiulevičius**		
9:40 – 10:00	**Information from the Head of the Conference Organizational Committee Prof. Dr. Aivaras Kareiva**		
10:00 – 11:00	Invited Speaker prof. dr. Pierre **Rabu**	University of Strasbourg, France	Strategy of Synthesis and Application of Nanostructured Materials
11:00 – 11:30	**Coffee break**		
Oral session I (Chairman Assoc. Prof. Dr. Ramūnas **Skaudžius**)			
11:30 – 12:30	Invited Speaker prof. dr. Vygandas **Rutkūnas,** Egidijus **Šimoliūnas**	Vilnius University, Lithuania	Dental Implantology and 3D Bioprinting. Clinical and Research Perspectives
12:30 – 14:00	**Lunch break**		
14:00 – 15:00	Invited Speaker prof. dr. Janis **Locs**	Riga Technical University, Latvia	Nanostructured Calcium Phosphate Biomaterials
15:00 – 16:00	Invited Speaker dr. Aleksej **Žarkov**	Vilnius University, Lithuania	Synthesis and Investigation of Tricalcium Phosphate Polymorphs
16:00 – 17:30	**Poster presentation session I** (Chairman Greta **Inkrataitė**)		

2nd December

Online Conference in MS „Teams“

Time	Presenter	Institution	Title of the Lecture
Oral session II (Chairman Assist. Prof. Dr. Aleksej **Žarkov**)			
9:00 – 10:00	Invited Speaker prof. dr. Karlis **Gross**	Riga Technical University, Latvia	Design and Nanostructuring of Calcium Phosphates for Bone Regeneration
10:00 – 11:00	Invited Speaker dr. Ramūnas **Skaudžius**	Vilnius University, Lithuania	Bioceramic Materials and its Application in Medicine
11:00 – 11:30	**Coffee break**		
11:30 – 12:30	Invited Speaker Prof. Dr. Vladimir **Sivakov**	Leibniz Institute of Photonic Technology, Germany	Novel Application Perspectives of Nanostructured Silicon: Green Hydrogen and Biotechnology
12:30 – 14:00	**Lunch break**		
Oral session III (Chairman Assist. Prof. Dr. Živilė **Stankevičiūtė**)			
14:00 – 15:00	Invited Speaker prof. dr. Mangirdas **Malinauskas**	Vilnius University, Lithuania	Optical Mesoscale 3D Printing: from Renewable Organics to Crystalline Inorganics
15:00 – 16:00	Invited Speaker dr. Edita **Garškaitė**	Lulea University of Technology, Sweden	Synthesis of Nanocrystalline Apatitic Bioceramics for Bone Tissue Engineering and Computed Tomography Studies of Hybrid Organic-Inorganic Biocomposites
16:00 – 17:30	**Poster presentation session II** (Chairman Dovydas **Karoblis**)		

3rd December

Online Conference in MS „Teams“

Time	Presenter	Institution	Title of the Lecture
Oral session IV (Chairman Prof. Dr. Aivaras **Kareiva**)			
9:00 – 10:00	Invited Speaker Ieva **Gendvilienė** and dr. Milda **Alksnė**	Vilnius University, Lithuania	3D Printed Bone: an Innovative Solution for Bone Regeneration
10:00 – 12:00	**Poster presentation session III** (Chairman Justinas **Januškevičius**)		
12:00 – 13:00	**Lunch break. Review of the results of the conference. Scientific discussions.**		

POSTER SESSION I 1st December 16:00 – 17:30		
P01	Afonina Anastasija	Low-Temperature Synthesis of Iron Doped Whitlockite Powders
P02	Aukštakojytė Rūta	Synthesis and Structural Characterization of Graphene Oxide and Thermally Reduced Graphene Oxide
P03	Bastakys Lukas	Structural and Tribological Properties of Ceramic Coatings Deposited by Plasma Spraying
P04	Beklešovas Benas	Chromium Oxide Synthesis by Reactive Magnetron Sputtering and Investigation
P05	Bilvinaitė Goda	A Micro-Computed Tomographic Evaluation of Single Cone Root Canal Fillings Performed by Undergraduate Student, Postgraduate Student, General Practitioner and Endodontist
P06	Bodylska Weronika	Bioactive Glass: Comparative Study on Particles with Different Sizes
P07	Budrevičius Darius	The Dependence of the Morphology Of $GdPO_4$ on pH
P08	Buzaitytė Eglė	Synthesis of $LaPO_4$:1%Eu Nanorods by Hidrothermal Method
P09	Diliautas Ramūnas	Preparation and Characterization of $Bi_{1-x}Gd_xFe_{0.85}Mn_{0.15}O_3$ Solid Solutions
P10	Dolmantas Paulius	Modified Maxwell-Garnett Mie Effective Medium Formulation for Investigation of LSPR in DLC:Ag Nanocomposite Thin Films
P11	Drobysh Maryia	The Development of Electrochemical-Based Immunosensor for SARS-CoV-2 Detection
P12	Dukstiene Nijole	SEM/EDS and XRD Studies of Ag-Cd-Se Thin Films Deposited on Polyamide 6
P13	Gabriūnaitė Inga	Phospholipid Membrane Formation on Fluorine Doped Tin Oxide for Biosensing of Toxins
P14	Gaidamavičienė Giedrė	Various Aqueous Synthesis Methods and Characterization Techniques for Nanocrystalline Calcium Molybdate as a Antimicrobial Component
P15	Griesiute Diana	Hydrothermal Synthesis of Copper-Containing Calcium Phosphate with Whitlockite Structure
P16	Griniuk Evelina	Influence of Synthesis Conditions on Formation Tungsten Oxide Thin Films
P17	Halubek-Gluchowska Katarzyna	Bioactivity and Optical Properties of SiO_2–CaO Glass Doped with Tm^{3+}/Yb^{3+} Ions
P18	Yang Chang Jen	Effect of Gamma-Polyglutatamic Acid/Nano-Hydroxyapatite (γ-PGA/Nano-HAp) Paste on Rehardening and Prevention of Surface Etched Enamel
POSTER SESSION II **2nd December 16:00 – 17:30**		
P19	Inkrataitė Greta	Determination of Different Garnet Films Characteristics Prepared Using Sol-Gel and Spin or Dip-Coatings Techniques
P20	Ivanets Andrei	Synthesis and Crystal Structure of Magnesium Ferrites Doped by Lanthanids
P21	Jonaitytė Eglė Marija	Evaluation of Microarchitecture and Collagen Coating of Regular and Irregular Structure 3D Polycaprolactone Scaffolds for Dental Pulp Tissue Regeneration

P22	Jreije Antonio	Development of Bone Equivalent 3D Printing Composites for Patient Specific Quality Assurance in Radiotherapy
P23	Jurgilevičius Jurgis	Comparison of 8 Different Impression Copings Splinting Methods
P24	Kalyk Fariza	Synthesis and Evaporation of Gadolinium-Doped Ceria Electrolyte for IT-SOFC Applications
P25	Kaminskas Algimantas	A Poly(1,10-Phenanthroline-5,6-Dione), Poly(Pyrrole-2-Carboxylic Acid), Gold Nanoparticles and Glucose Oxidase Nanobiocomposite Based Graphite Electrode as a Potential Anode for Biofuel Cell Powered by Glucose
P26	Kantminienė Kristina	Derivatives of 3-[(4-Methoxyphenyl)Amino]Propanehydrazide: Towards Anticancer and Antioxidant Agents
P27	Kavaliauskaitė Gabija	Ferric Hexacyanoferrate Modified Electrode for Impedimetric Urea Sensing
P28	Kyshkarova Viktoriia	Synthesis of Silica/PLGA Composites by Solution Mixing Method
P29	Kizalaitė Agnė	Synthesis of Zinc Whitlockite by Dissolution-Precipitation Process
P30	Knabikaitė Inga	Al^{3+} Influence on the Formation of Calcium Silicates by Using Two Step Synthesis
P31	Kusyak Andrii	Features of Biodegradation of Sol-Gel Bioactive Glass 60s Doped with Ge
P32	Latushka Siarhei	Crystal Structure and Magnetic Properties of $Bi_{1-x}Sm_xFeO_3$ Compounds Across the Phase Boundary: Effect of External Pressure
P33	Liustrovaitė Viktorija	Phospholipid Bilayer Formation and Characterization Immobilizing Chlorophyll A
P34	Lubinaitė Ernesta	Spectrophotometric Determination of Heparin Based on Aggregation of Gold Nanoparticles
P35	Markevičiūtė Henrieta	Morphological Study of Bio-Nanocomposites Based on PA6/Selenium Compounds
P36	Matijošius Tadas	Adhesion of Fibroblast Cells to Bioceramic Coatings on Aluminum
POSTER SESSION III 3rd December 10:00 – 12:00		
P37	Karoblis Dovydas	Sol-Gel Synthesis and Characterization of $SrTiO_3$-$BiMnO_3$ Solid Solutions
P38	Melnyk Inna	Perspectives of Sol-Gel Silica Particles Loaded with Cu, Eu for Biomedical Applications
P39	Merkininkaitė Greta	Application of Metalorganic Precursors for Laser Fabrication
P40	Michailova Laura	Role of Capping Agent in Formation of Photoelectrochemically Active Tungsten Oxide
P41	Navaruckiene Aukse	Vanillin Derivatives as Resins for Optical 3D Printing
P42	Norkus Mantas	Europium Doped Luminescent Glass Synthesis and Characterization
P43	Pakalniskis Andrius	Characterization of Sm-Doped $BiFeO_3$ Ceramics Crystal Structure and Magnetization Across the Phase Boundary Region

P44	Parvin Maliha	Bacterial Inactivation Using WO_3 Photoanode for Production of Reactive Chlorine Species in Situ
P45	Poderytė Margarita	Scanning Electrochemical Microscopy as a Tool for Targeted Electroporation Modeling
P46	Povilavičius Ignas	In Vitro Comparison of Different Cement Remnant Removal Efficiancy on Dental Implant-Supported Restorations
P47	Prozorovich Vladimir	Design of Manganese Oxide Sorbents for Selective Strontium Radionuclide Removal
P48	Pudule Anna	Carbonate in Amorphous Calcium Phosphate: Influence on Nanolevel Structuring
P49	Ramanavičius Simonas	Formation of Various TiO_{2-X} Nanostructures for Application in Biomedicine
P50	Rimkutė Gintarė	Investigation of Thermally Reduced Graphene Oxide and its Application in Amperometric Third Generation Biosensors
P51	Ruginytė Kristina	The Formation and Thermal Stability of Mayenite
P52	Sakalauskienė Laura	Electrochemical Synthesis of Dendritic Gold Nanostructures and Application for the Development of Glucose Biosensor
P53	Sinušaitė Lauryna	Effect of Mn Doping on Hydrolysis of Low Temperature Synthesized Metastable Alpha-Tricalcium Phosphate
P54	Skruodienė Monika	Sol-Gel and Molten Salt Synthesis of Novel $Y_{3-2x}Ca_{2x}Ta_xAl_{5-x}O_{12}$ Garnet Structure Phosphors
P55	Svazas Ernestas	Comparison of Two Different Healing Abutment Cleaning Protocols
P56	Šerpytis Lukas	Synthesis of $NaYF_4$ Nano/Micro Particles by Microwave-Assisted Solvothermal Method
P57	Šuopys Airingas	Microstructure and Corrosion Properties of Plasma Sprayed Al_2O_3 and Al_2O_3-TiO_2 Coatings
P58	Valeikienė Ligita	Sol–Gel Synthesis of $Mg_{2-x}M_x/Al_1$ (M = Ca, Sr, Ba) Layered Double Hydroxides
P59	Virbickas Povilas	Application of Transition Metals Hexacyanoferrates in Optical Sensing of Hydrogen Peroxide
P60	Zolubas Eimantas	Vesicle Immobilisation on Titanium Foil Nanopores
P61	Žalga Artūras	Aqueous Sol-Gel Synthesis and Characterization of Apatite-Type Materials
P62	Topa Monika	Nanosilica as the Inorganic Filler for Dental Composites Obtained by Photopolymerization

Oral presentations

Synthesis of Nanocrystalline Apatitic Bioceramics for Bone Tissue Engineering and Computed Tomography Studies of Hybrid Organic-Inorganic Biocomposites

E. Garskaite[1,2]*, Z. Stankeviciute[2], R. Golubevas[2], L. Alinauskas[2], A. Zarkov[2], R. Raudonis[2], A. Kareiva[2]

[1]*Wood Science and Engineering, Department of Engineering Sciences and Mathematics, Luleå University of Technology, Forskargatan 1, SE-931 87 Skellefteå, Sweden*

[2]*Institute of Chemistry, Faculty of Chemistry and Geosciences, Vilnius University, Naugarduko 24, Vilnius LT-03225, Lithuania*

e-mail: Edita.garskaite@ltu.se

ABSTRACT

With a growing world population, bone defects resulting from trauma, disease, or surgery are a significant worldwide problem. Currently due to clinical predictability, the autologous bone or autograft is regarded as the "gold standard" for bone defect repair, but complications such as limited supply and donor-site morbidity are stimulating the development of bone substitutes of biological and synthetic origin. The material used as a bone scaffold must satisfy a number of requirements, including biocompatibility, biodegradation with negligible toxicity, appropriate porosity, and mechanical properties, and the ability to integrate with biological molecules or cells to regenerate tissue.

Scaffolds made of synthetic polymers have been studied for bone-tissue engineering applications as they are able to produce materials that exhibit both toughness and plasticity. The most commonly used synthetic polymers are polylactic acid (PLA), poly-glycolic acid (PGA), copolymers of PLA and PGA, polycaprolactone, and polymethylmethacrylate (PMMA). Due to their different mechanical properties and degradation rates, as well as the absence of osteoconductivity, the synergistic combination of calcium phosphate (CaP) as an osteoconductive bioabsorbable ceramic in a polymeric matrix has been explored. Such inorganic-organic hybrids possess an advantage over single components as their interactions at a molecular level can provide interdependent properties while acting as a single-phase material.

The development of new bone-replacement materials and biofunctionalization strategies requires an accurate assessment of the scaffold structure. An established technique that provides three-dimensional information is computed tomography (CT), which is non-destructive and is used for imaging of internal structures based on the density distribution in the materials microstructure.

Herein, the synthesis and characterization of bioceramics, i.e. nanocrystalline hydroxyapatite and magnesium whitlockite, will be firstly described. The preparation of mixed ceramic biocomposites as well as hybrid inorganic(ceramic)-organic(polymer) composites then will be presented outlining their advantages and disadvantages [1-3]. The properties, such as dissolution in the simulated body fluid (SBF) under static conditions, mechanical compression strength before and after the dissolution, and surface hydrophilicity will be discussed. Finally, the assessment of density of the scaffolds and the distribution of ceramics within the polymeric matrix using CT and conventional dental radiography will be presented and discussed.

References:

1. E. Garskaite, L. Alinauskas et al. *RSC Advances*, 2016, 6, 72733.
2. R. Golubevas, A. Zarkov, et al. *RSC Advances*, 2017, 7, 33558.
3. R. Golubevas, Z. Stankeviciute et al. *Materials Advances*, 2020, 1, 1675.

3D Printed Bone: an Innovative Solution for Bone Regeneration

I. Gendviliene[1]*, M. Alksne[2]*
[1]Faculty of Medicine institute of Odontology, Vilnius University
[2]Life Sciences Center Institute of Biochemistry, Vilnius University
e-mail: ieva.gendviliene@mf.vu.lt; milda.peciukaityte@gf.vu.lt

ABSTRACT

More than 40 percent of people over the age of 65 have toothless jaws. One of the most advanced techniques for restoring lost teeth is dental implantation, but almost every second dental implantation procedure requires bone augmentation. There are several treatment options to solve bone deficiency with autologous bone grafts or various bone substitutes. However, all of them have several drawbacks which must be taken into consideration. One of the most promising treatment strategies is to create 3D structured and individually fabricated bone scaffolds. It is worth to mention that 3D printing technology stands out among bone tissue-engineered scaffold fabrication techniques. This technology can implement various imaging techniques, such as computed tomography, to create a patient-specific 3D tissue or scaffold model with controllable pore size, porosity, and internal architecture.

The lecture will present a new concept of using FFF 3D printed composite scaffolds for bone regeneration procedures, in vitro and in vivo investigation, and future directions.

Design and Nanostructuring of Calcium Phosphates for Bone Regeneration

K. A. Gross*
Biomaterials Research Laboratory, Riga Technical University, Latvia
e-mail: Karlis-Agris.Gross@rtu.lv

ABSTRACT

With bone loss from trauma and disease, there is a need to regenerate bone more actively compared to other hard tissue sites in the body. This pursuit requires a deeper understanding of the healing process and the changes in the biomaterial. It becomes particularly interesting with a material based on the chemistry of apatite that can nanostructure to resemble bone mineral in the body. Here, we shall track back to the bone generation process with a focus on bone mineral and see the changes that take place during growth. A review from a three decade pursuit will display the challenges in characterizing biomineral-like deposits, show the design considerations, and the preparation through nanostructuring and microstructuring.

Nanostructured Calcium Phosphate Biomaterials

J. Locs[1, 2]*

[1]*Rudolfs Cimdins Riga Biomaterials Innovations and Development Centre, Faculty of Materials Science and Applied Chemistry, Riga Technical University, Latvia*

[2]*Baltic Biomaterials Centre of Excellence, Headquarters at Riga Technical University, Riga, Latvia*

e-mail: janis.locs@rtu.lv

ABSTRACT

The research of nanostructured calcium phosphate materials in Rudolfs Cimdins Riga Biomaterials Innovations and Development Centre, Faculty of Materials Science and Applied Chemistry, Riga Technical University (RBIDC) have been performed already for more than 20 years. Although calcium phosphates are well known in bone tissue regeneration applications and bioactive substance delivery, continuous research is still actively ongoing in order to increase biocompatibility, control regenerative processes and mimic nanostructure of natural bone. In current presentation historically developed materials and progress achieved in several recent research projects at RBIDC will be presented and discussed.

Dental Implantology and 3D Bioprinting. Clinical and Research Perspectives

V. Rutkūnas[1]*, E. Šimoliūnas[2]*
[1]Institute of Odontology, Faculty of Medicine, Vilnius University
[2]Department of Biological Models, Institute of Biochemistry, Life Sciences Center, Vilnius University
e-mail: vygandas.rutkunas@mf.vu.lt; egidijus.simoliunas@gmc.vu.lt

ABSTRACT

The success of dental implantology depends on the quality of the planning and accuracy of implementation. Accurate planning and positioning of the implants enable to minimize tissue regeneration procedures and to simplify prosthetic procedures. Final prosthetic components can be fabricated before the surgical procedures and early loading protocols applied. However, bone defects of various origin compromise the success of such techniques. With advances in 3D bioprinting, new concepts of how digital implantology and 3D bioprinting could be applied emerge. The interdisciplinary research team will share the clinical and research results when applying new treatment concepts.

Bioceramic Materials and its Application in Medicine

R. Skaudžius[1]*, A. Pakalniškis[1], E. Buzaitytė[1], D. Budrevičius[1], K. Tsuru[2]
[1] Institute of Chemistry and Geosciences, Vilnius University, Naugarduko 24, 03225, Vilnius, Lithuania
[2] Section of Bioengineering, Department of Dental Engineering, Fukuoka Dental College, 2-15-1 Tamura, Sawara-ku, Fukuoka, 814-0193, Japan
e-mail: ramunas.skaudzius@chgf.vu.lt

ABSTRACT

During the past decades, lanthanide-doped nanoparticles (including upconverting particle) have been widely investigated due to the benefits related with their unique luminescent properties [1, 2]. Especially, Gd^{3+}-containing nanocrystals have received much attention due to the possibility of applying these materials as contrast agents in biomedicine for magnetic resonance imaging. This is due to the paramagnetic properties of Gd^{3+} ions due to the seven unpaired 4f layer electrons. By simultaneously inserting light-emitting lanthanide ions into the matrices of gadolinium compounds, an efficient, multifunctional nanomaterial with luminescent and magnetic properties is obtained. One such substance is gadolinium phosphate, which is widely studied for its bioavailability due to the phosphate moieties on the crystal surface [3]. With size around 100 nm it as a potential candidate for being a contrast material during magnetic resonance imaging. Doping by europium causes the orange-red light emission of Eu^{3+} ions, which might be used in luminescent imaging as well [4]. However, $GdPO_4$ has multiple crystallographic structures [5, 6] and many possible particle shapes, meanwhile its properties are dependent on the shape, size, and structure.

The $Gd_{1-x}La_xPO_4$:Eu · nH_2O compounds of monoclinic and hexagonal crystal structures were synthesized by hydrothermal, solid state, and co-precipitation methods. In order to determine phase purity and the structure itself at room temperature X-ray measurements were performed. Phase transition temperature and the amount of water in the compound were analyzed with high temperature in-situ X-ray diffraction analysis and TGA. Shape and size of particles were measured with TEM and SEM analysis. The dependence of luminescence properties on the amount of doped Eu^{3+} of hexagonal nanorods and cytotoxicity test were also investigated.

References

1.F. Zhang, Photon Upconversion Nanomaterials, Springer, Berlin, Heidelberg, 2015.
2.C.T. Yang, A. Hattiholi et al. *Acta Biomateriala,* Gadolinium-based bimodal probes to enhance T1-Weighted magnetic resonance/optical imaging, 2020, 110, 15–36.
3.M.F. Dumont, C. Baligand et al. *Bioconjugate Chemistry,* DNA Surface Modified Gadolinium Phosphate Nanoparticles as MRI Contrast Agents, 2012, 23, 951-957.
4., C.R. Patra, R. Bhattacharya et al. *Journal of Nanobiotechnology,* Inorganic phosphate nanorods are a novel fluorescent label in cell biology, 2006, 4, 11.
5., Y.P. Fang., A.W. Xu et al. *Journal of the American Chemical Society,* Systematic Synthesis and Characterization of Single-Crystal Lanthanide Orthophosphate Nanowires, 2003, 125, 16025-16034.
6.S. Rodriguez-Liviano, A.I. Becerro et al, *Inorganic Chemistry*, Synthesis and Properties of Multifunctional Tetragonal Eu:$GdPO_4$ Nanocubes for Optical and Magnetic Resonance Imaging Applications, 2013, 52, 647-654.

Synthesis and Investigation of Tricalcium Phosphate Polymorphs

A. Zarkov*, L. Sinusaite, H. Klipan, A. Kareiva
Institute of Chemistry, Vilnius University, Naugarduko St. 24, LT-03225 Vilnius, Lithuania
e-mail: Aleksej.zarkov@chf.vu.lt

ABSTRACT

Calcium phosphates (CPs) are the main inorganic part of biological hard tissues such as bones or teeth and play an essential role in human life. Due to the similarity to the mineral phase of bones and excellent biocompatibility, different synthetic CPs have been widely applied as biomaterials for bone repair. These materials are used in biomedical applications in different forms varying from thin coatings on metallic implants to sintered bioceramics. Tricalcium phosphate ($Ca_3(PO_4)_2$, TCP) is one of the representative biomaterials, which finds an application in bone cements and bone implants due to its excellent resorbability and osteoconductivity.

There are three known polymorphs of TCP: the low-temperature β-TCP and the high-temperature forms α- and α'-TCP. The last one is not suitable for practical applications, because it exists only at temperatures above 1430 °C and transforms to α-TCP on cooling below the transition temperature. In contrast, β-TCP is stable at room temperature and transforms at about 1125 °C to α-TCP phase, which can be retained during the cooling to room temperature. However, thermal quenching is often required for the synthesis of pure α-TCP without β-TCP secondary phase, which forms during the cooling of the sample, since phase transition from β- to α-TCP is reversible. Commonly, the synthesis of both α- and β-TCP polymorphs is performed by thermal treatment of a precursor with appropriate Ca to P molar ratio (1.5:1). Usually β-TCP powders are synthesized by solid-state reaction or wet precipitation method at temperatures about 800 °C or higher. The most common approach to the synthesis of α-TCP is thermal transformation of crystalline β-TCP at temperatures above 1125 °C. However, α-TCP can be also synthesized from amorphous CP at such low temperatures as 600−700 °C with further transformation to β-TCP at about 900 °C. Thereby, α-TCP can be obtained at low and high temperatures – below the temperature of formation of β-TCP and above the temperature of transition of β-TCP to α-TCP.

α- and β-TCP crystallize in the monoclinic and rhombohedral crystal systems, respectively. Theoretical densities of α- and β-TCP are 2.866 and 3.066 g cm^{-3}, respectively. These structural differences between α- and β-polymorphs are responsible for their different chemical and biological properties, such as solubility and biodegradability. The solubility of both structures is intermediate between orthophosphates, however α-TCP is much more reactive in aqueous solutions than β-TCP and easily hydrolyzes with a formation of calcium deficient hydroxyapatite, which is similar to bone hydroxyapatite. These differences in chemical properties of TCP polymorphs define their different practical applications. α-TCP is widely used as a major powder component of various bone cements, whereas β-TCP is an important component of mono- or biphasic bioceramics and composites. Both of these materials promote bone growth where implanted and support the proliferation of fibroblasts, osteoblasts and other bone cells.

In our work, we investigated phase-selective synthesis of TCP polymorphs, effect of doping with foreign ions on phase transformations between polymorphs and effect of doping on physical and biological properties of TCP.

Acknowledgements
This project has received funding from European Social Fund (project No 09.3.3-LMT-K-712-19-0069) under grant agreement with the Research Council of Lithuania (LMTLT).

Poster presentations

Low-Temperature Synthesis of Iron Doped Whitlockite Powders

Anastasija Afonina*, Inga Grigoravičiūtė-Puronienė, Aivaras Kareiva
Faculty of Chemistry and Geosciences, Institute of Chemistry, Vilnius University, Naugarduko 24, LT-03225 Vilnius, Lithuania.
**E-mail: anastasija.afonina@stud.chgf.vu.lt*

ABSTRACT

Human bone is a natural 3D assembled organic–inorganic composite of collagen fibrils and low crystalline nanoparticles of inorganic materials [1]. Biomimicking ceramics have been developed to induce efficient recovery of damaged osseous tissues. Among them, calcium phosphate-based bioceramics have been the most widely used because of their biocompatibilities [2]. In recent years, whitlockite (WH, $Ca_{18}Mg_2(HPO_4)_2(PO_4)_{12}$) has attracted much attention as a bone regenerative material. Being the second most abundant biomineral in human bones synthetic WH has an ability to enhance the proliferation and osteogenic differentiation of stem cells [3].

Trace elements are minerals present in living tissues in minor amounts. Fe is an essential trace element and is involved in numerous biological processes in mammalian body [4]. The main task of this work is development of a simple and low temperature process for the formation of iron doped whitlockite powder. The prepared powders phase was confirmed by using XRD analysis. The surface morphology has been analyzed by recording their SEM images.

References

1. M. Yaszemski et al. *Biomaterials*, Evolution of bone transplantation: molecular, cellular and tissue strategies to engineer human bone, 1996, 17, 175–185.
2. H.L. Jang et al. *Advanced Healthcare Mater*, In Vitro and In Vivo Evaluation of Whitlockite Biocompatibility: Comparative Study with Hydroxyapatite and β-Tricalcium Phosphate, 2016, 5, 128–136.
3. C. Wang et al. *Journal of Colloid and Interface Science*, Synthesis and formation mechanism of bone mineral, whitlockite nanocrystals in tri-solvent system, 2020, 569, 1–11.
4. N. Abbaspour et al. *Journal of Research in Medical Science*, Review on iron and its importance for human health, 2014, 9, 164– 174.

Synthesis and Structural Characterization of Graphene Oxide and Thermally Reduced Graphene Oxide

R. Aukstakojyte[1]*, J. Gaidukevic[1], J. Barkauskas[1]
[1]Institute of Chemistry, Faculty of Chemistry and Geosciences, Vilnius University, Naugarduko 24, LT-03225 Vilnius, Lithuania
e-mail: ruta.aukstakojyte@chgf.vu.lt

ABSTRACT

Graphene is a two-dimensional (2D) material with sp^2 hybridized carbon atoms configured in a honeycomb-like structure. Unique thermal, electrical, optical, physical and mechanical properties make it highly promising material for biomedical applications such as bioimaging, drug delivery, neural regeneration, and bone tissue engineering. Graphene and its derivatives such as graphene oxide (GO) and reduced GO can be used as reinforcement fillers for improving the mechanical and electrical characteristics of bioceramics. [1, 2] Today thermal reduction of GO is one of the potential synthesis methods to obtain graphene in a simple, low-cost, high yield and time-saving way. However, high volume of CO_2, CO and H_2O is released due to the deoxygenation of functional groups in GO lattice. The vigorous process of deoxygenation generates topological defects and C vacancies in the final product and causes poor electrical conductivity of graphene prepared this way. [2] To overcome these drawbacks, efficiency recovery of conjugated π-electron system could be achieved by using a suitable source of elemental carbon. According to the literature, the reaction between malonic acid (MA) and phosphorus pentoxide gives carbon suboxide (C_3O_2) that decomposes into carbon atoms at low temperatures. [3] By addition of these compounds in the reduction of GO lower defects concentration and better structural properties of thermal reduced graphene oxide can be achieved.

In this work, we present a new approach of thermal reduction of GO in the presence of additives. Two GO samples were synthesized using different oxidizing agents. Each purified and dried graphene oxide was mixed with MA, and P_2O_5 and thermally reduced under Ar gas atmosphere for 30 min at 100 ºC and 800 ºC temperatures. Structural changes caused by thermal exfoliation were determined by X-ray diffraction, Fourier transform infrared and Raman scattering spectroscopies. The morphology of the obtained products was evaluated using scanning and transmission electron microscopy methods. The surface area and pore volume of prepared samples were quantified using the Brunauer–Emmett– Teller method. Furthermore, measurements of electrical conductivity have also been carried out.

References

1.M. Li, P. Xiong et. al. *Bioactive Materials*, An overview of graphene-based hydroxyapatite composites for orthopedic applications, 2018, 3, 1–18.
2.S. Pei, H. Cheng *Carbon,* The reduction of graphene oxide, 2012, 50, 3210–3228.
3.Ganguly, Fundamentals of Inorganic Chemistry, 2011, ISBN 8131776220.

Structural and Tribological Properties of Ceramic Coatings Deposited by Plasma Spraying

L. Bastakys[1]*, J.S. Mathew[1], L. Marcinauskas[1,2], M. Aikas[2], S. Tučkutė[3]

[1]Kaunas University of Technology, Department of Physics, Studentų str. 50, LT- 51368 Kaunas, Lithuania
[2]Lithuanian Energy Institute, Plasma Processing Laboratory, Breslaujos str. 3, LT-44403 Kaunas, Lithuania
[3]Lithuanian Energy Institute, Center for Hydrogen Energy Technologies, Breslaujos str. 3, LT-44403 Kaunas, Lithuania
e-mail: lukas.bastakys@ktu.edu

ABSTRACT

Alumina ceramic coatings show resistance to wear, high strength, and hardness. Al_2O_3 coatings are also resistant to corrosion and high temperatures [1-2]. Due to the ability to reach high melting point of various ceramic materials, plasma spraying has been widely used as a deposition technique for ceramic coating formation. It has been reported that additions of graphene or chromia can further improve alumina coating properties [3-5]. Aim of this work was to showcase the ability to form coatings made from different kinds of powder compositions using plasma spraying technology as well as to compare alumina, alumina composite and chromia coating's structural and tribological properties.

Using atmospheric plasma spraying alumina (Al_2O_3), alumina-chromia (Al_2O_3-10 wt.% Cr_2O_3), alumina-graphite (Al_2O_3-10 wt.%C) and chromia (Cr_2O_3) coatings were deposited on P265GH steel substrate. Air and hydrogen mixture was used to create plasma jet. The surface morphology was investigated using scanning electron microscopy (SEM) Hitachi S-3400N. The elemental composition of the deposited coatings was determined by energy dispersive spectroscopy (EDS) using Bruker Quad 5040 spectrometer. The crystallography of the coatings was investigated by X-ray diffraction (XRD). Friction coefficient was measured using a CETR-UMT-2 ball-on-flat tribometer. Surface morphology investigation results revealed that a higher degree of melting occurred for alumina-based coatings. EDS results showed that 10 wt.% graphite addition to alumina powders resulted in only ~1.9 wt.% to be present on the coating surface. Meanwhile, the concentration of chromium was ~3.9 wt.% when alumina-chromia powders were used. XRD patterns indicated that alumina-based coatings consisted of α-Al_2O_3, β-Al_2O_3 and γ-Al_2O_3 phases. The XRD pattern of alumina-graphite coating had an additional (002) graphite peak. For alumina-chromia coating, XRD patterns revealed eskolaite (Cr_2O_3) peaks and relatively higher intensities of α-Al_2O_3 phase peaks. The tribological tests indicated that the friction coefficient (COF) of Al_2O_3 coating was ~0.55. The COF of chromia coating was similar (~0.56), meanwhile, a small addition of graphite or chromia into alumina powders resulted in a slight increase of COF values. The as-sprayed coatings exhibited superior wear-resistance and the specific wear rates were reduced up to 10 times compared to steel.

References

1. O. Sarikaya *Surface and Coatings Technology,* Effect of some parameters on microstructure and hardness of alumina coatings prepared by the air plasma spraying process, 2005, 190, 388-393.
2. M. Abyzov, *Refractories and Industrial Ceramics,* Aluminum Oxide and Alumina Ceramics (review). Part 1. Properties of Al_2O_3 and Commercial Production of Dispersed Al_2O_3, 2019, 60, 24-32.
3. X. Lu, S. Bhusal, et al., *Surface and Coatings Technology,* Efficacy of graphene nanoplatelets on splat morphology and microstructure of plasma sprayed alumina coatings, 2019, 366, 54-61.
4. P. Zamani, Z. Valefi *Surface and Coatings Technology,* Microstructure, phase composition and mechanical properties of plasma sprayed Al_2O_3, Cr_2O_3 and Cr_2O_3-Al_2O_3 composite coatings, 2017, 316, 138-145.
5. S. Tao, Z. Yin., et al. *Tribology International*, Sliding wear characteristics of plasma-sprayed Al_2O_3 and Cr_2O_3 coatings against copper alloy under severe conditions, 2010, 43, 69-75.

Chromium Oxide Synthesis by Reactive Magnetron Sputtering and Investigation

B. Beklešovas, V. Stankus
Department of Physics, Kaunas University of Technology
Studentų str. 50, LT-51368 Kaunas, Lithuania
e-mail: benas.beklesovas@ktu.edu

ABSTRACT

The properties of inorganic materials are mainly determined by their composition, structure, morphology. Materials such as chromium (III) oxide (Cr_2O_3) coatings and nanoparticles have received great attention due to its wide range of applications: super capacitor, liquid vibration sensors, pigments, heterogeneous catalysts. Especially there is a need of these coatings on a regular basis in medical industry. Cr_2O_3 is used in orthopedic implants because it eliminates the risk of chromium ion release into the patient as well as antimicrobial and antibacterial coatings [1]. Titanium alloys and stainless steel alloys have biocompatibility issues and are not immune to wear and corrosion. For instance, stainless steel implants show deterioration of the material, resulting in the release toxic for human body system Fe, Cr and Ni ions [2]. Chromium oxide coatings can be prepared using various techniques such as laser deposition, sputtering, sol-gel, solid thermal deposition, chemical vapour deposition, plasma spray pyrolysis [3].

In this work reactive magnetron sputtering was used and it is considered as the most preferable synthesis method for mass production. This technique allows the formation of high quality Cr_2O_3 coatings with desired properties for medical applications. Cr_2O_3 coatings were prepared in situ reactive magnetron sputtering at 500 °C in oxygen environment. The resulting Cr_2O_3 films were characterized by X-ray diffraction (XRD), UV-visible absorption.

References

1. R. Karimian, F. Pirib, S.J. Davarpanaha, *Journal of Applied Biotechnology Reports*, Synthesis of Zinc Oxide and Chromium (III) Oxide Nanoparticles with Diverse Physiological Properties,(2014), 1, 73-76.
2. A.M. Oje, A.A. Ogwu, *Royal Society Open Science*, Chromium oxide coatings with the potential for eliminating the risk of chromium ion release in orthopaedic implants,4: 170218.
3. B.B. Kamble, M. Naikwade, K.M. Garadkar, R.B. Mane, K.K.K. Sharma, B.D. Ajalkar, S.N. Tayade, *Journal of Materials Science: Materials in Electronics*, Ionic liquid assisted synthesis of chromium oxide (Cr_2O_3) nanoparticles and their application in glucose sensing,(2019), 30, 13984-13993.

A Micro-Computed Tomographic Evaluation of Single Cone Root Canal Fillings Performed by Undergraduate Student, Postgraduate Student, General Practitioner and Endodontist

G. Bilvinaitė[1], S. Drukteinis[1], P. Tušas[1], H. Shemesh[2]

[1] *Institute of Dentistry Faculty of Medicine Vilnius University, Vilnius, Lithuania*

[2] *Academic Centre for Dentistry Amsterdam (ACTA), Amsterdam, The Netherlands*

e-mail: goda.bilvinaite@gmail.com

ABSTRACT

Objective: In recent times, the single cone cold hydraulic obturation technique was suggested for use with bioceramic sealers, also known as hydraulic calcium silicate cements. It is predicted that this technique is less operator-dependent compared to other root canal filling methods [1; 2; 3; 4]. The aim of this study was to evaluate and compare the porosity distribution of bioceramic sealer *BioRoot RCS* and single cone root canal fillings performed by undergraduate student, postgraduate student, general practitioner and endodontist.

Methods: Twenty-eight plastic models of upper premolars with two roots were shaped with *HyFlex EDM* instruments to size 40, 0.04 taper and then randomly divided into four groups: undergraduate student (OS), postgraduate student (ER), general practitioner (GO) and endodontist (GE). A total of 14 canals in each group were filled with bioceramic sealer *BioRoot RCS* and one *HyFlex EDM* size 40 gutta-percha point. After the complete setting of the filling material, the specimens were scanned using microcomputed tomography scanner SkyScan 1272. The reconstruction of images was performed with CTAn software. Data were analyzed using Kruskall-Wallis and Mann-Whitney tests. The significance level was set at $p < 0,05$.

Results: The distribution of closed voids demonstrated statistically significant difference among all groups in the coronal ($p < 0,001$) and middle ($p < 0,001$) thirds while the distribution of open voids significantly differed only in the coronal third ($p = 0,002$). No significant difference was observed in the apical third of root canal fillings by comparing the amount of both open ($p = 0,182$) and closed ($p = 0,110$) voids.

Conclusions: The quality and homogeneity of single cone root canal fillings remain similar among groups in the apical and middle thirds. Significant differences are observed only in the coronal third.

Keywords: single cone, porosity, undergraduate student, postgraduate student, endodontist, general practitioner.

References

1. S. Kim, S. Kim., J.W. Park et al. Comparison of the percentage of voids in the canal filling of a calcium silicate-based sealer and gutta percha cones using two obturation techniques. *Materials (Basel)*. 2017; 10(10):1170.
2. D. Angerame, M. De Biasi et al. Filling ability of three variants of the single-cone technique with bioceramic sealer: a micro-computed tomography study. *J Mater Sci: Mater Med.* 2020; 31(11):91.
3. S. Drukteinis. Bioceramic Materials for Root Canal Obturation. In: Drukteinis S, Camilleri J, editors. Bioceramic Materials in Clinical Endodontics. Springer, Cham. 2020, 39–58.
4. Huang Y, Celikten B, de Faria Vasconcelos K, Ferreira Pinheiro Nicolielo L, Lippiatt N, Buyuksungur A, Jacobs R, Orhan K. Micro-CT and nano-CT analysis of filling quality of three different endodontic sealers. *Dentomaxillofac Radiol*. 2017; 46(8):20170223.

Bioactive Glass: Comparative Study on Particles with Different Sizes

W. Bodylska[1,2*], A. Paczkowska[1], Y. Gerasymchuk[1], D. Szymanski[1], M. Fandzloch[1],A. Lukowiak[1]

[1] *Institute of Low Temperature and Structure Research, Polish Academy of Sciences, Okólna 2, 50-422 Wrocław, Poland*

[2] *Faculty of Chemistry, Wrocław University of Science and Technology, Norwida 4/6, 50-373 Wrocław, Poland*

e-mail: werronikab@gmail.com

ABSTRACT

Bioglass® 45S5 developed by Larry Hench in 1970s is undoubtedly the first example of bioactive ceramics that has an outstanding ability to bond with bones and soft tissues and is successfully applied as an implantable material in orthopaedics and dentistry [1]. However, different clinical demands are challenging the design and development of new multifunctional material based on the bioglass for a specific application. The bioactivity of glasses strongly depends on their chemical composition, size and porosity therefore synthesis process and thermal treatment are crucial. Bioactive glasses are produced by the traditional melting method and sol-gel method, which has recently become very popular [2].

Following this topic, the aim of our research was the synthesis of nanometric and, above all, highly bioactive glass in both binary and ternary systems. Different types of amorphous bioglasses with the different compositions based on CaO, SiO_2 and P_2O_5 were obtained by wet chemical methods (solvothermal and sol–gel). The powders were characterized using XRD, IR, Raman, EDS, TEM and SEM (Fig. 1a) techniques.

In order to check the bioactivity of newly synthesized glasses, tests were conducted in the Dulbecco's phosphate-buffered saline (DPBS) during a different time of incubation at 37 °C. Tests were conducted simultaneously for nano- (obtained in solvothermal reaction), submicro- (sol–gel- derived), and microparticles (Bioglass® 45S5 as reference material). The results showed that nanoglass is the most active one - after 4 hours of incubation hydroxyapatite was formed (Fig. 1b-c) whereas, in case of commercial Bioglass®, crystalline phase appeared after 72h.

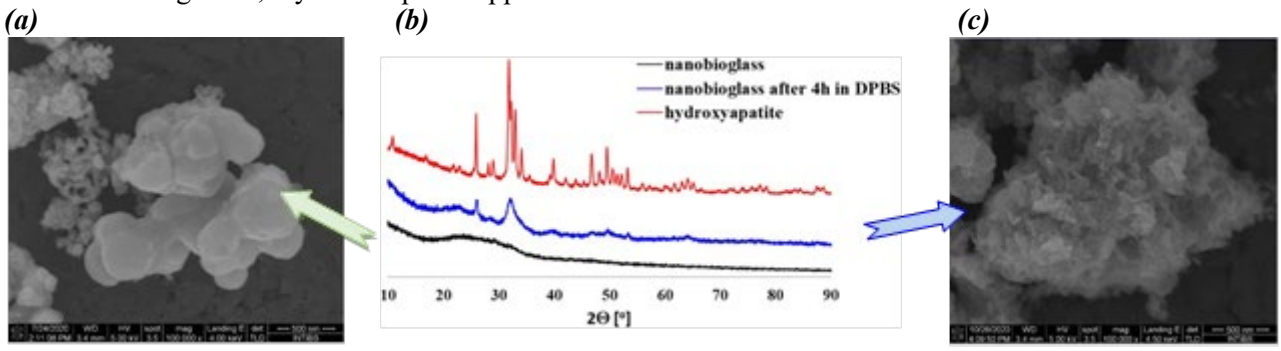

Fig. 1. SEM of selected nanobioglass before (a) and after 4 h of incubation in DPBS at 37°C (c); XRD pattern for solvothermally synthesized nanobioglass and hydroxyapatite as a reference (b).

References

1.L.L. Hench, *J. Biomed. Mat. Res.*, Bioactive materials: the potential for tissue regeneration, 1998, 41, 511–518.

2.Łukowiak, J. Lao, J. Lacroix, J.M. Nedelec, *Chem. Commun.,* Bioactive glass nanoparticles obtained through sol-gel chemistry, 2013, 49, 6620–6622.

Acknowledgement

This work was supported by the National Science Centre [grant number 2016/22/E/ST5/00530]. Authors would like to thank XL Sci-Tech for the supply of 45S5 glass.

The Dependence of the Morphology of $GdPO_4$ on pH

D. Budrevičius*, A. Pakalniškis, R. Skaudžius
Department of Inorganic Chemistry, Vilnius University, Naugarduko 24, LT-03225, Vilnius, Lithuania
E-mail: darius.budrevicius@gmail.com

ABSTRACT

Due to the wide nanoparticles application, the synthesis of nanoparticles and the study of their properties are of great interest to scientists. Special attention is paid not only to particle size but also to their morphology. Physical properties depend on the morphology of the nanoparticles. The Eu doped $GdPO_4$ has luminescent properties. These particles can be applicable in biomedicine, for example, in biological labels, biological images and drug delivery [1,2].

In this study Eu doped $GdPO_4 \cdot 2H_2O$ were prepared by hydrothermal synthesis. Our goal is to investigate how the morphology and size of nanoparticles depend on the synthesis conditions. One parameter was changed during each synthesis. The synthesis of $Gd_{0.85}Eu_{0.15}PO_4 \cdot 2H_2O$ had been performed by changing the time of hydrothermal synthesis, the pH of the solution (adjusted with ammonia), or the filling of the hydrothermal autoclave reactor. Samples were analyzed by X-ray diffraction and scanning electron microscopy. The luminescence properties also had been measured.

References

1. M. Janulevicius, V. Klimkevicius, A. Vanetsev, V. Plausinaitiene, S. Sakirzanovas, A. Katelnikovas. Controlled hydrothermal synthesis, morphological design and colloidal stability of $GdPO_4 \cdot nH_2O$ particles. Materials Today Communications Vol. 23, 2020, 100934.
2. H. Song, L. Zhou, L. Li, F. Hong, X. Luo. Hydrothermal synthesis, characterization and luminescent properties of $GdPO_4 \cdot H_2O:Tb^{3+}$ nanorods and nanobundles. Materials Research Bulletin Vol. 48, 2013, pp 5013–5018.

Synthesis of $LaPO_4$:1%Eu Nanorods by Hydrothermal Method

E. Buzaitytė[1]*, R. Skaudžius[1]
Institute of Chemistry, Faculty of Chemistry and Geosciences, Vilnius University, Naugarduko 24, LT-03225 Vilnius, Lithuania
e-mail: egle.buzaityte@chgf.stud.vu.lt

ABSTRACT

It has been showed that the physical properties of materials are strongly related to their sizes and morphologies. Monophosphates that are doped with rare-earth ions are important types of phosphors due to their great luminescent performance, which has been intensively applied in many fields, such as optical and optoelectronic devices, chemical labels, plasma display panels [1,2]. However, lanthanide-doped nanostructured materials have shown high sensitivity and low risk to living subjects and are considered as more suitable biological label, finding application in biological imaging, biomedicine, drug delivery and biosensors [3].

When synthesized, lanthanum monophosphate can form either hydrated hexagonal $LaPO_4 \cdot nH_2O$ or anhydrous monoclinic $LaPO_4$. Since zeolitic water may have an influence on the luminescent properties of doped-$LaPO_4$ [1], it is important to synthesize pure monoclinic $LaPO_4$. Hexagonal and monoclinic $LaPO_4:Eu^{3+}$ nanorods can be synthesized using hydrothermal method by simply adjusting the reaction temperature. Thus, the reaction was carried out in 180, 190 and 200°C. Also, $NH_4H_2PO_4$ and $(NH_4)_2HPO_4$ were chosen as PO_4 precursors. Physical properties of the composites were measured using XRD and SEM. Pure monoclinic nanorods were prepared at 190-200°C and grain size growth was also observed.

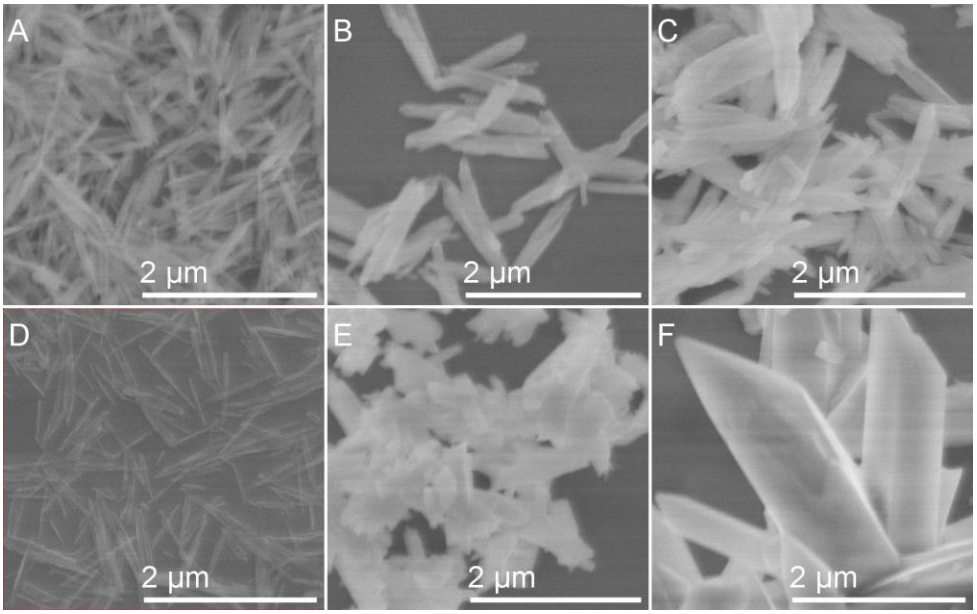

Fig. 1. SEM images of synthesised $LaPO_4$:1%Eu obtained using $NH_4H_2PO_4$ (A, B, C) and $(NH_4)_2HPO_4$ (D, E, F) as a PO_4 precursor. Products obtained at different temperatures: 180°C (A, D), 190°C (B, E), 200°C (C, F).

References

1. M. Ferhi, K. Horchani-Naifer, M. Férid, Hydrothermal synthesis and photoluminescence of the monophosphate $LaPO_4$:Eu(5%), J. Lumin. 128 (2008) 1777–1782. https://doi.org/10.1016/j.jlumin.2008.04.014.
2. M. Yang, H. You, G. Jia, Y. Huang, Y. Song, Y. Zheng, K. Liu, L. Zhang, Selective synthesis of hexagonal and monoclinic $LaPO_4:Eu^{3+}$ nanorods by a hydrothermal method, J. Cryst. Growth. 311 (2009) 4753–4758. https://doi.org/10.1016/j.jcrysgro.2009.09.027.
3. X. Guo, J. Yao, X. Liu, H. Wang, L. Zhang, L. Xu, A. Hao, $LaPO_4$:Eu fluorescent nanorods, synthesis, characterization and spectroscopic studies on interaction with human serum albumin, Spectrochim. Acta - Part A Mol. Biomol. Spectrosc. 198 (2018) 248–256. https://doi.org/10.1016/j.saa.2018.02.066.

Preparation and Characterization of $Bi_{1-X}Gd_xFe_{0.85}Mn_{0.15}O_3$ Solid Solutions

R. Diliautas[1]*, A. Beganskiene[1], D. Karoblis[1], A. Zarkov[1], A. Kareiva[1]
[1] *Faculty of Chemistry and Geosciences, Vilnius University, Naugarduko 24, LT-03225 Vilnius, Lithuania*
e-mail: ramunas.diliautas@chgf.stud.vu.lt

ABSTRACT

Multiferroics are class of solid-state materials, in which at least two of magnetic, electric or piezoelastic phases coexist. These type of compounds are extremely important for technological application due to the fact that externally applied electric or magnetic field can modify the shape of the material by inducing mechanical strain. Additionally, direct control of ferromagnetic and ferrolectric properties can be achieved via externally applied mechanical stress [1]. This combination of different properties leads to high variety of applicable fields, including biomedicine [2]. Astonishing progress has been made in two bio-medical areas: magnetically assisted in vivo targeted drug delivery, like ferrimagnetic $CoFe_2O_4$/ferroelectric $BaTiO_3$ composite nanoparticles [3] and enhanced scaffolds for tissue engineering. Preparing small particle size systems (below 10 nm), which can be excreted renally, remains great challenge, because ferroelectric and/or ferromagnetic properties are often not maintained at this size.

One of the most prominent single-phase multiferroic is bismuth ferrite ($BiFeO_3$). This material displays interesting magnetic and optical (nonlinear response) properties which makes it amenable for bio-oriented diagnostic applications as intra and extra membrane contrasts agent [4]. Another material, which exhibits multiferroic properties is gadolinium ferrite ($GdFeO_3$). This compound shows promising relaxivity properties and has potential as an MRI contrast agent [5]. Synthesis of composite materials and solid solutions can lead to tuning of physical properties of functional materials.

In this work $Bi_{1-x}Gd_xFe_{0.85}Mn_{0.15}O_3$ solid solutions (x from 0 to 1) were prepared by sol-gel synthesis route. Thermal behavior of precursor gel was investigated by thermogravimetric and differential scanning calorimetry (TG-DSC) measurements. For the characterization of obtained samples X-ray diffraction (XRD) analysis, scanning electron microscopy (SEM), Fourier transform infrared spectroscopy (FTIR) and other methods were used.

Acknowledgments
This work was supported by a Research grant BUNACOMP (No. SMIP-19-9) from the Research Council of Lithuania.

References

1. M. V. Vopson, *Critical Reviews in Solid State and Materials Sciences*, Fundamentals of multiferroic materials and their possible applications, 2015, 4, 223–250. A.B. Surname, C. Surname et al. *Name of journal*, Name of article, 2010, 20, 243–252.
2. N. A. Spaldin, *Proceedings of the Royal Society A*, Multiferroics beyond electric-field control of magnetism. 2020, 476.2233, 20190542.
3. R. Guduru et al, *Nature Communications*, Externally-controlled on-demand release of anti-HIV drug AZTTP using magneto-electric nanoparticles as carriers, 2013, 4, 1707-1713.
4. D. Staedler et al, *Nanomedicine: Nanotechnology, Biology, and medicine*, Cellular uptake and biocampatibility of bismuth ferrite harmonic advanced nanoparticles, 2015, 11, 815-824.
5. S. Deka et al, *Materials Science and Engineering: C*, Synthesis, characterization and in vitro analysis of α-Fe_2O_3-$GdFeO_3$ biphasic materials as therapeutic agent for magnetic hyperthermia applications, 2018, 92, 932-941.

Modified Maxwell-Garnett Mie Effective Medium Formulation for Investigation of LSPR in DLC:Ag Nanocomposite Thin Films

P. Dolmantas[1,2]*, K. Dagilis[2], A. Jurkevičiūtė[1,2], Š. Meškinis[1], T. Tamulevičius[1,2]

[1]Institute of Materials Science of Kaunas University of Technology, Baršausko St. 59, LT-51423 Kaunas, Lithuania

[2]Department of Physics, Kaunas University of Technology, Studentų St. 50, LT-51368 Kaunas, Lithuania e-mail: Paulius.Dolmantas@ktu.lt

ABSTRACT

Localized surface plasmon resonance (LSPR) in isolated noble metal nanoparticles (NPs) such as Ag or Au is notorious for confining electromagnetic fields at subwavelength scale. This effect can be utilized in range of applications including but not limited to bioimaging, surface – enhanced Raman scattering, and catalysis [1]. One field of particular interest is energy harvesting where resonant absorption band can be tuned in accordance with the structural absorption of the device seeking for efficiency [2]. Moreover, there have been reports on nearly perfect plasmonic absorbers with different host matrixes covering ultra-wide wavelength range [3]. Use of diamond-like carbon (DLC) as a matrix would be advantageous in such structures due to its chemical, mechanical stability, and deposition tailored optical properties [4].

An expression for calculation of effective dielectric function ε_{eff} which accounts for nanoparticle size dispersion with radius R distribution $P(R)$ in nanocomposite follows from Modified Maxwell-Garnett Mie (MMGM) theory [5]:

$$\frac{\varepsilon_{\text{eff}} - \varepsilon_{\text{m}}}{\varepsilon_{\text{eff}} + 2\varepsilon_{\text{m}}} = \frac{3i\lambda^3}{16\pi^3\varepsilon_{\text{m}}^{3/2}} \frac{f}{R_{avg}} \int \frac{R_{max}}{R_{min}} P(R)a_1(R)dR \quad (1)$$

Here ε_m is matrix dielectric function, λ – wavelength, f – filling fraction of silver nanoparticles, $a_1(R)$ – first electric Mie coefficient.

In the current work, influence of filling factor, NP radius and size distribution parameters on FWHM and central frequency of LSPR resonance band are presented. NP size distribution parameters were evaluated from SEM micrographs (see Fig. 1). It was obtained that for investigated samples R_{avg} is in between 1.26 nm and 11.4 nm, while σ is in the range from 0.77 to 5.34.

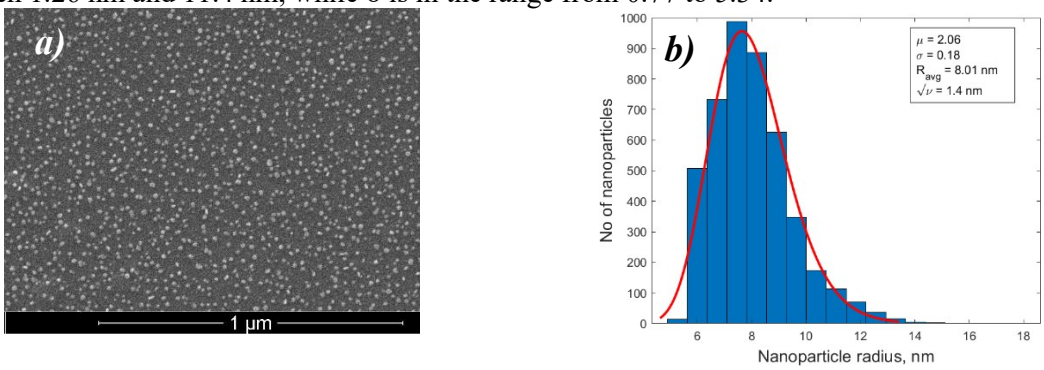

Fig. 1. a) SEM micrograph of a typical DLC:Ag sample surface, b) corresponding nanoparticle radius distribution with log-normal fitting parameters μ, σ and mean particle diameter R_{avg}

References

1.S. Tamulevičius, Š. Meškinis, T. Tamulevičius, and H.-G. Rubahn, "Diamond like carbon nanocomposites with embedded metallic nanoparticles," *Reports Prog. Phys.*, vol. 81, no. 2, p. 024501, Feb. 2018, doi: 10.1088/1361- 6633/aa966f.

2.N. Zhang *et al.*, "Reversibly tunable coupled and decoupled super absorbing structures," *Appl. Phys. Lett.*, vol. 108, no. 9, 2016, doi: 10.1063/1.4943089.

3.J. Y. Lu *et al.*, "Near-Perfect Ultrathin Nanocomposite Absorber with Self-Formed Topping Plasmonic Nanoparticles," *Adv. Opt. Mater.*, vol. 5, no. 18, pp. 1–8, 2017, doi: 10.1002/adom.201700222.

4.Yaremchuk, *et al.*, "Modeling of the plasmonic properties of DLC-Ag nanocomposite films," *Phys. Status Solidi Appl. Mater. Sci.*, vol. 211, no. 2, pp. 329–335, 2014, doi: 10.1002/pssa.201330067.

5.Y. Battie, *et al.*, "Extended Maxwell-Garnett-Mie formulation applied to size dispersion of metallic nanoparticles embedded in host liquid matrix," *J. Chem. Phys.*, vol. 140, no. 4, 2014, doi: 10.1063/1.4862995.

The Development of Electrochemical-Based Immunosensor for SARS-CoV-2 Detection

M. Drobysh[1]*, V. Liustrovaite[2], A. Ručinskienė[1], A. Ramanavičius[1]
[1]Center for Physical Sciences and Technology, Vilnius, LT-02300, Lithuania
[2]Institute of Chemistry, Vilnius University, Naugarduko 24, LT-03225, Vilnius, Lithuania
e-mail: maryia.drobysh@ftmc.lt

ABSTRACT

The treatment of the ongoing worldwide pandemic of COVID-19, which is caused by SARS-CoV-2 is requiring rapid, specific, and sensitive detection methods. The biosensor-based approaches can fully meet these needs. In our investigations, we were developing electrochemical biosensor methods for the diagnosis of SARS-Cov-2 induced COVID-19 disease. Sufficient immobilization of target biomolecules has been achieved by using a self-organizing monolayer. Such system is suitable for the detection and estimation of antibodies against nucleocapsid protein (N) of SARS-CoV-2. For the development of the bioanalytical system, we were modifying the working gold electrode surface by self-assembled monolayers (SAM) based on 11-mercaptoundecanoic acid (MUA)[1], which provided stable covalent binding and minimized non-specific protein adsorption on the working surface[2]. Later we were activating carboxylic groups of SAM forming materials by mixture of N-hydroxysuccinimide (NHS) and N-(3-dimethylaminopropyl)-N-ethyl-carbodiimide hydrochloride (EDC)[1] and were immobilizing the nucleocapsid protein of SARS-CoV-2. As an antigen, the recombinant nucleocapsid protein (rN) of SARS-CoV-2 was applied. Hence, we were assessing the interactions between the immobilized antigens and the antibodies, which were taking place on the electrode surface. It should be noted that used nucleocapsid protein is structurally bound to the RNA of the virus, and thus it participates in the viral replication cycle and the immune response of host cells[3]. Mouse polyclonal antibodies against SARS-CoV-2 nucleocapsid protein were used as analyte. During electrochemical investigations, we have used an electrochemical cell based on the working gold electrode, the counter electrode based on platinum, and the reference [Ag/AgCl/KCl_{sat}] electrode. The electrodes were immersed in the Phosphate-Buffered Saline (PBS) solution (pH 7.4).

Electrochemical measurements were performed with a potentiostat that was connected to the cell. We were applying the electrochemical detection methods based on the Chronoamperometry (CA) and Electrochemical Impedance Spectroscopy (EIS). Recent experiments showed the correlation between surface composition and formation of the antigen-antibody interactions. During experiments, we have applied different electrochemical parameters, such as different potentials of current alteration and we have calculated electrical impedance and capacitance. The present-day results give us the right to consider, that CA and EIS based approaches after selection of proper parameters will serve as the basis for the development of the electrochemical biosensor based approach for the immune-detection of antibodies against SARS-CoV-2 proteins.

References

1.Balevicius Z, Ramanaviciene A, Baleviciute I, Makaraviciute A, Mikoliunaite L, Ramanavicius A. Evaluation of intact- and fragmented-antibody based immunosensors by total internal reflection ellipsometry. *Sensors Actuators, B Chem.* 2011;160(1).
2.Kausaite-Minkstimiene A, Ramanaviciene A, Kirlyte J, Ramanavicius A. Comparative study of random and oriented antibody immobilization techniques on the binding capacity of immunosensor. *Anal Chem*. 2010;82(15):6401-6408.
3.Astuti I. Severe Acute Respiratory Syndrome Coronavirus 2 (SARS-CoV-2): An overview of viral structure and host response. Published online 2020.

SEM/EDS and XRD Studies of Ag-Cd-Se Thin Films Deposited on Polyamide 6

N. Dukštienė*, V.Krylova
Department of Physical and Inorganic Chemistry, Kaunas University of Technology
Radvilėnų pl. 19, LT-50254, Kaunas, Lithuania
e-mail: nijole.dukstiene@ktu.lt

ABSTRACT

The last decade has witnessed rapid progress in hybrid nanomaterials based on selenium compounds that are suitable for biomedical applications. The cation/anion exchange reactions from pre-synthesized nanostructures are an effective strategy to diversify inorganic-organic nanomaterials as it provides reactive capabilities in tuneable composition and property solutions [1]. Recently we have extended cation exchange reaction strategy to inorganic-organic hybrid materials synthesis [2].

In this study, the Ag-Cd-Se thin films were obtained via modification of nanostructured polyamide6-Se-CdSe composite material films with Ag^+ ions using a cation-cation exchange reaction. The surface morphology and phase structure of deposited films were examined. The morphological evolution of thin films was performed using a scanning electron microscope (SEM) JEOL JSM-5500LV equipped with an Energy Dispersive X-ray (EDS) microanalyzer IXRF Systems detector GRESHAM Sirius 10 with an accelerating voltage of 20 kV. The X-ray diffractometry (XRD) analysis was performed on the Bruker Advance D8 diffractometer, operating at the tube voltage of 40 kV and tube (emission) current of 40 mA.

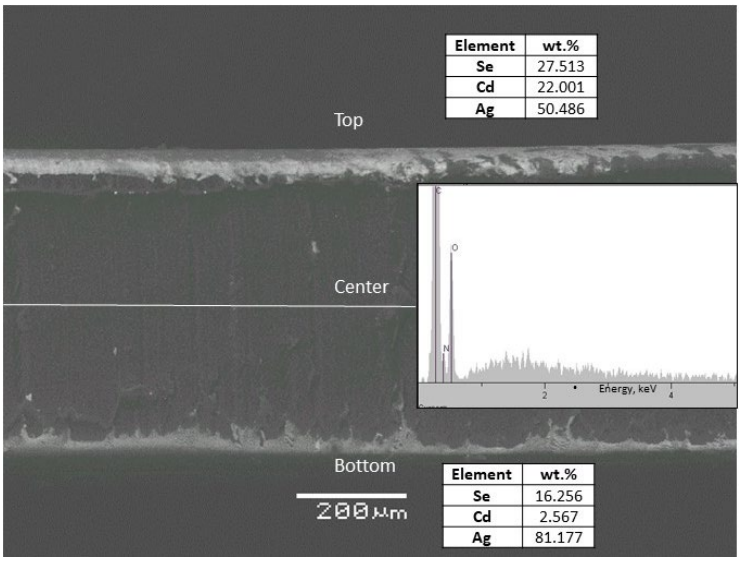

Fig. 1. SEM cross-section and elemental composition of Ag-Cd-Se thin films deposited on polyamide 6 surfaces.

SEM analysis confirms a very disordered morphology with a non-uniform coverage of different sized clusters. Moreover, EDS spectra analysis clarifies film of different chemical composition on the each side of polyamide (Fig. 1). These results were confirmed by XRD analysis showing a complex Se-CdSe-Ag_2Se film crystalline composition with trigonal Se (JCPDS#71-528), hexagonal CdSe (JCPDS#77-2307), orthorhombic Ag_2Se (JCPDS#24-1041) and Ag (JCPDS#24-1041) peaks.

References

1.G.D. Moon, S. Ko et al. *Nano Today*, Chemical transformations of nanostructured materials, 2011, 6, 186–203.
2.V. Krylova, S. Žalenkienė et al. *Appl. Surf. Sci.*, Modification of polyamide-CdS-CdSe composite material films with Ag using a cation–cation exchange reaction, 2015, 351, 203–208.

Phospholipid Membrane Formation on Fluorine Doped Tin Oxide for Biosensing of Toxins

I. Gabriunaite[1*], M. Poderyte[1], A. Valiūnienė[1]

[1] *Faculty of Chemistry and Geosciences, Vilnius University, Naugarduko str. 24, Vilnius, Lithuania*

[*] *e-mail: inga.gabriunaite@chf.vu.lt*

ABSTRACT

Toxins are substances made up of proteins which are released by bacteria to target host cells. They penetrate plasma membrane of living cells, which cause lysis and then death of the cells. Therefore, it is important to develop new sensing techniques for bacterial or venom toxins in order to prevent life threatening conditions or detect them at early stages.

Phospholipid bilayer membrane (BLM) on solid support (such as gold [1], titanium [2] or tin oxide [3, 4]) is a convenient substrate for immobilization of toxins [1]. BLM is relatively stable and could be investigated with surface sensitive techniques such as, various electrochemical methods, surface plasmon resonance or atomic force microscopy.

In this work, thin films of commercially produced fluorine doped tin oxide (FTO) were modified with silane-based self-assembled monolayer (SAM) and phospholipid bilayer membrane. Membrane consisted of 1,2-dioleoyl-sn-glycero-3-phosphocholine (DOPC) and cholesterol at molar ratio 6:4. Different toxins were investigated in this study: vaginolysin, α-hemolysin, phospholipase A_2 (PLA2) and melittin. Electrochemical measurements (cyclic voltammetry and electrochemical impedance spectroscopy) were carried out and some conclusions were made. First, toxin vaginolysin, which is characterized by the relatively large size (57 kDa), could not penetrate the membrane. Second, effect of smaller toxin, α-hemolysin (12 kDa), was non-specific. Third, even smaller toxin melittin (2.8 kDa) did penetrate the membrane. Last, due to different membrane targeting mechanism of phospholipase A_2 (30 kDa,), the toxin was also active because it hydrolyzes only the outer layer of phospholipids in the membrane (fig. 1) [3]. To sum up, in this work formed BLMs were functional only with smaller toxins, or with toxin characterized by specific targeting mechanism. It suggests that membranes are not fluidic enough and do not possess ionic reservoir between membrane and solid support. Therefore, in future, the fluidity of the membrane will be improved by modifying FTO surface with new anchor SAMs prior to membrane formation.

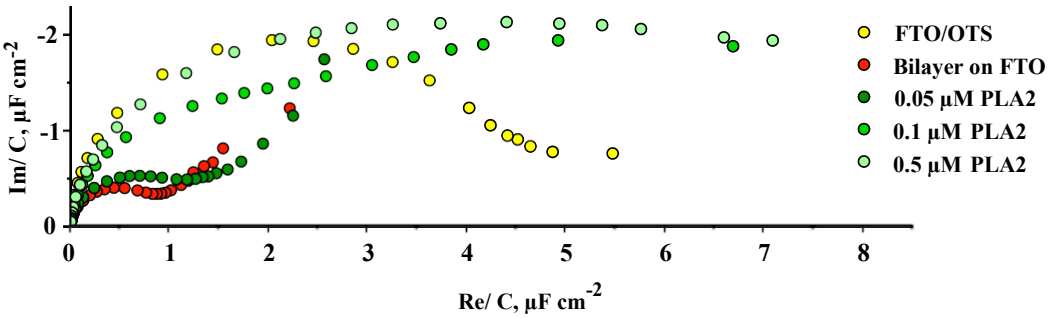

Fig. 1. Electrochemical impedance spectra in Cole - Cole plot after SAM formation on FTO with octadecyl trichlorosilane (OTS) – yellow circles; after bilayer membrane formation – red circles; after interaction with different concentrations of phospholipase A_2 (PLA2): 0,05 µM – dark green circles; 0,1 µM – green circles; 0,5 µM – light green circles.

References

1. T. Ragaliauskas, M. Mickevičius et. al., *Biochimica et Biophysica Acta*, Fast formation of low-defect-density tethered bilayers by fusion of multilamellar vesicles, 2017, 1859, 669-678.
2. T. Sabirovas, A. Valiuniene et al., *Journal of The Electrochemical Society*, Mechanically Polished Titanium Surface for Immobilization of Hybrid Bilayer Membrane, 2018, 165, G109-G115.
3. Gabriunaite, A. Valiuniene et al., *Electrochimica Acta,* Formation and properties of phospholipid bilayers on fluorine doped tin oxide electrodes, 2018, 283, 1351-1358.
4. Valiuniene, Z. Margarian et al., *Journal of The Electrochemical Society*, Cadmium Stannate Films for Immobilization of Phospholipid Bilayers, 2016, 163, H762-H767.

Various Aqueous Synthesis Methods and Characterization Techniques for Nanocrystalline Calcium Molybdate as an Antimicrobial Component

G. Gaidamavičienė*, A. Diktanaitė, A. Žalga
Department of Applied Chemistry, Institute of Chemistry, Faculty of Chemistry and Geosciences, Vilnius University, Naugarduko Str. 24, 03225 Vilnius, Lithuania
e-mail: giedre.prievelyte@chf.vu.lt

ABSTRACT

Developing novel compounds with antimicrobial properties can be an effective approach to decreasing the number of healthcare-associated infections, particularly in the context of medical devices and touch surfaces [1]. Recent publications describe the antimicrobial properties by silver nanoparticles, zinc oxide, titanic dioxide, silver molybdates, and silver tungstates [2]. The importance of silver for antimicrobial activity is clear, unquestionable and widely published in a significant amount of publications. Meanwhile, it has been reported that at high concentrations, the molybdenum (Mo^{6+}) is toxic not only to human health but also to other mammals and invertebrates. In despite that fact that many metal molybdates nanocrystals are attractive semiconductors, there are no reports of the toxic and genotoxic effects associated with these compounds. For example, calcium molybdate ($CaMoO_4$) has great potential applications in various fields, such as phosphors, optical fibres, scintillators, magnets and catalysts. The use of this compound in medical applications mainly depends on its structural, compositional and morphological characteristics. The synthesis techniques which provide the possibility control of obtained properties are highly desirable. From this point of view, we compared aqueous sol-gel synthesis and precipitation methods for the preparation of $CaMoO_4$ compound. The thermal analysis revealed the possible variations on the thermal decomposition of initial gel precursors. It was estimated that the nature of the starting compounds significantly influences the thermal decomposition of mixture for obtained metal salts. Besides, scanning electron microscopy clearly revealed the difference on the surface morphology of obtained final ceramics. In addition, the X-Ray diffraction analysis confirmed that the nature of the synthesis method significantly influences the structural properties of the nano $CaMoO_4$ crystals.

References

1.D. Tanasic, A. Rathner, et al., Silver-, calcium-, and copper molybdate compounds: Preparation, antibacterial activity, and mechanisms, *Biointerphases* 12(5) (2017) 05G607.
2.F. Nobre, R. Muniz, et al., Calcium molybdate: Toxicity and genotoxicity assay in Drosophila melanogaster by SMART test, *Journal of Molecular Structure* 1200 (2020) 127096.

Hydrothermal Synthesis of Copper-Containing Calcium Phosphate with Whitlockite Structure

D. Griesiūtė, A. Kizalaitė, H. Klipan, A. Žarkov
Institute of Chemistry, Vilnius University, Naugarduko g. 24, LT-03225, Vilnius, Lithuania
diana.griesiute@chgf.vu.lt

ABSTRACT

Calcium phosphates are the main inorganic constituents of human hard tissues (bones and teeth) and play an essential role in human life [1]. Despite the fact that magnesium whitlockite ($Ca_{18}Mg_2H_2(PO_4)_{14}$) is the second most abundant mineral in human body, synthetic whitlockite is not so frequently used in practice for regenerative medicine purposes. One of the reasons is that its preparation is challenging and synthesis products often contain impurities. On the other hand, whitlockite is biocompatible, have excellent osteogenic properties and it is more stable in acidic conditions than other calcium phosphates. These properties make whitlockite a promising candidate for the use in damaged bone regeneration or dental application [2].

Partially substituted calcium phosphates can possess improved physical and biological properties, which makes possible to use them in a wider application area. Copper is an essential element in metabolism processes and copper-doped biomaterials are useful for orthopedic application. Copper-substituted calcium phosphates are well known for their antibacterial [3], angiogenic, and osteogenic properties, which stimulate biological integration of new materials. These biomaterials with low copper concentration are not toxic like antibiotics, which were widely used in the past years [4]. For this reason, we hope, that copper-containing whitlockite will be a future candidate in orthopedic surgery due to copper biological and antibacterial properties.

In the present work, whitlockite powders were synthesized by dissolution-precipitation method under hydrothermal conditions. The main goal of this work is to optimize synthesis conditions (pH, temperature, reaction time, concentration of starting materials) and obtain low crystallinity whitlockite powders. Also, to analyze whitlockite phase purity and structural changes at different copper amounts. The crystallinity, crystal structure and structural changes were evaluated by powder X-ray diffraction (XRD), Fourier-transform infrared (FTIR) and Raman spectroscopies. Scanning electron microscopy (SEM) was used for the characterization of morphological features of products. Chemical composition of synthesized powders was analyzed by inductively coupled plasma optical emission spectrometry (ICP-OES).

References:

1. N. Eliaz, N. Metoki, *Materials,* Calcium phosphate bioceramics: A review of their history, structure, properties, coating technologies and biomedical applications, 2017, 10(4), 334.
2. H. L. Jang, H. K. Lee et al. *Journal of Materials Chemistry B,* Phase transformation from hydroxyapatite to the secondary bone mineral, whitlockite, 2015, 3, 1342–1349.
3. S. Gomes, C. Vichery et al. *Acta Biomaterialia,* Cu-doping of calcium phosphate bioceramics: From mechanism to the control of cytotoxicity, 2018, 65, 462–474.
4. A. Jacobs, G. Renaudin et al. *Acta Biomaterialia,* Biological properties of copper-doped biomaterials for orthopedic applications: A review of antibacterial, angiogenic and osteogenic aspects, 2020, 117, 21–39.

Influence of Synthesis Conditions on Formation Tungsten Oxide Thin Films

E. Griniuk[1*], L. Michailova[1], A. Griguceviciene[2], J. Juodkazytė[2], M. Petrulevičienė[2]
[1] *Institute of Chemistry, Faculty of Chemistry and Geosciences, Naugarduko str. 24, LT-03225 Vilnius University, Lithuania*
[2] *Center for Physical Sciences and Technology, Department of chemical engineering and technology Saulėtekio av. 3, LT-10257 Vilnius)*
e-mail: evelina.griniuk@stud.gchf.vu.lt

ABSTRACT

Hydrogen production via photoelectrochemical (PEC) water splitting is expected to play an important role in solving the problems related with global environmental pollution and energy crisis. The photocatalytic activity of most single component semiconductor photocatalysts is still far from satisfactory due to the fast recombination of the photoinduced charge carriers, which inhibits the migration of photoelectrons and holes towards semiconductor/electrolyte interface to participate in the redox reactions. Therefore, it is crucial to develop efficient and cost-effective photoelectrodes for water oxidation/reduction in PEC applications [1].

Among the numerous reported photoanode materials including α-Fe_2O_3, $BiVO_4$, WO_3, TiO_2, ZnO and Ag_3PO_4, tungsten (VI) oxide is considered to be one of the most attractive visible-light-responsive materials for PEC water splitting due to its narrower band gap (E_g 2.4–2.8 eV) compared to TiO_2 and ZnO, appropriate valence band (VB) position (approximately 3.0 V vs. NHE), which provides a sufficient potential for water, oxidation. Method and conditions of synthesis usually determine the morphology of photoactive layers, which is very important for efficient transport of photogenerated charge carriers.

In this work tungsten oxide coatings were synthesized using hydrothermal approach. Coatings were synthesized at 120°C, 140°C, 160°C and 180°C temperatures for 24 h. The composition of coatings was investigated using X-ray diffraction technique (Fig. 1). Surface area and roughness of coatings were analyzed using 3D optical microscope. Photoelectrochemical performance was investigated in three electrode cell in 0.5 M H_2SO_4 solution under light irradiation.

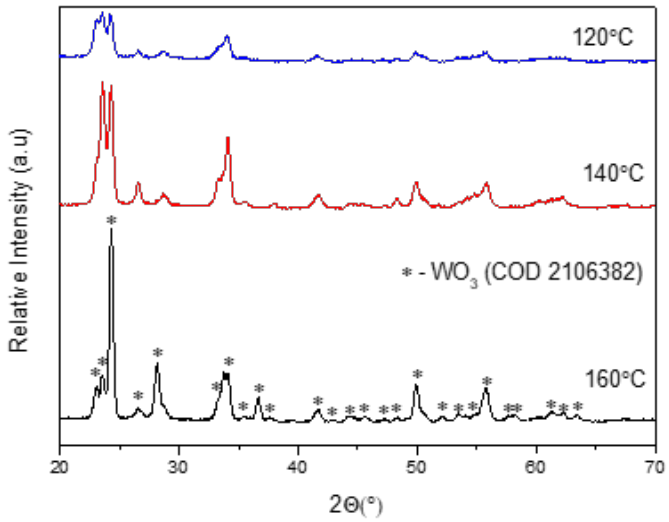

Fig. 1. XRD patterns of samples synthesized at different temperatures.

References

1.G. Zheng, J. Wang et al,. J. Mater. Chem. A, Sandwich structured WO3 nanoplatelets for highly efficient photoelectrochemical water splitting, 2019, 7, 26077.

Bioactivity and Optical Properties of SiO_2–CaO Glass Doped with Tm^{3+}/Yb^{3+} Ions

K. Halubek-Gluchowska*, D. Szymanski, A. Paczkowska, A. Lukowiak

Institute of Low Temperature and Structure Research, Polish Academy of Sciences, Okólna 2, 50-422 Wrocław, Poland

**Corresponding author: K.Gluchowska@intibs.pl*

ABSTRACT

Bioactive glasses are a class of inorganic biomaterials widely used in bone tissue engineering and regenerative medicine. Silica-calcia glass is described as a bioactive material able to form an hydroxyapatite (HA)-like surface layer when immersed in a simulated body fluid (SBF) similar to the blood plasma. It is a common method to evaluate bioactivity of silica-calcia glass by observing the formation of HA on the surface of material [1-4].

In the present work, silica–calcia glass powder doped with 0.3 mol% of Tm^{3+} and 4 mol% of Yb^{3+} ions was prepared by the sol–gel method. A structure, morphology and optical properties, including energy transfer upconversion (UC) mechanism, were described. XRD pattern indicated amorphous phase of the silica-based glass with partial crystallization in the case of systems with higher concentration of the doping ions. SEM images showed particles with diameter around 30 nm. The upconversion emission spectra and fluorescence lifetimes were registered under near infrared excitation (980 nm) at room temperature to study the energy transfer between Yb^{3+} and Tm^{3+} ions. The thulium emission bands were observed around 366, 475, 650 nm and 800 nm corresponding to the $^1D_2 \rightarrow {}^3H_6$, $^1G_4 \rightarrow {}^3H_6$, $^1G_4 \rightarrow {}^3F_4$ and $^3H_4 \rightarrow {}^3H_6$ transitions, respectively. To understand the mechanism of Yb^{3+}-Tm^{3+} UC energy transfer in the CaO–SiO_2 powders, the energy level diagram of the Yb^{3+} and Tm^{3+} ions was proposed. Furthermore, the ability of doped silica–calcia powders as an induction agent for the formation of apatite layer when soaked in simulated body fluid (SBF) was evaluated. After 3 weeks immersion in SBF, in XRD patterns appear the diffraction peak at $2\Theta \approx 26°$ and 32° which corresponded to the (002) and

(211) reflections of hydroxyapatite (HA). The EDX and ICP analysis showed the increase in the concentration of Ca and P elements on the sample surface indicating formation of HA layer.

Acknowledgment

This work was supported by the National Science Centre research grant No. 2016/22/E/ST5/00530.

References

1.F. Baino, S. Fiorilli, et al. *Acta Biomaterialia,* Bioactive glass-based materials with hierarchical porosity for medical applications: Review of recent advances 2016, 42, 18-32.

2.Dobrádi, M. Enisz-Bódogh et al. *Ceramics International,* Bio-degradation of bioactive glass ceramics containing natural calcium phosphates, 2016, 42, 3706-3714.

3.J.R. Jones *Acta Biomaterialia*, Review of bioactive glass: From Hench to hybrids, 2013, 9, 4457-4486.

4.P.N. Chavan, M.M. Bahir et al. *Materials Science and Engineering B,* Study of nanobiomaterial hydroxyapatite in simulated body fluid: Formation and growth of apatite, 2010, 168, 224-230.

Effect of Gamma-Polyglutatamic Acid/Nano-Hydroxyapatite (γ-PGA/Nano-HAp) Paste on Rehardening and Prevention of Surface Etched Enamel

N.C. Teng[1], A. Pandey[2], W.H. Hsu[3], C.S. Huang[1], W.F. Lee[4], T.H. Lee[2], T.C.K. Yang[3], T.S. Yang[5], J.C. Yang [2,*]

[1] School of Dentistry, College of Oral Medicine, Taipei Medical University, Taipei 110-31, Taiwan, ROC.
[2]Graduate Institute of Nanomedicine and Medical Engineering, College of Biomedical Engineering, Taipei Medical University, Taipei 11052, Taiwan, ROC.
[3] Department of Chemical Engineering and Biotechnology, National Taipei University of Technology, 1, Sec. 3, Chung-Hsiao E. Road, Taipei, 106, Taiwan, ROC.
[4] School of Dental Technology, College of Oral Medicine, Taipei Medical University, Taipei 110, Taiwan, ROC.
[5] Graduate Institute of Biomedical Optomechatronics, Taipei Medical University, Taipei 11031, Taiwan, ROC.
e-mail: yang820065@tmu.edu.tw

ABSTRACT

Pertaining to the high occurrence of tooth decay, which are the enduring challenges in the field of preventive dentistry, many revolutionary approaches are on the way. However, the ideal dental care material has yet to be fully developed. This research reports a dramatic enhancement in rehardening potential on surface-etched enamels by γ-polyglutamic acid (γ-PGA)/nano-hydroxyapatite (nano-HAp) paste within the limitations of the study. The percentage recovery of surface microhardness (SMHR%) and the surface parameters for 9 wt% γ-PGA/nano-HAp paste on acid-etched enamel were investigated by a Vicker microhardness tester and atomic force microscope (AFM), respectively. To test the hypothesis of the rehardening mechanism and the prevention effect of γ-PGA/nano-HAp paste, both the surface parameters of mean peak spacing (Rsm) and mean arithmetic surface roughness (Ra) were measured and compared to the specimens subjected to demineralization and/or remineralization. This in vitro study demonstrated that the γ-PGA/nano-HAp treatment could promote the SMHR% of etched enamel up to 39.59±6.69% in 30 min. After treatment of γ-PGA/nano-HAp on etched surface, the reduction of Rsm from 999±120 nm to 700±80 nm suggests the possible mechanism of void-filling within a short treatment time of 10 min. Furthermore, ΔRa-I, the roughness change due to etching before remineralization is 23.15±3.23 nm, while ΔRa-II, the roughness change after remineralization is 11.99±3.90 nm. This statistically significant reduction in roughness change ($p<0.05$) implies protection effect against demineralization process.

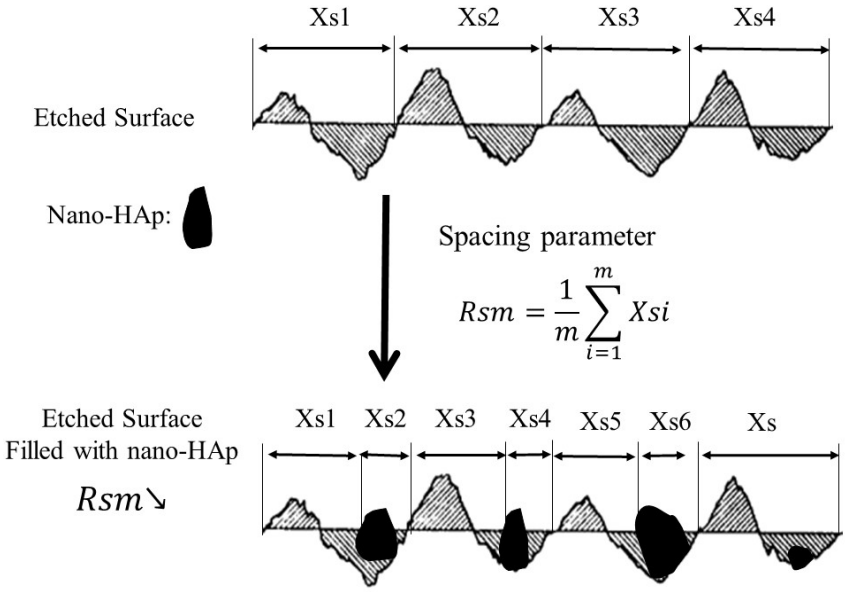

Fig. 1. Proposed fast repairing model for γ-PGA/nano-HAp paste using AFM spacing parameter.

Determination of Different Garnet Films Characteristics Prepared Using Sol-Gel and Spin or Dip-Coatings Techniques

G. Inkrataitė*, R. Skaudžius
Institute of Chemistry, Faculty of Chemistry and Geosciences, Vilnius University, Naugardukas st. 24, LT-03225 Vilnius, Lithuania
e-mail: greta.inkrataite@chgf.vu.lt

ABSTRACT

In recent years materials with luminescent properties have become very popular. In addition, these materials are very popular for usage in lamps and other light emitting devices, but nowadays scintillators and their research is becoming a very interesting subject for scientists. Scintillators are the basis for devices, that are used for radioactive contamination detection and measurement, nuclear material monitoring, also they are included in the computer detector composition of the tomography devices. There are various compounds that can be used as scintillators, but one of the most popular are those which have a garnet structure [1]. Amongst others, these can be yttrium or lutetium aluminum garnet, doped with different lanthanides (YAG:Ln; LuAG:Ln). These inorganics compounds have the required optical properties and radiation resistance and can, therefore, be used for thermal neutron and high energy radiation (X-ray, γ-radiation) detection [2]. The development of new scintillators is important. However, not the materials which are used are important but also their form. The preparation of powder is the simplest, but they are not suitable for the construction of scintillator detectors. Best suited and used for the manufacture of various devices are single crystals. In addition to single crystals, coatings on various pallets or microfibers can be used [3]. Using the sol-gel method we can obtain homogeneous multicomponent coatings at low temperatures, leaving the possibility of synthesizing compounds with emission intensity.

Improvement of luminescence is essential for getting the fastest scintillators properties. One way to do this is to additionally dope compounds with other elements. Replacing one element with another in the crystal lattice can influence the properties of the materials. The most common goal is to improve key parameters: compound emission intensity and decay times. One of the greatest scintillators drawbacks that is being addressed is that decay time is too long. When it is extremely long, then these second signal captured by the materials overlaps with the first, making the results unreliable and provides less data than it could. Scintillators such as YAG:Ce and LuAG:Ce doped with boron or magnesium can solve this problem. If a quick quench of decay time was obtained given result would be more accurate, and this method of synthesizing scintillators could be practically applicable [4].

In this work cerium boron and/or magnesium doped YAG and LuAG are synthesized on sapphire and quartz substrates using the dip-coating and spin-coating methods. Boron and magnesium are expected to improve required luminescent properties, and with the sol-gel method, homogeneous compounds will be synthesized at low temperatures. Phosphor coatings were analyzed by x-ray diffraction (XRD), scanning electron microscopy (SEM). Of course, emission, excitation spectra and decay times have been investigated as well.

Acknowledgments:
This project has received funding from European Social Fund (project No [09.3.3-LMT-K-712-15-0151]) under grant agreement with the Research Council of Lithuania (LMTLT).

References:

1. D. S. McGregor, *Annual Review of Materials Research*, Materials for Gamma-Ray Spectrometers: Inorganic Scintillators, 2018, 48, 254-277.
2. A.D. Sontakke, J. Ueda, et. al., *The Journal of Physical Chemistry C*, A Comparison on Ce3+ Luminescence in Borate Glass and YAG Ceramic: Understanding the Role of Host's Characteristics, 2016, 120, 31, 17683-17691.
3. S. Rawat, M. Tyagi, et. al., *Nuclear Instruments and Methods in Physics Research Section A: Accelerators, Spectrometers, Detectors and Associated Equipment*, Pulse shape discrimination properties of Gd3Ga3Al2O12:Ce,B single crystal in comparison with CsI:Tl, 2016, 840, 186-191.
4. C. Foster, Y. Wu, M. Koschan, et. al., *Journal of Crystal Growth*, Boron Codoping of Czochralski Grown Lutetium Aluminum Garnet and the Effect on Scintillation Properties, 2018, 486, 126-129.

Synthesis and Crystal Structure of Magnesium Ferrites Doped by Lanthanids

A. Ivanets[1*], V. Prozorovich[1], V. Sarkisov[1], Inga Grigoraviciute-Puroniene[2], Aleksej Zarkov[2], Aivaras Kareiva[2]

[1] *Institute of General and Inorganic Chemistry of National Academy of Sciences of Belarus, st. Surganova 9/1, 220072 Minsk, Belarus*

[2] *Institute of Chemistry, Vilnius University, Naugarduko 24, LT-03225 Vilnius, Lithuania*

e-mail: ivanets@igic.bas-net.by, AndreiIvanets@yandex.ru

ABSTRACT

Metal ferrites are widely used as Fenton-like catalysts for the oxidative degradation of organic pollutants. The catalytic activity of these materials significantly depends on the crystal structure, texture parameters, particle size and morphology [1]. Doping of metal ferrites with lanthanide ions leads to significant structural distortions and deformation of their lattice, which causes changes in the physicochemical and functional properties [2]. It is known that the introduction of lanthanides into the ferrite matrix can lead to an increase in their catalytic activity in a Fenton-like reaction due to the interaction of 3d-4f orbitals and increased generation of HO· radicals, and in the case of a photo- Fenton reaction due to the formation of impurity states in the band gap and a decrease in the electron transition energy [3].

This paper presents the results of a study of the effect of doping magnesium ferrite with lanthanide ions (La^{3+}, Ce^{3+}, Dy^{3+}, Gd^{3+}, Sm^{3+}) on their crystal structure. Magnesium ferrites were prepared by the glycine-nitrate method with the introduction of corresponding lanthanide nitrates into the reaction mixture and subsequent calcination at 600 °C.

X-ray diffractogrames of all obtained samples shown peaks corresponding to the (202), (311), (400), (511), (404) planes of magnesium ferrite, this confirms the formation of ferrites with spinel structure. The table shows the values of the lattice parameters (*a*), the unit cell volume (*V*), the average size of the crystallites (*D*) and the effective ionic radii (*r*) of the dopant cations.

Table. Structural parameters on magnesium ferrites.

Sample	a, *Å*	*V, nm³*	*D, nm*	*r(M^{3+}), Å*
$MgFe_{1.93}La_{0.07}O_4$	*8.431*	*0.599*	*19.4*	*1.032*
$MgFe_{1.93}Ce_{0.07}O_4$	*8.421*	*0.597*	*16,7*	*1.010*
$MgFe_{1.93}Sm_{0.07}O_4$	*8.406*	*0.594*	*13.0*	*0.958*
$MgFe_{1.93}Gd_{0.07}O_4$	*8.412*	*0.595*	*13.0*	*0.938*
$MgFe_{1.93}Dy_{0.07}O_4$	*8.411*	*0.595*	*12.4*	*0.912*
$MgFe_2O_4$	*8.387*	*0.590*	*16.8*	*0.645*

It was found that doping with lanthanide cations lead to an increase in the values of the lattice parameter *a*, which is associated with a large ionic radius of lanthanide ions compared to Fe^{3+} ion. The introduction of lanthanide cations into octahedral spinel voids lead to a distortion of the crystal lattice and an increase in the volume of the unit cell. However, there was no strict relationship between the ionic radius of the lanthanide and the average size of the crystallites.

Acknowledgments. This work was financial supported by BRFFR (No. X19LITG-007) and Research grant NOCAMAT (No. S-LB-19-2) from the Research Council of Lithuania

References

1. Ivanets, V. Prozorovich et al. *Journal of Nanomaterials*, Heterogeneous Fenton oxidation using magnesium ferrite nanoparticles for ibuprofen removal from wastewater: optimization and kinetics studies, 2020, Article ID 8159628.
2. M.A. Almessiere, Y. Slimani et al. *Journal of materials Research and Technology*, Effect of Nd-Y co-substitution on structural, magnetic, optical and microwave properties of NiCuZn nanospinel ferrite, 2020, 5, 11278-11290.
3. A.S. Weber, A.M. Grady et al. *Catalysis Science & Technology*, Lanthanide modified semiconductor photocatalysts, 2012, 4, 683-693.

Evaluation of Microarchitecture and Collagen Coating of Regular and Irregular Structure 3D Polycaprolactone Scaffolds for Dental Pulp Tissue Regeneration

E. M. Jonaitytė[1]*, M. Alksnė[2], P. Tušas[1], E. Šimoliūnas[2], V. Pečiulienė[1]
Institute of Odontology, Faculty of Medicine, Vilnius University, Lithuania
Department of Biological Models, Institute of Biochemistry, Life Sciences Centre, Vilnius University, Lithuania
egle.jonaityte@gmail.com

ABSTRACT

Background: 20 – 90 % of 6-year-old children in Europe have one tooth affected by dental caries [1]. Deep caries leads to inflammation and necrosis of the pulp-dentin complex. Thus, tooth maturation and root development are stopped, which leads to a worse prognosis of the tooth. However, current treatment outcomes and research data on the pulp-dentin complex regeneration are insufficient to reach the gold-standard procedure. Biodegradable 3D scaffold, which mimics the chemical composition and physical morphology of the pulp, is a promising method to aid pulp regeneration.

The aim of this study was to examine the pore size and porosity of regular and irregular structure 3D scaffold and to investigate the ability to coat scaffold with collagen.

Materials and methods: STL files of regular and irregular structure 3D scaffolds were designed with RegenHU software (BioCAD^{TM}). Polycaprolactone (PCL) scaffolds were printed with RegenHU 3D printer melted electrospinning writing (MESW) head. Images of the scaffolds were taken using optical microscope. Scaffold pores were blacked out using Adobe Photoshop (Adobe Systems Incorporated). Scaffold porosity, pore diameter, pore area and pore circularity were evaluated using the image processing program ImageJ (National Institutes of Health, LOCI, University of Wisconsin). PCL scaffolds were coated with type 1 acetylated collagen using ethylenediamine/n-propanol crosslinker. No collagen coating was used in the control group. Scaffolds were evaluated after application of Sirius Red dye. After 20 h incubation absorption of the solution was measured at 550 nm.

Results: Regular structure scaffold mean pore diameter was 194.23 µm. The smallest pore was 152.92 µm diameter, the largest 226.22 µm. Scaffold porosity was 77.43%, mean circularity 0.6 ± 0,04. Irregular structure scaffold mean pore diameter was 54.54 µm. The smallest pore was 5.82 µm diameter, the largest 373.72. 55,97% (361 pores) were smaller than 50 µm, 31,16% (201 pores) had 50 – 100 µm diameter, 9.46% (61 pores) had 100 – 150

µm diameter, 3.42 proc. (22 pore) were larger than 150 µm. Scaffold porosity was 58.62%, mean circularity 0,47 ± 0,18. Regular structure collagen coated scaffold light absorption was 0,0878 ± 0,02, irregular 0,0976 ± 0,03. There was no statistically significant difference between the groups (p=0.54).

Conclusions: Regular structure scaffold exhibited larger pore diameter and porosity percentage. Smaller than 50 µm pores were common in irregular structure scaffold. Both regular and irregular structure scaffolds displayed similar pore circularity. 3D PCL scaffold can be coated with collagen using acetylated collagen and ethylenediamine/n-propanol solution.

References:

1.World Health Organization. Diet and Oral Health: Fact sheet on oral health and sugars. 2018.

Development of Bone Equivalent 3D Printing Composites for Patient Specific Quality Assurance in Radiotherapy

Antonio Jreije[1], Diana Adlienė[1]
[1]Physics Department of Kaunas University of Technology.Studentų Str. 50, Kaunas, Lithuania
e-mail: antonio.jreije@ktu.lt

ABSTRACT

Additive manufacturing or 3-dimensional printing technology has gained popularity in recent years with a widespread application in medicine (e.g. implants or orthopaedic appliances, prostheses, surgical guides, etc). Given the flexibility and low cost of 3D printing, it is used for the creation of patient specific phantoms for radiotherapy quality assurance [1]. Previous publications demonstrated that commercially available 3D printing polymers can replicate soft tissues with high degree of accuracy. However, these studies failed to take into account that the human body is composed of different types of tissues which have a wide range of radiation attenuation and HU values.

This work aims at investigating the feasibility of creating a 3D printing composite with bone equivalent properties for future application in individualized anthropomorphic phantom. Specific features of the developed 3D printed materials i.e. tissue equivalency and X-ray attenuation were characterised.

The methodology presented in this study was to dope the commercially available 3D printing material High Impact Polystyrene (HIPS) with selected Tantalum metal powder (Ta, Z = 73) at appropriate ratio in order to achieve mass attenuation profiles equivalent to that of the bone. The weight percentage of the doping powder can be calculated theoretically in first approximation using mathematical modeling (NIST XCOM database) [2]. The x-ray attenuation properties were investigated in the energy range 50-150 keV which is relevant for phantom based analysis using Orthovoltage X-ray therapy. Using this approach, it was found that X- ray attenuation similar to that of bones can be achieved by the the addition of 0,47 wt % Ta powder to HIPS. In order to verify the results of the modeling, the attenuation properties of HIPS samples doped with different weight percentage of Ta (0.28%, 0.47%, 0.74% and 1.4%) was measured experimentally. Using 3D printer Zortrax 300M, experimental samples were manufactured by applying layer-by-layer printing technique while depositing Ta (powder, - 100 mesh, Sigma Aldrich) between the printed layers.

Experimental evaluation of the physical density and attenuation properties of the printed samples provided promising results for their application as a bone equivalent material. However, inhomogeneity of powder distribution was identified and will be discussed in future work dedicated for the fabrication of Ta doped HIPS filament for 3D printing.

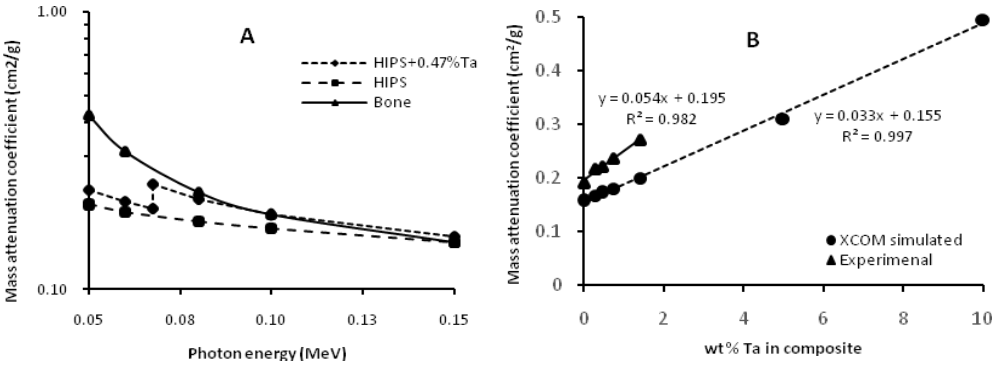

Fig. 1. (A) XCOM simulated X-ray attenuation HIPS with/without Ta (50-150 KeV). (B) X-ray attenuation of HIPS with different concentrations of Ta (121 kVp).

References

1.Sevcik et al. *Nuclear Instruments and Methods in Physics Research Section B: Beam Interactions with Materials and Atoms.* Low energy deposition patterns in irradiated phantom with metal artefacts inside: a comparison between FLUKA Monte Carlo simulation and GafChromic EBT2 film measurements, 2020, 478, 142-149.

2.M. J. Berger et al. (2010). Xcom: Photon cross sections database, nist standard reference database 8 (xgam). URL http://physics.nist.gov/PhysRefData/Xcom/Text/XCOM.html.

Comparison of 8 Different Impression Copings Splinting Methods

V. Rutkūnas[1] , V. Bilius[2], J. Jurgilevičius[3]

[1]Associate Professor, Department of Prosthodontics, Institute of Odontology, Faculty of Medicine, Vilnius University, Vilnius, Lithuania.

[2]Predoctoral student, Institute of Odontology, Faculty of Medicine, Vilnius University, Vilnius, Lithuania.

[3]Student, Institute of Odontology, Faculty of Medicine, Vilnius University, Vilnius, Lithuania.

e-mail: jurgis.jurgilevicius@gmail.com

ABSTRACT

Background: In clinical dentistry implant impression coping splinting tecnique is used to splint 2 or more impression copings, especially in angulated implants. This is done to ensure better impression accuracy by using more rigid materials than for overall impression(1). Though there is no consensus which splinting material exibits best physical properties(2).

Aim/Hypothesis: Analyze and compare accuracy of different materials used for impression copings splinting by measuring polymerization distortions.

Materials and Methods:

The research was conducted in Vilnius University Institute of Dentistry. In total 8 different splinting methos were evaluated by using optical scanner (4E, 3Shape) at dental technicians' labaratory.

1. Test group 1 – 10 impression coping pairs splinted with impression plaster, PLA
2. Test group 2 – 10 impression coping pairs splinted with autopolymerizing acrylic resin (GC pattern resin, GC Europe), cut and rejoin technique, PTR
3. Test group 3 – 10 impression coping pairs splinted with light cured acrylic resin (Individo Lux, Voco), cut and rejoin technique, ILC
4. Test group 4 – 10 impression coping pairs splinted with light cured acrylic resin, no cut, ILN
5. Test group 5 – 10 impression coping pairs splinted with VPS bite registration material (Futar, Kettenbach GmbH & Co. KG), SBR
6. Test group 6 – 10 impression coping pairs splinted with bis-acryl bite registration material (Luxabite, DMG), LXB
7. Test group 7 – 10 impression coping pairs splinted with bis-acryl composite resin (Protemp, 3M ESPE), PTP
8. Test group 8 – 10 impression coping pairs splinted with 3D printed splint and fastened with autopolymerizing acrylic resin.

Scaning protocol includes 3 scans: first - non splinted impression copings, second - 2 hours after splinting, and third - 24 hours after splinting.

Results: In total – 80 splinted impression copings were observed.

The lowest mean and interquartile range in X axis distace shift was found among ILC group (17,5 +-12 µm) at 2H and (21 +-12 µm) at 24H. Accordingly in Y axis lowest distace shift was found among ILC group (11,5 +-15 µm) at 2H. The lowest mean and interquartile range in angulation shift was found among ILC group (0,0395 +-0,05°) at 24H. The lowestmean and interquartile range in rotation shift was found among LXB group (0,151 +-0,165°) at 2H.

Conclusion and Clinical implications: All splinting materials, used in this study expressed some level of polymerization dimentional distortion. Using light cured custom tray material is slightly better method than using traditional pattern resin cut and rejoin technique and should be used practically. Angulation and distace discreptancies are detrimental to overall impression accuracy. More clinical *in vivo* researches should be done, in order to back up studies, conducted in labaratory environment.

References:

1. Aggarwal R, Jain S, Choudhary S, Saini HS, Reddy NK. Evaluating the Effect of Different Impression Techniques and Splinting Methods on the Dimensional Accuracy of Multiple Implant Impressions: An *in vitro* Study. J Contemp Dent Pract. 2018 Aug;19(8):1005–12.
2. Baig M. Accuracy of Impressions of Multiple Implants in the Edentulous Arch: A Systematic Review. Int J Oral Maxillofac Implants. 2014 Jul 10;29:869–80.

Synthesis and Evaporation of Gadolinium-Doped Ceria Electrolyte for IT-SOFC Applications

Fariza Kalyk[1*], Brigita Abakevičienė[1,2]

[1]Department of Physics, Kaunas University of Technology, Studentų str. 50, Kaunas, Lithuania
[2]Institute of Materials Science, Kaunas University of Technology, K. Baršauskas str. 59, Kaunas, Lithuania
**fariza.kalyk@ktu.edu*

ABSTRACT

Solid oxide fuel cells (SOFCs) have become one of the most used and researched types of fuel cells as they can operate over a wide temperature range from 400 °C to 1000 °C. The electrolyte of SOFC as initial material has important requirements such as high density and good ionic conductivity. These requirements can be achieved by controlling the concentration of impurities in the sample, e.g., mol% of gadolinia in gadolinium-doped ceria (GDC) thin films and selecting the appropriate method for the deposition of thin films. Comparing to other methods of producing electrolytes, e-beam evaporation technique has large deposition area and high deposition rate. In this research, gadolinium-doped ceria (GDC) ceramic powders with the molar content of Gd_2O_3 10, 15, 20 mol% were synthesised by co-precipitation (CP) synthesis method. Pellets with diameter of 13 mm were formed from synthesized and calcined at 900 °C powders; and annealed at 1200 °C for 5 h in the air. Synthesised pellets were further used as targets to form thin films on Si (100) substrate using e-beam evaporation technique. Crystal structure and surface area were studied by using X-ray diffraction (XRD) and Brunauer–Emmett–Teller (BET) methods. Structural properties and thermal decomposition of the samples were analysed using scanning electron microscopy (SEM) and thermogravimetric analysis (TGA) technique. Electrical properties of 10GDC pellets were investigated by impedance spectroscopy in 200 - 800 °C temperature range, from 1 Hz to 1 MHz frequencies. In this research, it was aimed to synthesize and characterize target material, to form dense electrolyte thin films using EB-PVD technique. Due to the fact that the target may influence the chemical composition of the film, the chemical composition of evaporated thin films was estimated using XPS measurement. XRD analysis of synthesised GDC powders indicates that 10, 15, and 20 GDC have a cubic fluorite-type crystalline lattice (Fm$\bar{3}$m space group) with dominating (111) crystallographic plane and were observed at a relatively low calcination temperature. SEM images revealed that the average grain sizes of GDC ceramics were about 201 and 317 nm, with no visible defects observed. Arrhenius plots of total ionic conductivities and activation energies for synthesized 10 GDC electrolytes were obtained from impedance plots, and showed that 10 GDC had the highest total ionic conductivity (0.011 $S \cdot cm^{-1}$ at 600 °C) with the lowest activation energies both at LT and HT (0.85 and 0.65 eV). Complex impedance plots, obtained from the impedance spectroscopy showed four types of different processes occurring in the structure, which include grain, grain boundary at the low temperature range and polarisation of platinum electrodes at the higher temperature range.

A Poly(1,10-Phenanthroline-5,6-Dione), Poly(Pyrrole-2- Carboxylic Acid), Gold Nanoparticles and Glucose Oxidase Nanobiocomposite Based Graphite Electrode as a Potential Anode for Biofuel Cell Powered by Glucose

Algimantas Kaminskas, Asta Kaušaitė-Minkštimienė
NanoTechnas – Centre of Nanotechnology and Material Science, Institute of Chemistry, Faculty of Chemistry and Geosciences, Vilnius University, Naugarduko str. 24, LT-03225 Vilnius, Lithuania
e-mail: Algimantas.Kaminskas@chgf.stud.vu.lt

ABSTRACT

Fuel cells (FC) have been in development for over 50 years and are still of great interest because has a potential application as alternative energy sources and as self-powered electrochemical biosensors whose main advantage is the use of simplified two electrode system, while external power source is not required for the operation. It is expected that in the future they will be used as implanted biosensors to measure various substances that cause heart disease or cancer, as well as blood glucose [1,2]. For this, they should be small and light, operate at body temperature, pH and salt concentration, and must be able to generate sufficient amount of energy. The use of gold nanoparticles (AuNP) allows for improving the efficiency of electron transfer, stability and sensitivity of biosensors. Conjugated polymers has good biocompatibility and may also improve electron transfer and provide stable matrix for enzyme immobilization. The goal of this work was to design an anode for FC powered by glucose with improved characteristics by exploiting unique properties of these nanomaterials. In order to accomplish this, 1,10-phenanthroline-5,6-dione (PD) was absorbed on the surface of the graphite rod (GR) and GR was immersed into electrochemical cell filled with buffer solution containing pyrrole-2-carboxylic acid (PCA) and colloidal AuNP (Fig. 1). Polymerization of PD and PCA was performed by cyclic voltammetry. AuND were encapsulated in a poly(pyrrole-2-carboxylic acid) (PPCA) layer during the polymerization. Finally, glucose oxidase (GOx) was covalently linked with the carboxyl groups of the PPCA layer. Immobilized GOx acted as a catalyst oxidizing glucose by molecular oxygen and converting chemical energy of this chemical reaction into a potentiometric signal.

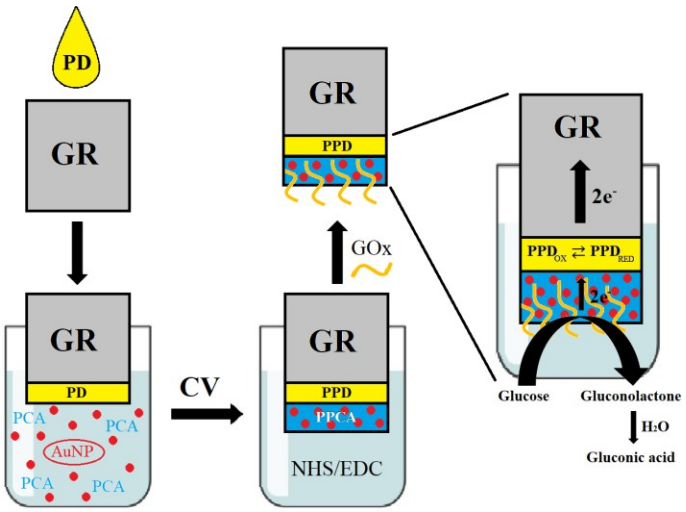

Fig. 1 Scheme of GE/PPD/(AuNP)PPCA-GOx electrode preparation and operation

Acknowledgement
This research was funded by a grant (No. S-LU-20-11) from the Research Council of Lithuania.

References

1.Y. Chen et al. *Nano Energy*, Fuel cell-based self-powered electrochemical sensors for biochemical detection, 2019, 61, 173.
2.C. Gonzalez-Solino et al. *Biosensors*, Enzymatic fuel cells: towards self-powered implantable andwearable diagnostics, 2018, 8, 11.

Derivatives of 3-[(4- Methoxyphenyl)Amino]Propanehydrazide: Towards Anticancer and Antioxidant Agents

I. Tumosienė[1], V. Petrikaitė[2,3,4], I. Jonuškienė[1], K. Kantminienė[5]*

[1]Department of Organic Chemistry, Kaunas University of Technology, Lithuania;
[2]Laboratory of Drug Targets Histopathology, Institute of Cardiology, Lithuanian University of Health Sciences,
[3]Institute of Physiology and Pharmacology, Faculty of Medicine, Lithuanian University of Health Sciences, Lithuania;
[4]Institute of Biotechnology, Life Sciences Center, Vilnius University, Lithuania;
[5]Department of Physical and Inorganic Chemistry, Kaunas University of Technology, Lithuania
e-mail: kristina.kantminiene@ktu.lt

ABSTRACT

Recently, thiadiazole, triazolethione and isatin derivatives have been attracting attention of medicinal chemists as promissing chemical scaffolds with a broad spectrum of activity, low toxicity and excellent pharmacokinetic properties.

A series of novel 1,3,4-thiadiazole, 1,2,4-triazolin-5-thione, and isoindoline-1,3-dione derivatives were synthesized from 3-[(4-methoxyphenyl)amino]propanehydrazide and their structures were confirmed by IR, ^{1}H, ^{13}C NMR spectroscopy and mass spectrometry data.

Anticancer activity of the synthesized compounds was screened by MTT assay against human glioblastoma U-87 and triple-negative breast cancer MDA-MB-231 cell lines. The tested compounds were more cytotoxic against U-87 cell line than MDA-MB-231 one. 1-(4-Fluorophenyl)-2-((5-(2-((4- methoxyphenyl)amino)ethyl)-4-phenyl-4*H*-1,2,4-triazol-3-yl)thio)ethanone (**12**) has been identified as the most active compound against glioblastoma U-87 cell line. It has shown different activity on both cell lines, possibly due to selectivity on specific targets in glioblastoma cells, and, therefore, has been identified as possessing the promising anticancer activity.

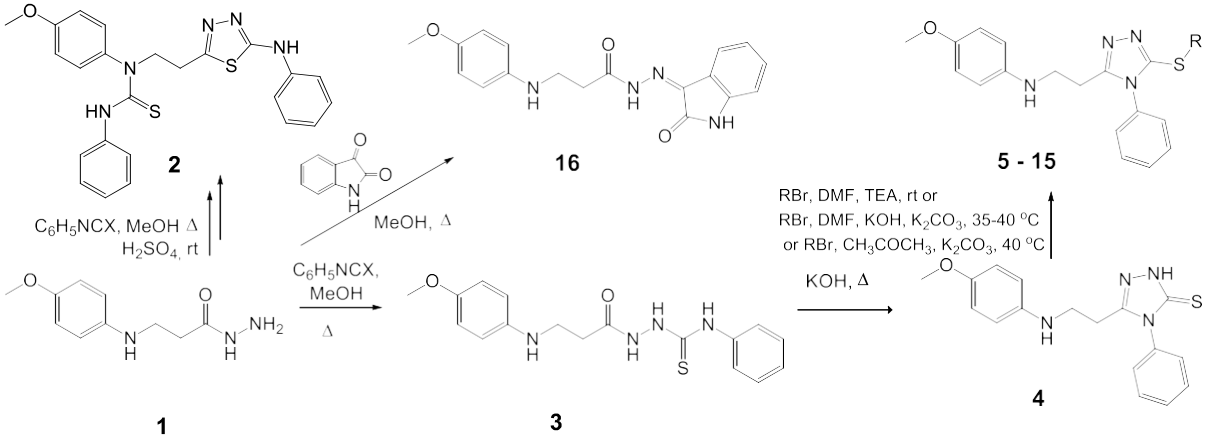

Scheme 1. Synthesis of compounds **2-16**.

The antioxidant activity of the synthesized compounds was screened by DPPH radical scavenging method. 2-(3-((4-Methoxyphenyl)amino)propanoyl)-*N*-phenylhydrazinecarbothioamide (**3**), ((5-(2-((4-methoxyphenyl)amino)ethyl)-4-phenyl-4*H*-1,2,4-triazol-3-yl)thio)methyl propionate (**5**), and 3-((4-methoxyphenyl)amino)-*N*′-(2-oxoindolin-3-ylidene)propanehydrazide (**16**) have been identified as possessing quite high antioxidant activity in respect of the well-known antioxidant ascorbic acid.

References

1. I. Tumosienė, I. Jonuškienė, et al. *Research* on *Chemical Intermediates*, Synthesis and biological activity of 1,3,4-oxa(thia)diazole, 1,2,4-triazole-5-(thio)one and *S*-substituted derivatives of 3-((2-carboxyethyl)phenylamino)propanoic acid, 2016, 42, 4459–4477.
2. R. Meleddu, V. Petrikaitė, et al. *ACM Medicinal Chemistry Letters*, Investigating the Anticancer Activity of Isatin/Dihydropyrazole Hybrids, 2018, 10, 571–576.
3. Tumosienė, K. Kantminienė, et al. *Molecules*, Antioxidant and Anticancer Activity of Novel Derivatives of 3-[(4-Methoxyphenyl)amino]propanehydrazide, 2020, 25, 2980.

Sol-Gel Synthesis and Characterization of $SrTiO_3$-$BiMnO_3$ Solid Solutions

D. Karoblis[1]*, A. Zarkov[1], K. Mazeika[2], D. Baltrunas[2], A. Beganskiene[1], A. Kareiva[1]
[1]Institute of Chemistry, Vilnius University, Naugarduko 24, LT-03225, Vilnius, Lithuania
[2]Center for Physical Sciences and Technology, Vilnius, LT-02300, Lithuania
e-mail: dovydas.karoblis@chgf.vu.lt

ABSTRACT

Perovskites are the large family of compounds that have crystal structure related to the mineral $CaTiO_3$. ABX_3 is the general formula for perovskites, where A and B are two cations and X is anion (halide, nitride, sulfide or oxygen) that bonds to both [1]. Due to multiple combinations of A and B elements and different crystal structures, this type of materials display large variation of physical properties, including piezoelectricity [2], multiferroicity [3], colossal magnetoresistance [4] etc. As a result of high variety of physical properties, inorganic perovskite-type materials have wide ranges of applications such as information storage devices, fuel cells, gas sensors. Moreover, these materials can be used in medicine as well. For example, $La_{0.75}Sr_{0.25}MnO_3$ (LSMO) based magnetic fluids (MF) were applied for treatment of rat tumors. It was observed that single intratumoral administration of LSMO-based MF results in complete tumor regression for 15-35 % of rats [5].

$SrTiO_3$ is another perovskite-type material, which can be used in medicine. Well-ordered $SrTiO_3$ nanotube arrays, which are capable of Sr release at slow rate and for a long time, was succesfully fabricated on titanium. This material showed good biocompatability, also it can induce precipitation of hydroxyapatite from stimulated body fluids and can be considered an ideal candidate for osteoporotic bone implants [6]. Furthermore, Ni^{2+} and Er^{3+} co-doped $SrTiO_3$ demonstrated applicative potential for luminescent nanothermometer for biomedical purposes [7].

In present study, solid solutions of $SrTiO_3$-$BiMnO_3$ have been synthesized using an aqueous sol-gel method. The maximal substitution level was determined. The thermal behaviour of precursor gels was investigated by thermogravimetric and differential scanning calorimetry (TG-DSC) measurements. X-ray diffraction (XRD) analysis was performed for the characterization of phase purity and crystallinity. Scanning electron microscopy (SEM) was employed for the estimation of morphological features. Moreover, $SrTiO_3$-$BiMnO_3$ specimens were also characterized by FT-IR and magnetization measurements were carried out for all samples.

Acknowledgments
This work was supported by a Research grant BUNACOMP (No. SMIP-19-9) from the Research Council of Lithuania.

References

1. M. Johnsonn, P. Lemmens. *Journal of Physics: Condensed Matter*, Perovskites and thin films—crystallography and chemistry, 2008, 4, 1–9.
2. F. P. Sun et al. *Journal of Intelligent Materials Systems and Structures*, Truss structure integrity identification using PZT sensor-actuator, 1995, 6.1, 134-139
3. H. Liu, X. Yang. *Ferroelectrics*, A brief review on perovskite multiferroics, 2017, 1, 69-85.
4. M. Baldini et al. *Proceedings of the National Academy of Sciences*, Origin of colossal magnetoresistance in $LaMnO_3$ manganite, 2015, 112.35, 10869-10872.
5. G. Belous et al. *AIP Conference Proceedings*, Nanoparticles of spinel and perovskite ferromagnets and prospects for their application in medicine, 2014, 13-18.
6. Y. Xin et al. *ACS nano*, Bioactive $SrTiO_3$ nanotube arrays: strontium delivery platform of Ti-based osteoporotic bone implants, 2009, 3.10, 3228-3234.
7. C. Matuszewska et al. *The Journal of Physical Chemistry C*, Transition metal ion-based nanocrystalline luminescent thermometry in $SrTiO_3$:Ni^{2+}, Er^{3+} nanocrystals operating in the second optical window of biological tissues, 2019, 123.30, 18646-18653.

Ferric Hexacyanoferrate Modified Electrode for Impedimetric Urea Sensing

G. Kavaliauskaitė[1]*, P. Virbickas[1], A. Valiūnienė[1]
[1]*Vilnius University, Faculty of Chemistry and Geosciences, Institute of Chemistry, Physical Chemistry department, Naugarduko str. 24, Vilnius, Lithuania LT-03225*
e-mail: gabija.kavaliauskaite@chgf.stud.vu.lt

ABSTRACT

Ferric hexacyanoferrate, also known as Prussian Blue (PB), is an inorganic compound, which is characterized by the property of selectivity for K^+, NH^+, Rb^+, Cs^+ ions, that intervene in its crystal lattice when electrochemical methods are used [1,2]. For this reason, PB is a preferable signal transducer material for ion selective sensors [3,4].

Carbamide (urea) is the final product of protein degradation. Medical detection of carbamide is important as high levels of blood urea can be related with kidney failure or liver malfunction [4,5]. For this reason, new, faster analytical systems for urea detection are relevant and important in nowadays world.

This research work is based on PB selectivity for NH^+ ions, which are obtained during electrochemical oxidation of carbamide. An electrochemical NH^+ ion sensor was formed on glass/FTO substrate, then analyzed by using electrochemical impedance spectroscopy (EIS). Electrochemical impedance spectra were measured at potential of + 0.8 V vs $Ag|AgCl|KCl_{sat}$, in the frequency range from 610 mHz to 20 kHz. By analyzing the obtained EIS data, according to Randles equivalent circuit model, the values of charge transfer resistance, R_{ct}, were calculated at various urea concentrations and are presented in Table 1.

c(UREA), mM	*R_{ct}, Ω•cm²*
0.050	*177.7*
0.149	*234.0*
0.249	*286.9*
0.495	*346.6*
0.739	*432.1*
0.980	*497.3*
1.22	*625.8*
1.47	*685.8*

Table 1. Values of charge transfer resistance of glass/FTO/BM electrode (geometric surface area = 2.25 cm^2) at various urea concentrations in PBS, pH 7.1.

References

1.A.A. Karyakin, E.E. Karyakina, L. Gorton, Electrochem. Commun. 1, p. 78 – 82 (1999)
2.P. Virbickas, G .Kavaliauskaitė, A. Valiūnienė, A. Ramanavicius, J. Electrochem. Soc., 166 (12), B927-B932 (2019)
3.Arkady A. Karyakin, Electroanalysis 13, No. 10, p. 813 – 819 (2001)
4.Valiūnienė, P. Virbickas, G. Medivikytė, A. Ramanavičius, Electroanalysis, val. 32 (3), p. 503-509 (2019)
5.C.S. Pundir, S. Jakhar, N. Vinay, Biosens. Bioelectron. 123, p. 36 – 50 (2019)

Synthesis of Silica/PLGA Composites by Solution Mixing Method

V. Kyshkarova*, I. Melnyk
Institute of Geotechnics, Slovak Academy of Sciences, Košice, Slovakia
e-mail: kyshkarova@saske.sk

ABSTRACT

Hybrid organic-inorganic materials have been widely studied over the past 30 years due to the unique combination of properties [1]. The potential intermixture of the advantages of inorganic materials with the use of tetraethyl orthosilicate (TEOS) (environmental compatibility, high mechanical strength, good thermal and chemical stability, hydrophilicity, and low cost) with the benefits of organic polymers poly(D,L-lactide-co-glycolide) (PLGA) (biocompatible, biodegradable, and non-toxic) can provide a wide range of applications for these composites. Among all polymers, the request of the biodegradable polymer poly(D,L-lactide-co-glycolide) (PLGA) has demonstrated great potential in biomedicine. PLGA is a family of FDA-approved decomposable polymers that are physically strong and highly biocompatible and have been widely studied as a means of delivering drugs, proteins, and various other macromolecules such as DNA, RNA, and peptides [2-4]. PLGA is the most common among the various ecologycal polymers because of its long clinical experience, propitious degradation characteristics, and opportunities for persistent drug delivery.

The aim of this work was to develop a one-step solution mixing method using tetraethyl orthosilicate and PLGA composite materials with various catalysts. The synthesis was carried out in acetone for polymer solubility. The ratio TEOS/PLGA was 130/1 (mass.). TEOS hydrolysis was performed in the presence of HCl catalyst, and then the polymer was added. NaF (sample SPC1) and NH_4OH (sample SPC2) were added to accelerate the condensation reaction having prepared silica/PLGA composites. After 24h gels were formed, they were crushed, washed and dried in an oven at 100°C (Fig.1). Some data on the composition and structure of the obtained composites are presented in Table 1.

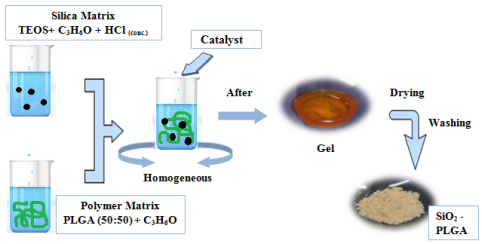

Fig.1. Schema of synthesis

Table 1. Elemental analysis data and content of functional groups

Sample	Elemental analysis data, %		EDX,wt %	pI	$C_{acidic\ groups}$, mmol/g	S_{BET}, m^2/g
	C	H	Si			
SPC1	18.5	4.2	39.2	2.2	5.6	22
SPC2	5.1	2.5	31.6	3.5	4.6	15

On the basis of the conducted researches, it is possible to conclude that the synthesized hybrid composites are non-porous materials with acid groups on the surface, capable of interactions with organic and inorganic substances.

The research is supported by the REA No. 734641-NanoMed and APVV-19-0302 projects.

References

1.H.Zou, S Wu, J. Shen. *Chem. Rev.,* Polymer/Silica Nanocomposites: Preparation, Characterization, Properties, and Applications, 2008, 108, 3893–3957.
2.C.Bouissou, J.J. Rouse, et al. *Pharm Res*, The influence of surfactant on PLGA microsphere glass transition and water sorption: Remodeling the surface morphology to attenuate the burst release, 2006, 23,1295–1305.
3.R.A. Jain. *Biomaterials*, The manufacturing techniques of various drug loaded biodegradable poly(lactide-*co*-glycolide) (PLGA) devices, 2000, 21, 2475–2490.
4.P.Q. Ruhe, E.L. Hedberg, et al. *J Bone Jt Surg Am,* rhBMP-2 release from injectable poly (DL-lactic-*co*-glycolic acid)/calcium-phosphate cement composites, 2003;85, 75–81.

Synthesis of Zinc Whitlockite by Dissolution-Precipitation Process

A. Kizalaite*, H. Klipan, I. Grigoraviciute-Puroniene, A. Kareiva, A. Zarkov
Institute of Chemistry, Vilnius University, Naugarduko g. 24, LT-03225 Vilnius, Lithuania
agne.kizalaite@chgf.vu.lt

ABSTRACT

Magnesium whitlockite ($Ca_{18}Mg_2H_2(PO_4)_{14}$) is the second most abundant mineral in human body and one of the main components of the human hard tissue, constituting to approximately 20–35 wt% [1]. This compound is known for its excellent biocompatibility and osteogenic capability which makes this material a promising candidate for application in bone regeneration [2]. Using other ions instead of Mg could further improve biological properties of the material and make it more appealing for medical usage. Zn substituted calcium phosphates are characterized by enhanced rate of metabolic processes and antibacterial properties which makes these materials very attractive for usage in medicine [3].

In the present work, whitlockite powders with different amounts of Zn ions were synthesized by dissolution-precipitation method using calcium hydrogen phosphate dihydrate and zinc acetate dihydrate as starting materials. Synthesis conditions such as temperature, time and pH were carefully studied and optimized. All synthesized compounds were obtained at low temperatures (75 °C) under atmospheric pressure. Synthesized compounds were analysed by X-ray diffraction, Fourier-transform infrared spectroscopy, scanning electron microscopy, inductively coupled plasma optical emission spectroscopy and Raman spectroscopy. Rietvield analysis was employed for calculations of lattice parameters.

Amount of Zn ions in the crystal structure was varied by varying their ratio with Ca ions in reaction mixture. It was demonstrated that single-phase Zn whitlockite can by synthesized when Ca to Zn ratio in a reaction mixture is in the range from 9 to 20. With an increase of Zn amount in the crystal lattice, decrease of lattice parameters was observed. Also, a significant change in morphology of the particles can be observed when amount of Zn in the crystalline lattice changes. When Zn concentration is low, particles are shaped like hexagonal platelets but with increase of Zn concentration it changes to a rhombic shape. Thermal stability studies revealed that Zn whitlockite is thermally unstable above 500 °C and after heat treatment decomposes to β-tricalcium phosphate and calcium pyrophosphate. As for our knowledge, whitlockite compounds with Zn instead of Mg ions were synthesized for the first time.

Acknowledgements
This project has received funding from European Social Fund (project No 09.3.3-LMT-K-712-19-0069) under grant agreement with the Research Council of Lithuania (LMTLT).

References

1.H. Cheng, R. Chabok et al. *Acta Biomaterialia*, Synergistic interplay between the two major bone minerals, hydroxyapatite and whitlockite nanoparticles, for osteogenic differentiation of mesenchymal stem cells. 2018, 69, 342–351.
2.H. L. Jang, G. Bin Zheng et al. *Advanced Healthcare Materials*, In Vitro and In Vivo Evaluation of Whitlockite Biocompatibility: Comparative Study with Hydroxyapatite and β-Tricalcium Phosphate, 2015, 5, 128–136.
3.V. Fadeeva, M. R. Gafurov et al. *BioNanoScience, Barinov*, Tricalcium Phosphate Ceramics Doped with Silver, Copper, Zinc, and Iron (III) Ions in Concentrations of Less Than 0.5 wt.% for Bone Tissue Regeneration, 2017, 7, 434–438.

Al^{3+} Influence on the Formation of Calcium Silicates by Using Two Step Synthesis

I. Knabikaite*, A. Eisinas, K. Baltakys

Departament of Silicate Technology, Faculty of Chemical Technology, Kaunas University of Technology, Radvilenu road 19, LT-50254 Kaunas, Lithuania

**e-mail: inga.knabikaite@ktu.lt*

ABSTRACT

Recently, extensive interest has been shown to developing of bioactive materials containing CaO-SiO_2 components for biomedical applications. One of the most recognized bioactive ceramics is hydroxyapatite because of its bioactivity and osteoconductivity. However, the low hardness of mentioned material limits its application [1]. Thus, importance of calcium silicates (CaO-SiO_2 component) is becoming very important not only for traditional ceramics (cement industry), but also for bioactivity technologies. Because of the favorable properties such as low shrinkage, good strength, lack of volatile constituents, body permeability, fluxing characteristics etc. [2].

Usually, calcium silicates are synthesized during solid-state sintering at high temperature (1100-1450 °C) [3]. However, it can be received by two-stages approach. Firstly, hydrothermal treatment is carrying out in CaO-SiO_2-H_2O system at 100-200 °C temperature; then synthesis products are treating by 800-1000 °C temperature for a final product [4]. Following method is better not only because of lower temperature, but also for opportunity by changing temperature, pressure, C/S ratio, etc., control synthesis products structure and other properties. Moreover, Al^{3+} ions can improve mentioned compound properties [5]. Thus, the aim of this work is to investigate Al^{3+} influence on the formation of calcium silicates by using two steps synthesis.

The molar ratio of primary mixture was equal to CaO/SiO_2 = 1.5 and $Al_2O_3/(Al_2O_3+SiO_2)$ = 0.05. Dry primary mixture (with Al^{3+} additive or without) was mixded with H_2O to reach solution/solid ratio of the suspension equal to 10.0. The synthesis carried out in unstired suspensions, isothermal treatment at 200 °C temperature duration changing from 8 to 72 h. The structure synthesis products mainly were characterized by XRD and thermal properties investigated by STA.

XRD showed that after 8 h of isothermal treatment in both systems (with and without Al^{3+} additive) unreacted raw material – portlandite was identified and semi-crystalline type C-S-H (I) and/or C-S-H (II) formed. However, other results differed from each other. In CaO-SiO_2-H_2O system hydraulically active α-C_2SH formed, while in CaO-SiO_2-Al_2O_3-H_2O system γ-C_2S was observed, which are stable even at room temperature. Moreover, together with mentioned compounds calcium alumosilicate hydrate – katoite was identified. By prolonging synthesis duration to 72 h, in both systems observed that higher crystallinity compounds formed: xonotlite, kilchoanite, pavloskyite and scawtite.

Although the XRD results were similar, simultaneous thermal analysis confirmed, that Al^{3+} had positive influence on wollastonite recrystallization from primary synthesis products. Exothermic effects on temperature higher than 850 °C showed that small amount of aluminium ions let to compose higher quantity of wollastonite.

Acknowledgments

This research was supported by the Research and Innovation Fund of Kaunas University of Technology (grant No. PP59/2002)

References

1. Z. Gou, J. Chang et al. *J Eur Ceram Soc,* Preparation and characterization of novel bioactive dicalcium silicate ceramics, 2005, 25, 1507-1514
2. X. Liu, M. Morra et al. *Biomed & Pharmacother,* Bioactive calcium silicate ceramics and coatings, 2008, 62, 526-529
3. R.A. Rashid, R. Shamsudin et al. *J Asian Ceram Soc,* Low temperature production of wollastonite from limestone and silica sand through solid-state reaction, 2014, 2, 77-81
4. K. Lin, J. Chang et al. *J Cryst Growth,* A Simple Method Synthesize Single-Crystalline Wollastonite Nanowires, 2007, 300, 267-271
5. L. Hermansson. *J Korean Ceram Soc,* A Review of Nanostuctured Ca-aluminate Based Biomaterials within Odontology and Orthopedics, 2018, 2, 95-107

Features of Biodegradation of Sol-Gel Bioactive Glass 60s Doped with Ge

A.P. Kusyak[1*], V.A. Dubok[2], V.S. Chornyi[3], A.L. Petranovska[1], I.V. Bohomol.[4], P.P. Gorbyk[1]

[1] Chuiko Institute of Surface Chemistry, NAS of Ukraine, Kyiv
[2]Frantsevich Institute of Problems of Materials Science, NAS of Ukraine, Kyiv
[3]Bogomolets National Medical University, Kyiv
[4] Ivan Franko State University of Zhytomyr, Natural Sciences Faculty, Zhytomyr
a_kusyak@ukr.net

ABSTRACT

The development of the latest bioceramic materials for medical and biological purposes is a significant segment of modern scientific technology. One of the classes of such materials that attracts special attention is bioactive sol-gel glass (BG). Due to its biocompatibility and ability to integrate with bone and soft tissues, BG is an attractive material for creating implants with osteoconductive properties [1, 2], and increasing requirements for them stimulates the emergence of more technological materials and medical procedures. Promising are the research and search for new implant materials and coatings based on known but insufficiently studied BG (45S5, 58S, 77S, 60S and others), which have the necessary properties for use in orthopedics, traumatology and other fields [3].

Samples of BG 60S (4% P_2O_5, 36% CaO, 60% SiO_2) (1) and doped with GeO_2 (1%) (2) were synthesized by the sol-gel method. In the environment of model physiological fluid (Kokubo's SBF) *in vitro* biodegradation processes of synthesized BG samples were studied and *in vivo* studies of bone formation were performed. The methods of atomic absorption (for Ca^{2+}, Mg^{2+}) and photometric (for HPO_4^{2-}) analysis were used to study the change in the ionic composition of the model physiological fluid, the pH changes of which were recorded potentiometrically. BG samples before and after *in vitro* bioresorption studies were tested by IR spectroscopy. The studied dependences of the activity of ion exchange processes and the rate of formation of hydroxy-carbonate apatite on the surface from doping additives confirm the bioactivity of the synthesized samples. The highest bioactivity according to the results of in vitro and *in vivo* studies shows BG 60S without alloying additives.

The results of studies of changes in the concentration of ions in the model environments during the biodegradation of the studied samples indicate active ion exchange processes, as a result of which changes in the chemical composition and surface structure of BG are possible. In Kokubo's SBF medium, ion exchange processes involving Ca^{2+}, Mg^{2+}, HPO_4^{2-} - ions occur throughout the observation time. Active adsorption of Mg^{2+} ions on the glass surface occurs throughout the period. Ca^{2+} ions actively pass into the solution from the surface of BG. The highest activity is observed for the undoped sample 60S, for the sample doped with Ge the extremum of release of Ca^{2+} in the first day of researches is characteristic. In Kokubo's SBF, the most active adsorption of HPO_4^{2-} ions was observed for the undoped sample throughout the study period.

Synthesized samples before and after interaction with the physiological fluid model were investigated by FTIR spectroscopy. According to the research results, the peak at 1095 cm^{-1} is assigned as a Si-0-Si stretching. The peak at 482 $cm^{-1}$is assigned as a Si-0-Si bending mode. An increase in the intensity of the peak at 1436 cm^{-1}, which is characteristic of the structural hydroxyl groups of the surface; an increase in the intensity of peaks at 480 $cm^{-1}$and 1055 cm^{-1}, as well as the appearance of low-intensity at 796 cm^{-1}, which are characteristic of fluctuations in Si-0-Si bonds indicate active processes of changes in the structure of the siloxane network. The peak at 598 and 566 cm^{-1} belong to P - O oscillations in tetrahedra [PO_4].

In vivo studies confirm the high level of bioactivity of unalloyed BG (60S) and the decrease in bioactivity of BG (60S) as a result of the addition of GeO_2 as evidenced by a 22.3% increase in bone tissue at 4 weeks after implantation for samples undoped BG (60S) compared to doped GeO_2.

References

1.L. L. Hench, *J Mater Sci: Mater Med*., The story of Bioglass, 2006, 17(11), 967-978.
2.H.Ylänen, Bioactive Glasses: Materials, Properties and Applications, *Elsevier Woodhead Publishing, UK*., 2017.
3.M.Bosetti , L.Zanardi , L.L.Hench , M. Cannas,. *J. Biomed. Mater. Res. A*., Type I collagen production by osteoblast-like cells cultured in contact with different bioactive glasses, 2003, 64(1), 189-195.

Crystal Structure and Magnetic Properties of $Bi_{1-x}Sm_xFeO_3$ Compounds Across the Phase Boundary: Effect of External Pressure

S.I. Latushka[1*], D.V. Zhaludkevich[1], M. Silibin[2], A. Pakalniškis[3], A. Kareiva[3], R. Skaudžius[3], D.V. Karpinsky[1]

[1]*Scientific-Practical Materials Research Centre of NAS of Belarus, 220072 Minsk, Belarus*
[2]*National Research University of Electronic Technology "MIET", 124498 Zelenograd, Moscow, Russia*
[3]*Institute of Chemistry, Vilnius University, LT-03225 Vilnius, Lithuania*
e-mail: latushkasi@gmail.com

ABSTRACT

Over the last decades, ferrites and manganites have attracted great attention of scientific society [1, 2]. Especially the compounds with chemical composition near the phase boundary and characterized by metastable structural state. Metastable structural state provides frustration of ferroic orders which opens up new possibilities for practical applications of the BiFeO3-based multiferroic materials [3]. Samples of the Bi1-xSmxFeO3 system with dopant ion concentrations up to x = 0.20 were prepared by the sol-gel reaction method. Structural measurements for the compounds Bi1-xSmxFeO3 showed a transition from the rhombohedral phase to the nonpolar orthorhombic phase through the antipolar orthorhombic phase with an increase in the dopant content, followed by stabilization of the nonpolar orthorhombic phase. An application of external pressure (P~5GPa) to the compounds having chemical composition across the phase boundary region leads to significant modification of the crystal structure and magnetic properties of the compounds. Thus, an application external pressure provides a stabilization of the orthorhombic states, viz. the polar rhombohedral phase diminishes and transforms to the anti-polar orthorhombic phase, while the anti-polar orthorhombic phase transforms to the non- polar orthorhombic phase. Magnetic properties of the compounds subjected to external pressure demonstrate increase in the magnetization of the compounds having dominant rhombohedral phase, wherein coercivity significantly increases, while the spontaneous magnetization remains nearly constant.

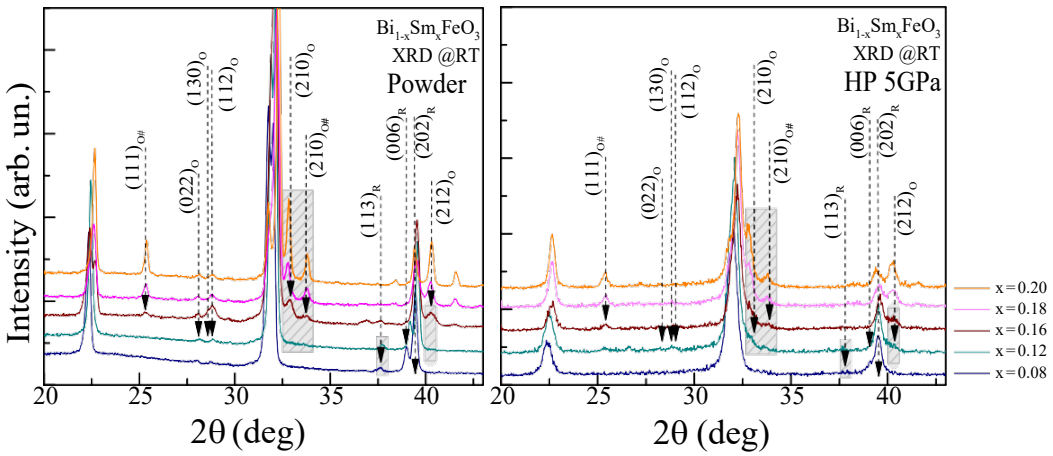

Fig. 1. Room-temperature XRD patterns obtained for the compounds powder and HP $Bi_{1-x}Sm_xFeO_3$ with x = 0.08, 0.12, 0.16, 0.18 and 0.20.

Acknowledgement

This work was supported by the European Union's Horizon 2020 research and innovation programme (RISE No. 778070), BRFFR and RFBR (project F20R-123. №20-58-00030).

References

1. R. Masrour, A. Jabar et al. *Solid State Commun*, Experiment, mean field theory and Monte Carlo simulations of the magnetocaloric effect in $La_{0.67}Ba_{0.22}Sr_{0.11}MnO_3$ compound, 2017, 268, 64–69.
2. R. Masrour, A. Jabar et al. *J. Magn. Magn. Mater*, Monte Carlo simulation study of magnetocaloric effect in $NdMnO_3$ perovskite, 2016, 401, 91–95.
3. G. Catalan, J.F. Scott, *Adv. Mater*, Physics and Applications of Bismuth Ferrite, 2008, 634, 2463.

Phospholipid Bilayer Formation and Characterization Immobilizing Chlorophyll A

Viktorija Liustrovaitė[1*], Aušra Valiūnienė[1], Gintaras Valinčius[2], Arūnas Ramanavičius[1]
[1]Institute of Chemistry, Vilnius University, Naugarduko 24, LT-03225, Vilnius, Lithuania
[2]Department of Bioelectrochemistry and Biospectroscopy, Institute of Biochemistry, Vilnius, Lithuania
e-mail: viktorija.liustrovaite@chgf.stud.vu.lt

ABSTRACT

Nature has created chlorophyll (Chl) to harvest light energy. Chl is responsible for capturing the photons of the sun and converting their energy into the energy of chemical bonds in a form that is available to virtually all life forms[1]. It is known that chlorophyll is located in the plasma membrane of the cell, which ensures the separation of space between the outer and inner medium of the cell, and its composition and structure give the cell a shape[2]. Naturally Chl is embedded within plant cell membrane. Therefore, for better understanding of Chl action tethered bilayer lipid membranes (tBLMs) can be applied. tBLMs is a complex system that allows it to be used as an experimental platform for basic studies of bio membrane structure and their function. In this work, one of such models is tBLM, which was deposited on the gold surface by the fusion of vesicles[3]. This modification of immobilized membranes allows the development of various biosensors by the incorporation of lipid components such as DOPC and cholesterol[4], which provide stability and can be variously altered by the incorporation of molecules such as chlorophyll a (Chl-a).

The aim of this study is to create phospholipid bilayer model with immobilized Chl-a and to characterize it. The investigation is performed with electrochemical impedance spectroscopy (EIS) and cyclic voltammetry (CV) to measure dielectric capacity and conductivity changes. Fluorescence microscopy (FM) is used to estimate the morphology of the membranes. The goal of this work is to immobilize Chl-a within the tethered bilayer lipid membrane (tBLM) in order to adapt this structure in the future to the production of structural models based on tBLM that could be useful for the imitation of the plant leaf cell membrane and are likely to be ideal for the further development of new biosensors and 'artificial leaves'.

References

1. Kräutler, B. & Hörtensteiner, S. Chlorophyll Catabolites and the Biochemistry of Chlorophyll Breakdown. in *Chlorophylls and Bacteriochlorophylls* (2007).
2. El-Khouly, M. E., El-Mohsnawy, E. & Fukuzumi, S. Solar energy conversion: From natural to artificial photosynthesis. *Journal of Photochemistry and Photobiology C: Photochemistry Reviews* (2017)
3. McGillivray, D. J. *et al.* Structure of functional Staphylococcus aureus α-hemolysin channels in tethered bilayer lipid membranes. *Biophys. J.* (2009)
4. Valincius, G. & Mickevicius, M. Tethered Phospholipid Bilayer Membranes. An Interpretation of the Electrochemical Impedance Response. in *Advances in Planar Lipid Bilayers and Liposomes* (2015).

Spectrophotometric Determination of Heparin Based on Aggregation of Gold Nanoparticles

E. Lubinaite[1]*, B. Brasiunas[1], A. Popov[1], A. Kausaite-Minkstimiene[1], A. Ramanaviciene[1]

NanoTechnas – Center of Nanotechnology and Materials Science, Institute of Chemistry, Faculty of Chemistry and Geosciences, Naugarduko str. 24, Vilnius, Lithuania

ernesta.lubinaite@chgf.stud.vu.lt

ABSTRACT

Heparin is a widely used anticoagulant in medicine that prevents the formation of blood clots. Excessive levels of heparin in the body can lead to severe circulatory diseases [1]. For this reason, it is very important to monitor the level of this drug in the blood during surgery and its regular use. From the structural point of view, it is a highly sulfated and negatively charged linear polysaccharide [2]. This property can be successfully applied for the development of an analytical systems based on an aggregation of gold nanoparticles for sensitive heparin determination [3].

In this work, 13 nm gold nanoparticles were synthesized by reducing hydrogen tetrachloroaurate(III) with trisodium citrate in the presence of tannic acid [4]. Positively charged polymer poly-L-lysine can be used to aggregate gold nanoparticles in the solution. However, if negatively charged heparin is present, poly-L-lysine binds to heparin instead, resulting that gold nanoparticles aggregation is being stopped (Fig. 1). This interaction was successfully applied for the sensitive detection of heparin. It was determined that the limit of detection is 0.0018 units/ml of heparin. The absorbance ratio at A_{650nm}/A_{520nm} has a linear dependence in heparin concentration range from 0.0031 to 0.04 units/ml allowing heparin in the sample to be quantified using the calibration curve.

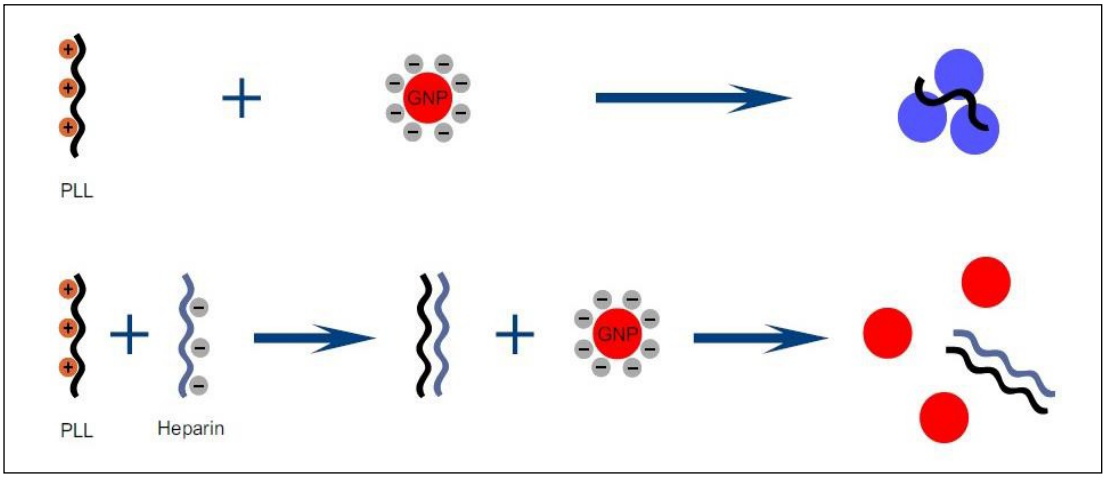

Fig. 1. Scheme representing the analytical system for heparin detection using gold nanoparticles and positively charged poly-L-lysine.

References:

1. L. Tian, H. Zhao, Z. Zhao, J. Zhai, and Z. Zhang, "A facile voltammetric method for detection of heparin in plasma based on the polyethylenimine modified electrode," *Anal. Methods*, vol. 11, no. 10, pp. 1324–1330, 2019.
2. M. A. Smythe, J. Priziola, P. P. Dobesh, D. Wirth, A. Cuker, and A. K. Wittkowsky, "Guidance for the practical management of the heparin anticoagulants in the treatment of venous thromboembolism," *J. Thromb. Thrombolysis*, vol. 41, no. 1, pp. 165–186, 2016.
3. X. Ma, X. Kou, Y. Xu, D. Yang, and P. Miao, "Colorimetric sensing strategy for heparin assay based on PDDA- induced aggregation of gold nanoparticles," *Nanoscale Adv.*, vol. 1, no. 2, pp. 486–489, 2019.
4. J. Turkevich, P. C. Stevenson, and J. Hillier, "A study of the nucleation and growth processes in the synthesis of colloidal gold," *Discuss. Faraday Soc.*, vol. 11, no. c, pp. 55–75, 1951.

Morphological Study of Bio-Nanocomposites Based on PA6/Selenium Compounds

H. Markevičiūtė*, V. Krylova, N. Dukštienė
Kaunas University of Technology, Department of Physical and Inorganic Chemistry
e-mail: henrieta.markeviciute@ktu.edu

ABSTRACT

In recent years, nanotechnology and the potential of forming bio-nanocomposites by incorporation of nanosized particles in biopolymer matrices have drawn increased attention. So far, the most studied matrices for the bio-nanocomposites sythesis are various artificial and natural polyamides.The application of highmolecular compounds as matrix for the synthesis of selenium compounds- containing nanocomposites is of particular interest [1]. The present work aims to characterize the surface morphology of PA6/selenium compounds-containing bio-nanocomposites. These bio- nanocomposites were obtained applying different chemical synthesis methods: the PA6/Se via chemical bath deposition, the PA6/Cd-Se by successive ionic layer adsorption and reaction and the PA6/Ag-Cd-Se by cation exchange method. The bulk chemical composition was determined using atomic absorption spectroscopy (AAS). Atomic force microscopy (AFM) was used to characterize surface morphology.

From the AFM images (Fig. 1), it can be seen that the local areas of the PA6 and PA6/Se surfaces exhibited a different morphological structure. Surface roughness is also an important parameter for quantitatively describing the surface. The Z_{mean} and R_a of PA6/Se composite were clearly different from those of the virgin PA6 (Table 1).

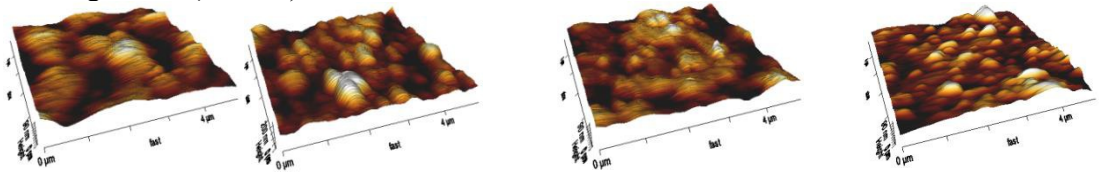

PA6 *PA6/Se* *PA6/Cd-Se* *PA6/Ag-Cd-Se*

Fig. 1. Three-dimensional AFM topographical images of obtained composites.

Table 1. Composition and surface roughness parameters of the obtained composites.

Sample	*Composition, at%*	*Average height, Z_{mean} (nm)*	*Average roughness, R_a (nm)*	*RMS roughness, R_q (nm)*	*Peak-to-valley roughness R_t (nm)*
PA6	–	*60.4*	*10.78*	*13.73*	*94.61*
PA6/Se	*Se – 100*	*156.9*	*27.61*	*35.66*	*225.9*
PA6/Cd-Se	*Se – 73.2* *Cd – 26.8*	*53.57*	*9.82*	*12.17*	*96.75*
PA6/Ag-Cd-Se	*Se – 38.96* *Cd – 1.18* *Ag – 59.86*	*50.81*	*8.36*	*11.55*	*97.15*

When PA6/Se samples were exposure in an aqueous medium containing Cd^{2+} cations, insoluble nanoparticles of CdSe deposited in situ on PA6/Se template and produce the PA6/Cd-Se nanocomposite. Some pyramidal-like single crystals of crystalizes Se and/or CdSe were observed. The Z_{mean} and R_a of PA6/Cd-Se composite, significantly decreased in comparison with those of the PA6/Se (Table 1). After the PA6/Cd-Se composite exposure in an aqueous $AgNO_3$ solution, the surface of the obtained composite showed the presence of nano-sized particles, assumed to be of Ag_2Se. As a result, the quantitative parameters of the surfaces decreased. Furthermore, R_t of the PA6/Se-CdSe and PA6/Cd-Se-Ag composite surface like no undergoes. It should be noted, that the RMS of deposited films decreased with the formation of the CdSe and Ag_2Se nanoparticles as compared to deposited amorphous Se films on PA6 surface.

References

1.L.M. Sosedova, V.S. Rukavishnikov et all. *Nanotechnologies in Russia,* Synthesis of chalcogen-containing nanocomposites of selenium with arabinogalactan and a study of their toxic and antimicrobial properties, 2018, 13,290–294.

Adhesion of Fibroblast Cells to Bioceramic Coatings on Aluminum

T. Matijošius[1]*, J. Kavaliauskaitė[2], A. Kazlauskaitė[2], A. Stirkė[2], S. Asadauskas[1]
[1]Center for Physical Sciences and Technology, Department of Chemical Engineering and Technology
[2]Center for Physical Sciences and Technology, Department of Functional Materials and Electronics
e-mail: tadas.matijosius@ftmc.lt

ABSTRACT

Bioceramic materials are often used in medicine for dental and bone implants due to their chemical inertness, biocompatibility, high hardness and resistance to abrasion. However, their inertness might lead to insufficient cell adhesion. Anodic coatings, which are composed mainly of bioinert Al_2O_3, offers high porosity which can be beneficial for adhesion of various cell types.

Industrial Al alloys 1050 and 6082 of 99.6% and 96.7% purity respectively as well as Ti BT1 alloy of 96.32% purity were employed as substrates. Hard anodization of Al was performed in Type III H_2SO_4/oxalic a. electrolyte for 70 min at 200 A/m² and 15 ºC to obtain bioceramic coatings of ~60 µm thickness [1]. Phospho-anodization was performed in 4% H_3PO_4 for 150 min at 150 V to produce coatings of ~10 µm thickness. The cells were grown on the plates of over 50 cm² spreading area, where the submerged specimen occupied 2.5 cm². Cell interaction with the specimen surface was analyzed using Eclipse Ti-E microscope after 48 hours of incubation at 37 °C [2].

Murine fibroblast cells L929, which are isolated from connective tissue, show good viability and proliferation rates on Ti alloy BT1. Therefore, they were further evaluated on anodized 1050 (higher purity) and 6082 (lower purity) alloys, see Fig. 1.

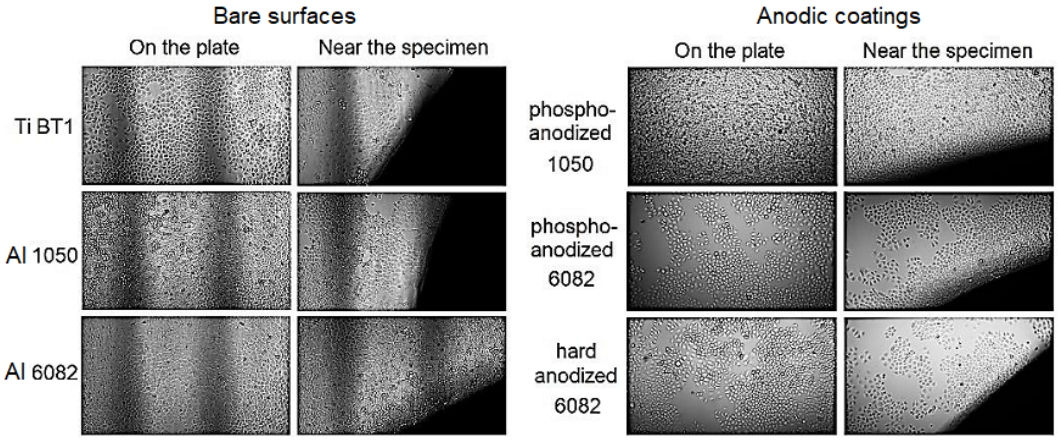

Fig. 1. Morphological appearance of L929 cells on the plate and near the bare alloys (left) and anodic coatings (right) after 48 h under 10× magnification

The interaction between the fibroblast cells and the specimen was evaluated by comparing their abundance in the vicinity near the specimen. Cell density was higher near phospho-anodized 1050 alloy of 99.6% purity. They were less abundant near bare 1050 and 6082. Even Ti specimen, which was not porous, appeared less populated compared to the phospho-anodized 1050. The cell growth was slower near phospho-anodized or hard anodized 6082 with pore ID of ~200 nm and ~15 nm resp. Lower purity at 96.7% could result in significant release of Mn, Zn and other alloying elements and inhibit cell proliferation. Hard-anodized surfaces also are less porous compared to phospho-anodized ones. This suggests that alloy purity, electrolyte components and surface pore density might influence cell adhesion and proliferation. These factors require detailed analysis and further experimentation to assess the viability of industrial aluminum alloys as the substrates for bioceramic coatings.

References

1. T. Matijošius, A. Pivoriūnas et al. *Ceramics International*, Friction reduction using Nanothin Titanium layers on anodized aluminum as potential bioceramic material, 2020, 46, 15581–15593.
2. T. Matijošius, J. Kavaliauskaitė et al. *9th Conference of PhD Students and Young Researchers FizTech2019*, Influence of titanium and bioceramic coatings on cell adhesion, 2019, 15.

Perspectives of Sol-Gel Silica Particles Loaded with Cu, Eu for Biomedical Applications

I. Melnyk[1,2]*, V. Tomina[2], N. Stolyarchuk[2], I. Furtat[3], M. Vaclavikova[1], A. Kareiva[4], A. Beganskienė[4]

[1]Institute of Geotechnics of SAS, Watsonova 45, Kosice-04001, Slovak Republic. [2]Chuiko Institute of Surface Chemistry of NASU, Generala Naumova 17, Kyiv-03164, Ukraine. [3]National University of Kyiv-Mohyla Academy, Skovorody 2, Kyiv-04070, Ukraine. [4]Vilnius University, Naugarduko 24, Vilnius LT-03225, Lithuania
e-mail: in.melnyk@gmail.com

ABSTRACT

Sol-gel technique has got a huge potential for material production within the research communities worldwide. Obtained via one-step sol-gel synthesis functionalized polysiloxanes are hybrid polymer materials with different functional groups, possessing such characteristics as resistance to highly acidic environments, biocompatibility, lack of swelling in organic solvents, etc. Fabrication of silica particles with different chemical structures and various mechanisms of action is widely used in bionanotechnology. One of the most important requirements of the successful application of such materials is the high content of the available hydrolytically stable functional groups to form the complexes with metal ions which can add antibacterial or biomarker activities. Recently, the task of preparing eco-friendly materials usable for multiple purposes has become of increasing concern [1]. Functionalized amino-silica particles (especially with bifunctional surface layers) are widely used as adsorbents for heavy metal ions. We designed the adsorbents combining on the surface hydrophilic (-NH_2, -OH) and hydrophobic (phenyl, ethyl) groups, basic (amino) and acidic (silanol) groups, complex-forming (amino) and ion-exchange (silanol) groups for solving a complex of water treatment problems, including the removal of Cu(II) and Eu(III) ions (Fig. 1a).

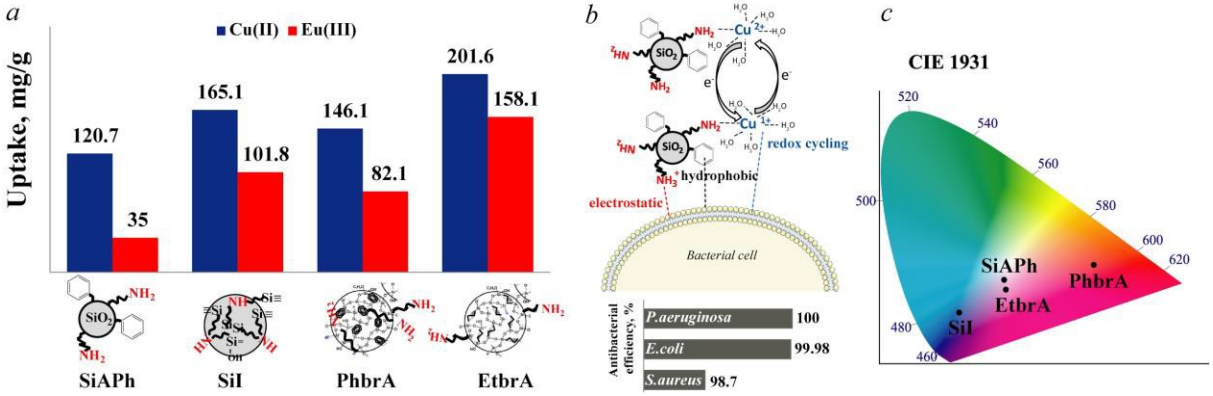

Fig.1. Sorption capacities of aminosilica particles to Cu(II) and Eu(III) ions (a); types of interactions on bacterial cells' surface (b); chromaticity diagram obtained from the luminescence spectra (c)

Water suspension (1%) of Cu(II) loaded SiO_2/-$(CH_2)_3NH_2$/-C_6H_5 particles showed complete growth inhibition (in 120 min) of the bacterial cultures such as *P. aeruginosa, E.coli,* and *S.aureus* on the solid medium due to multiple and nonspecific interactions between the particle surfaces and the surface layers of bacteria, revealing the perspectives of such materials as antimicrobial agents [2] (Fig.1b). Meanwhile, Eu(III) loaded samples, especially with bridges within silica networks, exhibited different light emission (Fig.1c) and this feature can be used for some specific applications, e.g. bioimaging [3].

The study is funded by the APVV-19-0302 and REA No. 734641-NanoMed projects.

References

1. V.V. Tomina, I.M. Furtat, et al. Surface and structure design of aminosilica nanoparticles for multifunctional applications: adsorption and antimicrobial studies, *Biocompatible Hybrid Oxide Nanoparticles for Human Health: From Synthesis to Applications* (ISBN 9780128158753), Elsevier, 2019, 15–31.
2. V.V. Tomina, I.M. Furtat, et al. *ACS Omega,* Diverse pathway to obtain antibacterial and antifungal agents based on silica particles functionalized by amino and phenyl groups with Cu(II) ions complexes, 2020, 5, 25, 15290–15300.
3. V.V. Tomina, N.V. Stolyarchuk, et al. *Colloids and Surfaces A*, Preparation and luminescence properties of europium(III)-loaded aminosilica spherical particles, 2021, 608, 125552

Application of Metalorganic Precursors for Laser Fabrication

G. Merkininkaitė[1,2]*, V. Padolskytė[3], E. Aleksandravičius[3], D. Gailevičius[2,3], M. Malinauskas[3], S. Šakirzanovas[1]

[1] *Faculty of Chemistry and Geosciences, Vilnius University, Lithuania*
[2] *Femtika Ltd., Lithuania*
[3] *Laser Research Center at Vilnius University, Lithuania*
greta.merkininkaite@chgf.vu.lt

ABSTRACT

Direct laser writing using multi-photon polymerization has become a powerful technique for the fabrication of free form micro- and nano-structures for diverse applications in microfluidic, micro mechanic and electronic, biomedical, metamaterial as well as nano-photonic research fields [1, 2]. Such numerous applications require precursors with different chemical, physical and optical properties. Therefore, development of new chemical composition materials remains an urgent and timely task.

The purpose of this research was to synthesize a series of organic-inorganic polymer precursors [3] and investigate the prospects of 3D formation of these materials as well as to estimate the inhibitor influence on polymerization reactions. The following steps have been accomplished to achieve this goal. Firstly, organometallic polymer precursors with different silicon (Si) and zirconium (Zr) compound amounts with and without inhibitor were prepared *via* sol-gel method. Differences in chemical composition of synthesized materials were determined using Fourier transform infrared spectroscopy (FTIR). Measurements of refractive indices were performed for preliminary characterization of optical properties and suitability of precursors for laser lithography. Scanning electron microscopy (SEM) images of fabricated 3D structures confirmed the resolution change dependency on the material composition and manufacturing parameters.

The study shows that silicon and zirconium hybrid organic-inorganic compounds synthesized by the sol-gel method are suitable for 3D laser lithography (Fig. 1) and the inhibitor has an effect on structure resolution.

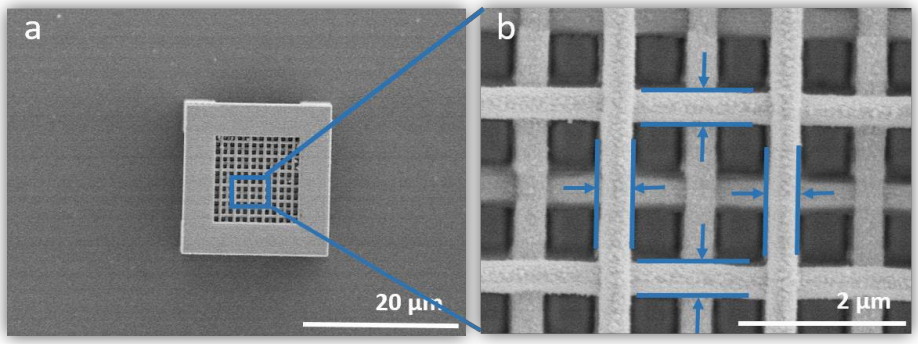

Fig. 1. SEM micrographs of printed periodic lattice.

References

1. Gailevičius, D., et al., Additive-manufacturing of 3D glass-ceramics down to nanoscale resolution. Nanoscale Horizons; **4**, 647-651; (2019)
2. Sakellari, I., et al., Diffusion-Assisted High-Resolution Direct Femtosecond Laser Writing. ACS Nano; **6**(3), 2302-2311; (2012)
3. Ovsianikov, A., et al., Ultra-Low Shrinkage Hybrid Photosensitive Material for Two-Photon Polymerization Microfabrication. ACS Nano; **2**(11), 2257-2262; (2008)

Role of Capping Agent in Formation of Photoelectrochemically Active Tungsten Oxide

L. Michailova[1*], E. Griniuk[1], G. Plečkaitytė[2], M. Petrulevičienė[2], J. Juodkazytė[2]
[1] *Institute of Chemistry, Faculty of Chemistry and Geosciences, Naugarduko str. 24, LT-03225 Vilnius University, Lithuania*
[2] *Center for Physical Sciences and Technology, Department of chemical engineering and technology Saulėtekio av. 3, LT-10257 Vilnius*
e-mail: laura.michailova@chgf.stud.vu.lt

ABSTRACT

The scarcity and growing demands for fossil fuels require to develop efficient and sustainable methods for fuel production using renewable energy sources. Photoelectrochemical (PEC) water splitting to produce H_2 using semiconductor photoelectrodes and solar energy is a promising approach to address these issues. Tungsten (VI) oxide WO_3 with a moderate band gap of 2.4–2.8 eV has been considered as suitable visible light responsive photoanode for PEC water splitting. Moreover, WO_3 is characterized by moderate hole diffusion length (~150 nm) compared with α-Fe_2O_3 (2–4 nm) and better electron mobility (~12 $cm^2\ V^{-1}\ s^{-1}$) compared to TiO_2 (~0.3 $cm^2\ V^{-1}\ s^{-1}$) [1].

Properties of tungsten oxide coatings strongly depend on synthesis conditions and additives used in the synthesis. A variety of synthesis techniques such as sol–gel, microwave, hydrothermal, solvothermal, chemical precipitation, and flame spray pyrolysis have been used to prepare WO_3 nanomaterial [2]. Particle size, porosity and morphology of tungsten oxide can be controlled with the help of structure directing agents.

In this work sol-gel approach was applied to synthesize tungsten oxide coatings using ethylendiamintetraacetic acid (EDTA) as a structure directing agent. It was investigated how different molar ratios of W:EDTA influence the morphology and photoelectrochemical response of the films. Following W:EDTA ratios were investigated: 1:0.5, 1:1, 1:1.67 and 1:2. Morphology of coatings was analyzed using scanning electron microscope (SEM). Photoelectrochemical activity of WO_3 films was studied by means of cyclic voltammetry in three electrode cell in 0.5 M H_2SO_4 solution under illumination.

It was found that morphology of coatings strongly depends on amount of EDTA used in the synthesis. Voltammetric investigations (Fig. 2) revealed differences in photoelectrochemical performance and electrochemically active surface area of the coatings.

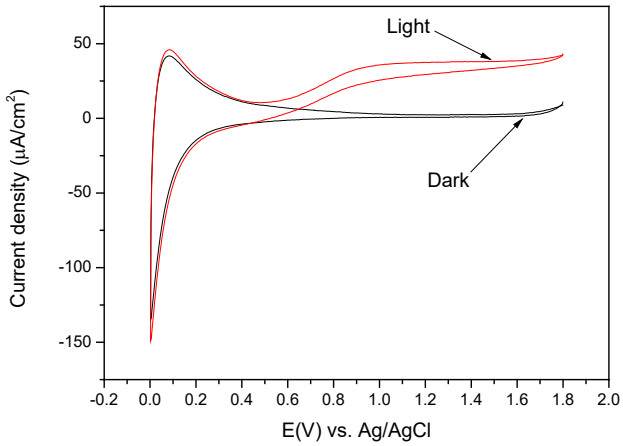

Fig. 1. Cyclic voltammograms of WO_3 sample prepared with W:EDTA ratio 1:2; 0.5 M H_2SO_4, potential scan rate 50 mV/s, intensity of illumination ~ 100 mW cm^{-2}.

References

1. G. Zheng, J. Wang et al. Nanoscale, Tungsten oxide nanostructures and nanocomposites for photoelectrochemical water splitting, 11, 18968-18994 (2019).
2. T. Govindaraj, C. Mahendran et al. J Mater Sci: Mater Electron, The remarkably enhanced visible-light-photocatalytic activity of hydrothermally synthesized WO3 nanorods: An effect of Gd doping, 40, 1-15 (2020).

Vanillin Derivatives as Resins for Optical 3D Printing

A. Navaruckiene[1], E. Skliutas[2], M. Malinauskas[2], J. Ostrauskaite[1]*
[1]*Department of Polymer Chemistry and Technology, Kaunas University of Technology*
[2]*Laser Research Center, Faculty of Physics, Vilnius University*
**e-mail: jolita.ostrauskaite@ktu.lt*

ABSTRACT

3D printing, also known as additive manufacturing has drawn increasing attention globally and has made a revolutionary impact on product fabrication in such areas like food industry, textiles, architecture, medicine, and construction [1]. Polymers are widely used in our everyday life due to their diverse properties and relatively low cost; however, it is difficult to form intricate geometries from them. Additive manufacturing is a solution to create complex geometries from plastics [2].

In this study, the cross-linked polymers were obtained by free-radical photocross-linking of vanillin diacrylate and vanillin dimethacrylate using ethyl(2,4,6-trimethylbenzoyl) phenylphosphinate as photoinitiator. The chemical structure of obtained polymers was confirmed by FT-IR spectroscopy. The yield of insoluble fraction obtained after Soxhlet extraction with acetone after 24 hours was in the range of (77-96) %. The cross-linking density calculated from the real-time photorheometry storage modulus curve at the steady state was in the range of (49-7928) mol/m^3. Thermal and mechanical properties of vanillin diacrylate-based and vanillin dimethacrylate-based polymer films were investigated.

Real-time photorheometry was used to monitore the evolution of free-radical photocross-linking process. The tests were performed on a MCR302 rheometer from Anton Paar equipped with the plate/plate measuring system. The samples were irradiated by UV/Vis light in a wavelength range of 250-450 nm through the glass plate using UV/Vis spot curing system OmniCure S2000, Lumen Dynamics Group Inc. The sufficient amount of photoinitiator was determined by comparing compositions containing 1-5 mol.% of photoinitiator. In most cases photopolymerization was faster and more rigid polymers were obtained when 3 mol.% of ethyl(2,4,6-trimethylbenzoyl) phenylphosphinate were used. The most rigid polymers were obtained by free-radical photocross-linking of vanillin dimethacrylate, however its films were fragile.

Optical printing techniques, direct laser writing and microtransfer molding, were used to produce 3D objects out of vanillin diacrylate-based photocross-linkable resin. A test to assess the optimal fabrication parameters was performed and the capability to produce 3D microporous 75 × 75 μm^2 woodpile structures out of the resin via direct laser writing was demonstrated. 3D printed objects of vanillin diacrylate-based resin with 3 mol.% of ethyl(2,4,6-trimethylbenzoyl) phenylphosphinate corresponded to the used 3D model.

Acknowledgements
Financial support from EU ERDF, through the INTERREG BSR Programme, (ECOLABNET project #R077) is gratefully acknowledged.

References
1.J. Liu, L. Sun et al. *Carbohydrate Polymers*, Current advances and future perspectives of 3D printing natural-derived biopolymers, 2019, 207, 297-316.
2.N. Li, S. Huang et al. *Journal of Materials Science & Technology*, Progress in additive manufacturing on new materials: A review, 2019, 35, 242–269.

Europium Doped Luminescent Glass Synthesis and Characterization

M. Norkus[1]*, G. Niaura[2,3], R. Skaudžius[1]

[1]Faculty of Chemistry and Geosciences Institute of Chemistry, Naugarduko st. 24, LT-03225 Vilnius, Lithuania
[2]Department of Organic Chemistry, Center for Physical Sciences and Technology (FTMC), Saulėtekio Ave. 3, LT-10257, Vilnius, Lithuania
[3]Institute of Chemical Physics, Faculty of Physics, Vilnius University, Saulėtekio Ave. 3, LT-10257, Vilnius, Lithuania
e-mail: mantas.norkus@chgf.vu.lt

ABSTRACT

Since the commercialization of white LED in 1996, incandescent and fluorescent light sources have been steadily overturned by LEDs in all of their usage spheres [1]. The most prevalent way for white light production is the combination of yellow phosphor (YAG:Ce^{3+}) and organic resin composite with blue light emitting diode. To drive LEDs for high brightness applications high current densities are required, however, after a certain threshold value the amount of generated light diminishes due to so-called efficiency droop phenomena [2]. In practice this is circumvented by using a larger number of individual LED chips instead of increasing operating current of a single module.

Another most apparent drawback of present technology is the aging and instability of yellow phosphor composite: as the junction temperature between phosphor composite and blue emitting chip increases, the organic matrix inevitably suffers from luminous efficiency degradation and evident color shift throughout its lifespan [3]. In order to improve thermal characteristics and extend LEDs operating temperature range several solutions have been proposed in recent literature, such as, the usage of various inorganic glasses as matrices for phosphors, crystallizing phosphors directly in molten glass precursors or synthesizing transparent ceramic phosphor plates [4].

In this work phosphate glasses with different compositions were synthesized. The glass precursors and luminescent materials were ground and mixed together, melted in muffle furnace: molten liquid was poured into premade molds and heated again at lower temperatures to relieve internal stress. As obtained samples were polished and characterized by x-ray diffractometry, scanning electron microscopy, Raman spectroscopy, photoluminescence measurements and inductively coupled plasma optical emission spectrometry.

References

1. S. Nakamura, M. Senoh et al. *Japanese Journal of Applied Physics*, InGaN-Based Multi-Quantum-Well-Structure Laser Diodes, 1996, 35, L74-L76.
2. J. J. Wierer, J. Y. Tsao, D. S. Sizov, *Laser & Photonics Reviews*, Comparison between blue lasers and light-emitting diodes for future solid-state lighting, 2013, 7, 963-993.
3. M.H. Chang, D. Das, et al. *Microelectronics Reliability*, Light emitting diodes reliability review, 2012, 52, 762-782.
4. H. Lin, T. Hu, et al. *Laser & Photonics Reviews*, Glass Ceramic Phosphors: Towards Long-Lifetime High-Power White Light-Emitting-Diode Applications-A Review, 2018, 12, 1700344.

Vanillin Derivatives as Resins for Optical 3D Printing

A. Navaruckiene[1], E. Skliutas[2], M. Malinauskas[2], J. Ostrauskaite[1]*
[1]*Department of Polymer Chemistry and Technology, Kaunas University of Technology*
[2]*Laser Research Center, Faculty of Physics, Vilnius University*
**e-mail: jolita.ostrauskaite@ktu.lt*

ABSTRACT

3D printing, also known as additive manufacturing has drawn increasing attention globally and has made a revolutionary impact on product fabrication in such areas like food industry, textiles, architecture, medicine, and construction [1]. Polymers are widely used in our everyday life due to their diverse properties and relatively low cost; however, it is difficult to form intricate geometries from them. Additive manufacturing is a solution to create complex geometries from plastics [2].

In this study, the cross-linked polymers were obtained by free-radical photocross-linking of vanillin diacrylate and vanillin dimethacrylate using ethyl(2,4,6-trimethylbenzoyl) phenylphosphinate as photoinitiator. The chemical structure of obtained polymers was confirmed by FT-IR spectroscopy. The yield of insoluble fraction obtained after Soxhlet extraction with acetone after 24 hours was in the range of (77-96) %. The cross-linking density calculated from the real-time photorheometry storage modulus curve at the steady state was in the range of (49-7928) mol/m^3. Thermal and mechanical properties of vanillin diacrylate-based and vanillin dimethacrylate-based polymer films were investigated.

Real-time photorheometry was used to monitore the evolution of free-radical photocross-linking process. The tests were performed on a MCR302 rheometer from Anton Paar equipped with the plate/plate measuring system. The samples were irradiated by UV/Vis light in a wavelength range of 250-450 nm through the glass plate using UV/Vis spot curing system OmniCure S2000, Lumen Dynamics Group Inc. The sufficient amount of photoinitiator was determined by comparing compositions containing 1-5 mol.% of photoinitiator. In most cases photopolymerization was faster and more rigid polymers were obtained when 3 mol.% of ethyl(2,4,6-trimethylbenzoyl) phenylphosphinate were used. The most rigid polymers were obtained by free-radical photocross-linking of vanillin dimethacrylate, however its films were fragile.

Optical printing techniques, direct laser writing and microtransfer molding, were used to produce 3D objects out of vanillin diacrylate-based photocross-linkable resin. A test to assess the optimal fabrication parameters was performed and the capability to produce 3D microporous 75 × 75 μm^2 woodpile structures out of the resin via direct laser writing was demonstrated. 3D printed objects of vanillin diacrylate-based resin with 3 mol.% of ethyl(2,4,6-trimethylbenzoyl) phenylphosphinate corresponded to the used 3D model.

Acknowledgements
Financial support from EU ERDF, through the INTERREG BSR Programme, (ECOLABNET project #R077) is gratefully acknowledged.

References
1.J. Liu, L. Sun et al. *Carbohydrate Polymers*, Current advances and future perspectives of 3D printing natural-derived biopolymers, 2019, 207, 297-316.
2.N. Li, S. Huang et al. *Journal of Materials Science & Technology*, Progress in additive manufacturing on new materials: A review, 2019, 35, 242–269.

Characterization of Sm-Doped $BiFeO_3$ Ceramics Crystal Structure and Magnetization Across the Phase Boundary Region

A. Pakalniškis[1*], A. Kareiva[1], G. Niaura[2], D. Karpinsky[3], S. Latushka[3], M. Kaya[4], R. Skaudžius[1]

[1]*Institute of Chemistry, Vilnius University, Naugarduko 24, LT-03225 Vilnius, Lithuania*
[2]*Institute of Chemical Physics, Faculty of Physics, Vilnius University, Sauletekio Ave. 9, LT-10222, Vilnius Lithuania*
[3]*Scientific-Practical Materials Research Centre of NAS of Belarus, 220072 Minsk, Belarus*
[4]*Ankara University, Institute of Accelerator Technologies, 06830, Golbasi, Ankara, Turkey*
andrius.pakalniskis@chgf.vu.lt

ABSTRACT

Chemical substitution of bismuth ions by rare-earth elements (La - Sm) causes the structural transition from the polar rhombohedral phase (described by the space group *R3c, R-phase*) to the non-polar orthorhombic phase (s.g. *Pnma, O_1-phase*) via stabilization of $PbZrO_3$-like anti-polar orthorhombic phase (*O_2-phase*) [1,2]. The concentration ranges of the structural stability of the rhombohedral and the anti-polar orthorhombic phases strongly depend on the type of rare-earth element and the reduction in the ionic radius of the dopant ions leads to a shrinkage of the mentioned ranges [3]. The concentration range attributed to the anti-polar orthorhombic phase reduces down to 1% in the system $Bi_{1-x}Sm_xFeO_3$, while a chemical doping with rare earth elements having ionic radius smaller than that specific for samarium ions leads to a structural transition directly to the non-polar orthorhombic phase [4,5]. Chemical doping with samarium ions attracts particular attention due to very narrow concentration range ascribed to the single phase anti-polar orthorhombic state. It is known that the concentration ranges attributed to the phase coexistence regions can be modified using different synthesis methods and preparation conditions thus allowing a stabilization of relaxor -type ferroelectric behavior and/or diluted magnetic structure [3,6]. In the case of Sm-doping the concentration range ascribed to structural stability of the antipolar orthorhombic phase becomes extremely dependent on the preparation conditions and post synthesis treatment of the samples [1].

It should be noted that a formation of the metastable structural state in the compounds having frustrated ferroic orders opens up new possibilities for applications of the $BiFeO_3$-based multiferroic materials. In the present study, we report on the correlation between the type of structural distortion, morphology of crystallites and an onset of remanent magnetization for Sm-doped $BiFeO_3$ compounds prepared by different methods. In contrast to the structural results obtained for the solid-state ceramics the single-phase state with anti-polar orthorhombic structure is not stabilized in the compounds under study. The compounds having single phase rhombohedral structure are characterized by a notable release of remanent magnetization in contrast to the solid-state compounds having the same chemical compositions.

Acknowledgements
The work has been done in frame of the project TransFerr. This project has received funding from the European Union's Horizon 2020 research and innovation programme under the Marie Sklodowska-Curie grant agreement No. 778070.

References

1. I. O. Troyanchuk, et al. *J. Am. Ceram. Soc,* Phase Transitions, Magnetic and Piezoelectric Properties of Rare-Earth-Substituted $BiFeO_3$ Ceramics. 2011, 94, 4502–4506.
2. D. A. Rusakov, et al. *Chem. Mater.* Structural evolution of the $BiFeO_3$ - $LaFeO_3$ system, 2011, 23, 285–292.
3. D. Arnold, *IEEE Trans. Ultrason. Ferroelectr. Freq. Control,* Composition-driven structural phase transitions in rare-earth-doped $BiFeO_3$ ceramics: A review, 2015, 62, 62–82.
4. S.Karimi, Reaney, et al. *J. Mater. Sci,* Crystal chemistry and domain structure of rare-earth doped $BiFeO_3$ ceramics, 2009, 44, 5102–5112.
5. M. Kubota, et al. *Jpn. J. Appl. Phys,* Sequential Phase Transitions in Sm Substituted $BiFeO_3$, 2011, 50.
6. D. V. Karpinsky, et al. *Nanomaterials,* Peculiarities of the Crystal Structure Evolution of $BiFeO_3$–$BaTiO_3$ Ceramics across Structural Phase Transitions, 2020, 10, 801.

Bacterial Inactivation Using WO_3 Photoanode for Production of Reactive Chlorine Species in Situ

M. Parvin[1,*], M. Petrulevičienė[1], I. Savickaja[1], B. Šebeka[1], A. Naujokaitis[1], V. Pakštas[1], A. Gegeckas[2], J. Virkutis[2], J. Juodkazytė[1]

[1]Center for Physical Sciences and Technology, Saulėtekio av. 3, LT-10257 Vilnius, Lithuania
[2]Life Sciences Center, Vilnius University, Saulėtekio av. 7, LT-10257 Vilnius, Lithuania
e-mail: maliha.parvin@ftmc.lt

ABSTRACT

Reactive chlorine species (RCS) such as hypoclorous acid (HOCl), hypochlorite ion (ClO^-) and chlorine radicals ($Cl^•$, $Cl^{•-}$) have been used for disinfection of drinking water, swimming pools, and waste water due to their proper oxidation power. Recently, tungsten trioxide (WO_3) has attracted the attention of researchers as antimicrobial material also suitable for air purification, pollutants degradation, etc. [1, 2]. Herein, we investigated photoelectrochemical (PEC) production of RCS using WO_3 photoanode and the applicability of PEC chlorination for microbial inactivation under visible light irradiation.

Coatings of WO_3 on fluorine-doped tin oxide (FTO) substrate were formed by sol-gel method. Different reducing agents, deposition times and annealing temperatures were applied to investigate the effect of photoelectrochemical activity and properties of WO_3 photoanodes. The coatings were characterized using X-ray diffraction (XRD), scanning electron microscopy (SEM), thermogravimetric (TG), differential scanning calorimetry (DSC) analysis. Photoelectrochemical behavior was investigated by cyclic voltammetry (CV), electrochemical impedance spectroscopy (EIS) and chronoamperometry (CA). PEC chlorination was performed in a two-electrode cell in NaCl solution. After photoelectrolysis, faradaic efficiency (FE) of photoelectrochemical ClO^- generation was evaluated with the help of iodometric titration. The FE was found to decrease with duration of electrode exploitation (Fig. 1). Antimicrobial effect of PEC chlorination with sol-gel derived WO_3 photoanodes was successfully demonstrated in suspensions of Gram-positive Bacillus spp. and Gram-negative E.coli bacteria strains in NaCl electrolyte.

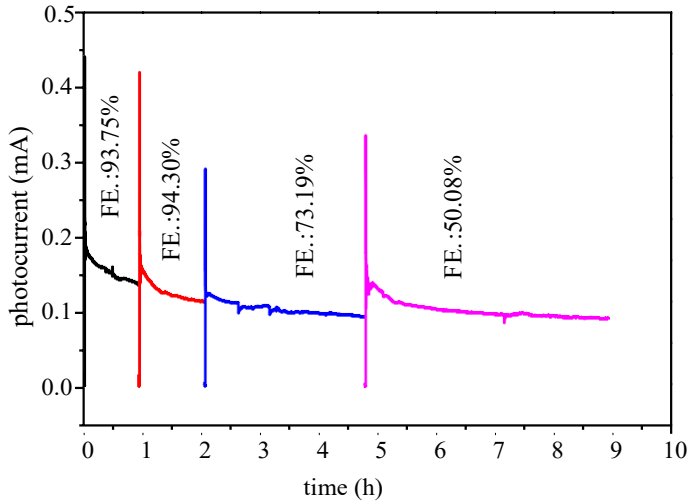

Fig. 1. Chronoamperograms of WO_3 photoanode recorded consecutively in a two-electrode cell in 0.05 M NaCl at voltage of 1.6 V under illumination (~100 mW cm^{-2}); values of faradaic efficiency of ClO^- production from photoelectrochemical Cl^- oxidation are indicated for each experiment; WO_3 coating was prepared using isopropanol as reductant, applying 180 min deposition time and 400°C annealing temperature.

References

1. M.S. Koo, X. Chen, K. Cho, T. An, et al. *Environmental science & technology*, In situ photoelectrochemical chloride activation using a WO_3 electrode for oxidative treatment with simultaneous H_2 evolution under visible light. 2019, *53*, 9926-9936.
2. C.C. Mardare, & A.W. Hassel, A. W. *physica status solidi (a)*, Review on the versatility of tungsten oxide coatings. 2019, *216*, 1900047.

Scanning Electrochemical Microscopy as a Tool for Targeted Electroporation Modeling

M. Poderytė*, I. Gabriūnaitė, A.Valiūnienė
Faculty of Chemistry and Geosciences, Vilnius University, Naugarduko str. 24, Vilnius, Lithuania
margarita.poderyte@chgf.stud.vu.lt

ABSTRACT

Scanning electrochemical microscopy (SECM) is a technology in which a current flowing through a very small electrode (usually an ultramicroelectrode with a working surface diameter of no more than 25 µm) is used to characterize the properties of a substrate (analyte) immersed in a solution. SECM maintains the great interest of biomedical scientists' investigations since the environment of the experiments can be easily biocompatible[1].

The plasma membrane is a complex system that is responsible for vital cellular functions. Membranes have a selective permeability that can be modified[2]. One of the modification methods is electroporation - a physical method in which cells are exposed to a strong electrical pulse (about 1 kV cm^{-1}), as a result of which temporary or permanent pores are formed in the phospholipid layer. Electro-permeabilization can be applied for introduction of small organic compounds into microorganisms, electroporation is applied in medical practice for cancer treatment, food industry[3]. The use of high voltages affects sensitive biological systems, so it is especially important to look for alternative electroporation models. Although electroporation is already used in practice certain studies on the size of the pores formed and the time of pore closure are still relevant[4].

In this work scanning electrochemical microscope in feedback mode is used to investigate and modificate hybrid bilayer membrane (prepared using the vesicle fusion method from 1,2-dioleoyl-sn-glycero-3-phosphocholine (DOPC) and cholesterol in phosphate buffer solution (PBS)) formed on a glass plate coated with a layer of tin oxide doped with fluorine atoms (FTO). Through targeted UME approach experiments a non-polarized hBLM is recorded and then modified (Fig. 1) using a relatively low voltage (under 2 V vs Ag/AgCl reference electrode). Using SECM scanning mode, surface changes has been visualized after the electroporation and it was determined that a pore has been formed exactly below the working electrode.

Another goal is to apply this electroporation model to living cells. Yeast cells is one of the simplest eukaryotic organisms, but many important cellular processes in yeast and human cells are the same, so they can be used as a model to study human cells. It was demonstrated that the approach curves to live yeast cells and dead are different. This leads to promising experiments in which SECM can be successfully applied to electroporate live yeast cells and to capture the changes in them.

Such research is particularly important in medicine because, even though electroporation is already used in practice, it is still a random and incompletely controlled process.

This project has received funding from the European Social Fund (project number [09.3.3.-LMT-K-712-22-0045] under a grant agreement with the Research Council of Lithuania (LMTLT)

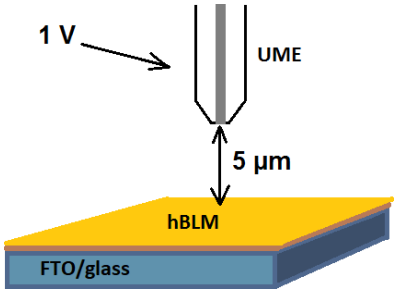

Fig. 1. Scheme of electroporation process using SECM

References

1. Daniel, M. (2012). Micro- and Nanopatterning Using Scanning Electrochemical Microscopy. Scanning Electrochemical Microscopy, Second Edition, 489–524.
2. D.C. Chang, Reviews in Cell Biology and Molecular Medicine, John Wiley & Sons, New York, 2006
3. R. Stampfli, Reversible electrical breakdown of the excitable membrane of a Ranvier node. Ann. Acad. Brasil. Ciens. 30, 57–63 (1958)
4. Valiuniene, I. Gabriunaite, M. Poderyte, A. Ramanavicius. Electroporation of a hybrid bilayer membrane by scanning electrochemical microscope. Bioelectrochemistry 2020, 2020

In Vitro Comparison of Different Cement Remnant Removal Efficiency on Dental Implant - Supported Restorations

I.Povilavičius
email: ignasp1998@gmail.com

ABSTRACT

Objectives: The aim of this study was to evaluate the amount of excess cement after cementation and cleaning of implant-supported restorations with different cements.

Material and methods: The same amount of metal-ceramic crowns was luted to prosthetic abutments with three different cements: resin modified glass ionomer, zinc-oxide eugenol and zinc phosphate cement, excess cement was cleaned and restorations were removed to evaluate the amount of undetected cement. All quadrants were photographed and ratios between the cement remnants area and total area were evaluated using Adobe Photoshop.

Results: Results showed significant increase of undetected cement between the groups when resin modified glass ionomer cement was used ($p < 0,05$).There was no significant difference between zinc phosphate cement and zinc-oxide eugenol cement.

Groups	p
1 and 2	p=0.092
1 and 3	p=0,001
2 and 3	p=0.001

Table 1. Mann - Whitney U test results.

Conclusions: The removal efficiency of residual cement after cementation depends on type of cement used. Resin modified glass ionomer cement is more difficult to remove than zinc-oxide eugenol and zinc phosphate cement.

References

1.Linkevicius T, Vindasiute E, Puisys A, Linkeviciene L, Maslova N, Puriene A. The influence of the cementation margin position on the amount of undetected cement. A prospective clinical study. Clinical oral implants research. 2012; 24(1): 1-6 10.

2.Linkevicius T., Puisys A., Vindasiute E. Linkeviciene L. Does residual cement around implant-supported restorations cause peri-implant disease? A retrospective case analysis.Clinical Oral Implants Research, November 2013, Vol.24(11), pp.1179-1184

3.Patel B, Patel V, Ramesh TR, Soundharya A. Effect of modified cementation technique on marginal fit and apical spread of excess cement for implant restorations: An in vitro study. Journal of Dental Research and Review. 2016; 3(1): 8-13.

Design of Manganese Oxide Sorbents for Selective Strontium Radionuclide Removal

V.G. Prozorovich, A.I. Ivanets, T.F. Kouznetsova
Institute of General and Inorganic Chemistry of National Academy of Sciences of Belarus, st. Surganova 9/1, 220072 Minsk, Belarus
e-mail: vladimirprozorovich@gmail.com

ABSTRACT

Liquid radioactive waste (LRW) generated during the operation of nuclear power facilities poses a great danger to the public and the environment [1]. This determines the relevance of the development of effective materials and technologies for the removal and immobilization of radionuclides. The long half-life of ^{90}Sr and its ability to replace calcium ions in the tissues of living organisms make it one of the most dangerous components of LRW [2]. Due to the complex composition of real LRW and low concentration of ^{90}Sr radionuclide, the problem of their purification can be solved using highly selective sorbents [3].

In this paper, manganese oxide sorbents of ^{90}Sr radionuclide were developed. The synthesis of the sorbents was carried out in a controlled reduction of potassium permanganate in aqueous solution. A comprehensive study of the effect of synthesis conditions on the physical and chemical characteristics of manganese oxides was carried out. The influence of the nature of the reducing agent (hydrogen peroxide, manganese(II) salt, ethanol and polyvinyl alcohol) and their concentration on the phase and chemical composition, the parameters of the crystalline and porous structure of sorbents was studied. The possibility of directional regulation of structural and phase organization of the manganese oxides by ion-exchange introduction of cations (K^+, Na^+, Mg^{2+} and Ca^{2+}) with different sizes into the interlayer space of the birnessite with its subsequent heat treatment at 200-600 °C was shown [4].

The study of sorption and selective characteristics of manganese oxides on model solutions containing background electrolytes (0.15-1.30 M Na^+ and 0.01-0.10 M Ca^{2+} ions), characterized by pH of 2.0-12.0, as well as modeling the composition of seawater with salinity of 5.0-50.0 g/L was carried out. The distribution coefficient, static exchange capacity and Sr/Ca ions separation coefficient were calculated on the basis of experimental data as criteria for evaluating the efficiency of the developed sorbents [5].

Thus, the conducted studies allowed to establish the relationship between the synthesis conditions – physical and chemical properties – sorption and selective characteristics of manganese oxide sorbents for selective strontium radionuclide removal, as well as the main factors affecting on their selectivity was determined.

Acknowledgments. The authors are grateful to Vitaly V. Milyutin, head of the laboratory of chromatography of radioactive elements of Frumkin Institute of Physical chemistry and Electrochemistry Russian academy of science, and to Artem V. Radkevich, scientific secretary of The State Scientific Institution «The Joint Institute for Power and Nuclear Research – Sosny» of the National Academy of Sciences of Belarus for their help in performing of sorption experiment.

References

1. J. Iqbal, F.M. Howari et al. Pollution Assessment for Sustainable Practices in Applied Sciences and Engineering, Chapter 20 - Assessment of radiation pollution from nuclear power plants, 2021, 1027-1053.
2. S. Pors Nielsen. *Bone*, The biological role of strontium, 2004, 35 (3), 583-588.
3. D. Alby, C. Charnay et al. *Journal of Hazardous Materials*, Recent developments in nanostructured inorganic materials for sorption of cesium and strontium: Synthesis and shaping, sorption capacity, mechanisms, and selectivity - A review, 2018, 344, 511-530.
4. A.I. Ivanets, V.G. Prozorovich, T.F. Kouznetsova, A.V. Radkevich, A.M. Zarubo. *Environmental Nanotechnology, Monitoring & Management*, Mesoporous manganese oxides prepared by sol-gel method: Synthesis, characterization and sorption properties towards strontium ions, 2016, 6, 261-269.
5. A.I. Ivanets, V.V. Milutin, V.G. Prozorovich, T.F. Kouznetsova, N.A. Nekrasova. *Journal of Radioanalytical and Nuclear Chemistry*, Adsorption properties of manganese oxides prepared in aqueous-ethanol medium toward Sr(II) ions, 2019, 321 (1), 243-253.

Carbonate in Amorphous Calcium Phosphate: Influence on Nanolevel Structuring

A. Pudule[1]*, L. Komarovska[1], K. Tonsuaadu[2], A. Viksna[3], K.A. Gross[1]
[1]Biomaterials Research Laboratory, Riga Technical University, Latvia; [2]School of Engineering, Tallinn University of Technology, Estonia; [3]Dept. of Analytical Chemistry, University of Latvia
e-mail: aiga-anna.pudule@rtu.lv

ABSTRACT

The ubiquitous carbonate ion and calcium phosphate are so commonplace in nature, but the effect of carbonate on stabilizing the amorphous calcium phosphate and further transitions remains unknown. This is especially interesting for calcium phosphates that may exist as apatites since different processing routes markedly influence the transition to nanostructures. The purpose is to investigate the chemical diversity of carbonated amorphous calcium phosphates and then investigate nanolevel structuring.

Amorphous calcium phosphate was synthesized with increasing amounts of carbonate to determine the extent of incorporation. Since carbonate is readily associated with calcium, increasing carbonate was directly related to the larger quantity in the double decomposition reaction between calcium nitrate hexahydate and ammonium phosphate. The larger inclusion was confirmed by more intense carbonate absorption peaks in Fourier transform infra-red spectroscopy. An amorphous phase identified by X-ray diffraction was stable for Ca/P ratios from 1.5 to 2.6.

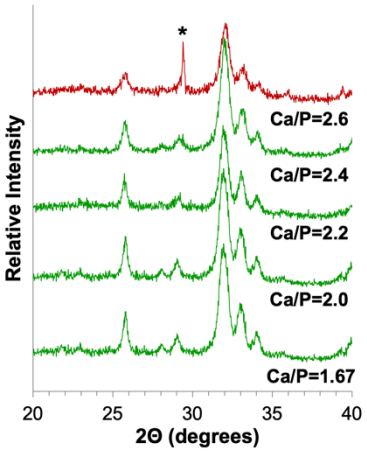

The amorphous phase was thermally crystallized in air at 700 °C and hydrothermally crystallized at 150 °C to determine nanostructuring. Structuring was investigated from looking at the evolved heat in a wide temperature sweep by thermal analysis and the assembled nanostructure characterized by X-ray diffraction. Hydrothermal treatment allowed for the largest chemical diversity in apatite up to a Ca/P molar ratio of 2.4, Fig. 1. Rietveld analysis showed 20nm sized domains. Heating in air destabilized the carbonate and an apatite structure was only retained up to a Ca/P ratio of 2. This corresponds to tetracalcium phosphate that has previously been structured as apatite.

Fig. 1. Hydrothermal processing retains an apatite up to a Ca/P molar ratio of 2.4. More carbonate produces a calcium carbonate (shown as an asterisk).

Carbonate can be integrated into amorphous calcium phosphate at a higher concentration than in crystalline phases. The process path influences the degree of inclusion in a crystalline phase. Nanostructuring in hydrothermal conditions allows for more carbonate inclusion than heating in air.

Formation of Various TiO_{2-X} Nanostructures for Application in Biomedicine

S. Ramanavicius[1]*, A. Naujokaitis[1], A. Jagminas[1]
[1]State research institute Center for Physical Sciences and Technology, Vilnius, Lithuania
** simonas.ramanavicius@ftmc.lt*

ABSTRACT

Titanium dioxide (TiO_2) nanomaterials are known for their numerous and diverse applications from common daily products to biomedicine. To extend TiO_2 application there is a high interest in synthesis of titanium suboxide structures (Ti_xO_y) with new properties. Thus, there is a high demand for a simple and efficient method for the production of new materials with desirable properties [1,2].

This research is dedicated to show a simple technology for formation of controllable composition titanium suboxides from aqueous solutions to extend materials of titanium oxide applications. It was investigated that our formed nanostructures have strong hydrophilic properties as well as significantly lower bandgap and nanoplatelet-shaped morphology. In order to prove the formation of suboxides, EPR and XRD were employed. Ellipsometry was used to measure thickness and calculate band gaps of the films. The modeling was also used to calculate porosity of structures showing it is nearly 80%. This parameter could be useful for application of such structures for various implants and other biomedical applications.

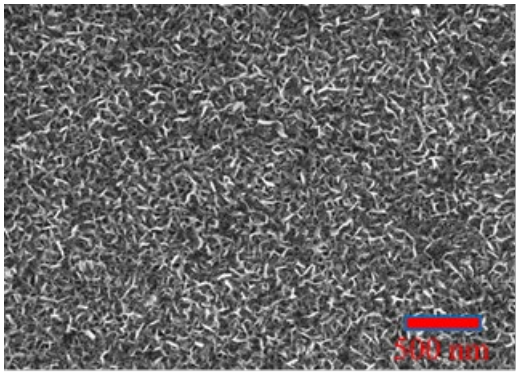

Fig. 1. Scanning electron microscope image of nanoplatelet-shaped titanium suboxide thin film.

References

1.X. Chen, et al. *Chem. Rev*. Titanium Dioxide Nanomaterials: Synthesis, Properties, Modifications, and Applications, 2007, 107, 2891-2959.
2.Jagminas, et al. *RSC Adv.* Hydrothermal synthesis and characterization of nanostructured titanium monoxide films, 2019, 9, 40727-40735.

Investigation of Thermally Reduced Graphene Oxide and its Application in Amperometric Third Generation Biosensors

G. Rimkutė[1*], J. Razumienė[2], J. Barkauskas[1], J. Gaidukevič[1], I. Šakinytė[2], V. Gurevičienė[2]

[1]Institute of Chemistry, Faculty of Chemistry and Geosciences, Vilnius University, Lithuania
[2]Institute of Biochemistry, Life Sciences Center, Vilnius University, Lithuania
gintare.rimkute@chgf.stud.vu.lt

ABSTRACT

In the last decade, graphene-related materials have been intensively investigated due to their excellent properties. One of the most remarkable carbon nanomaterials is graphene oxide, which can be described as chemically modified graphene containing a range of reactive oxygen functional groups such as epoxides, hydroxyl, carbonyl and carboxyl groups. This functionalized graphene has a lot of applications and can be used in supercapacitors, batteries, water decontamination systems, bioceramic-based composites, drug delivery agents, biosensors and much more [1-4].

In this work, the focus was directed toward the use of functionalized graphene in biosensors. Using modified graphene could help to create third-generation biosensors based on direct electron transfer (DET) between the enzyme and the electrode. Design of the analytical systems acting on DET principle do not require any intermediate mediating materials, so biosensors created by this technology are becoming simpler in design and more cost-effective [5].

The purpose of this work was to synthesize and analyse fractions of thermally reduced graphene oxide (TRGO) and to use them in construction of third-generation biosensors based on pyrroloquinoline quinone-dependent glucose dehydrogenase (PQQ-GDH) from *Acinetobacter calcoaceticus* sp. While PQQ-GDH possesses substrate specificity to wide range of carbohydrates, the enzyme could be very promising for creation of new technologies for investigation of diseases related to release of carbohydrates.

Using modified Hummers‘ method graphite oxide (GO) was synthesized and thermally reduced, thus obtaining three fractions of TRGO (TRGO1, TRGO2, TRGO3). Properties of carbon materials were characterised by Raman spectroscopy, thermogravimetric (TGA), x–ray diffraction (XRD) and Brunauer–Emmett–Teller (BET) analysis. The amperometric biosensors were constructed using membranes made from PQQ-GDH immobilised into the layer of carbon material. DET was implemented only using TRGO fractions and biosensor with TRGO2 was the most effective with sensitivity 77.7±3.8 $\mu A \cdot mM^{-1} \cdot cm^{-2}$. TRGO2 had the largest surface area (708.0±0.3 $m^2 \cdot g^{-1}$), the highest number of defects and optimal number of functional groups, which determined the highest sensitivity of this biosensor. Other characteristics of proposed biosensors, such as limit of detection (LOD) and stability were determined as well.

ACKNOWLEDGEMENTS:
This project has received funding from European Social Fund (project No [09.3.3-LMT-K-712- 16-0125]) under grant agreement with the Research Council of Lithuania (LMTLT).

References

1. M. P. Lavin-Lopez, A. Patón-Carrero, N. Muñoz-Garcia, V. Enguilo, J. L. Valverde, A. Romero. *Colloids Surfaces A*, The influence of graphite particle size on the synthesis of graphene-based materials and their adsorption capacity, 2019, 582, 123935.
2. M. Kralj, A. Supina, D. Čapeta, I. Sović, I. Halasz. *Materialia*, Mechanochemical oxidation of graphite for graphene-hydrogel applications: Pitfalls and benefits, 2020, 14, 100908.
3. Z. Li, W. Zhu, S. Bi, R. Li, H. Hu, H. Lin, R.S. Tuan, K.A. Khor. *Journal of Biomedical Materials Research*, Incorporating silica-coated graphene in bioceramic nanocomposites to simultaneously enhance mechanical and biological performance, 2020, 108, 1016–1027.
4. O. C. Compton, S. T. Nguyen. *Small,* Graphene oxide, highly reduced graphene oxide, and graphene: Versatile building blocks for carbon-based materials, 2010, 6, 711–723.
5. Šakinyte, J. Barkauskas, J. Gaidukevič, J. Razumiene. *Talanta*, Thermally reduced graphene oxide: The study and use for reagentless amperometric d-fructose biosensors, 2015, 144, 1096–1103.

The Formation and Thermal Stability of Mayenite

K. Ruginytė[1]*, A. Eisinas[1]
Department of Silicate Technology, Faculty of Chemical Technology, Kaunas University of Technology, Radvilenu road 19, LT–50270 Kaunas, Lithuania
kristina.ruginyte@ktu.edu

ABSTRACT

Calcium aluminate as a biomaterial has been studied since the beginning of the 1990s in relation to its physical and mechanical properties, as well as its biocompatibility [1]. Mayenite ($C_{12}A_7$), one of calcium aluminate minerals with CaO/Al_2O_3 =1.7, has stimulated the research interest because of its better accelerator effect-rapid hardening activity, oxygen mobility, ionic conductivity and catalytic properties in comparison with the other calcium aluminates [2]. $C_{12}A_7$ hydration exhibits an induction period of a few minutes during which pastes have suitable rheological properties and remain workable. Besides, the setting can be controlled by adding additives to the blend and the resulting hydrated cements have shown to be biocompatible in vivo and in vitro [3]. Mayenite can be synthesized through solid state reaction, however, the main disadvantages is a very high calcination temperature (1300–1500 °C), low surface area, low porosity. Sol–gel procedure increases the operation cost due its complexity, the use of energy at different synthesis steps and the required precursor, which has to be calcined in a 600–900°C temperature range. Another method of $C_{12}A_7$ preparation is a hydrothermal synthesis of precursors, which is followed by the thermal treatment at temperatures ranging from 25 to 1000 °C. It was determined that this method allows to synthesize $C_{12}A_7$ powders with relatively high specific surface area [4]. For this reason, the main objective of the present work is to determine the formation and thermal stability of mayenite by using two steps synthesis in a 25 – 1150 °C temperature range.

In this paper, the following reagents were used: calcium oxide from $Ca(OH)_2$ was additionally burned at 550 °C temperature for 1.5 h, the quantity of free CaO is equal to 92 wt. %. γ-Al_2O_3 was produced by burning aluminium hydroxide at 475 °C for 4 hours. Dry primary mixture with molar ratio of CaO/Al_2O_3 = 2.8 was mixed with water to reach the water/solid ratio (W/S) of the suspension equal to 10.0. The hydrothermal synthesis was carried out in unstirred suspensions, in “Parr instruments” (Germany) autoclave, under saturated steam pressure at 130 °C temperature for 1-72 hours (the temperature was reached within 2 h). After hydrothermal treatments, the autoclave was quenched to a room temperature. The suspensions after synthesis were filtered, products rinsed with acetone to prevent carbonization of materials, dried at 50 °C ± 5 temperature for 24 h, and sieved through a sieve with a size width of 60 μm. In-situ XRD analysis was made with a high-temperature camera MTC-hightemp (Bruker AXS, Karlsruhe, Germany).

It was found that, in unstirred $CaO–Al_2O_3$ suspensions, when CaO/Al_2O_3 molar ratio of primary mixture was equal to 2.8, within 1 hour of isothermal curing at 130 °C, katoite, was formed. Also, the basic reflections of partially unreacted gibbsite were observed in X-ray diffraction patterns. Moreover, the carbonation appeared, when the products and/or partially unreacted primary components were dried in an air conditioned chamber (50 °C, 24 h), because the diffraction peaks characteristic to calcium monocarboaluminate. After 4 h of hydrothermal treatment, XRD analysis data showed that gibbsite was fully reacted and more intensive diffraction maximums characteristic to katoite were observed. The thermal stability of products obtained after 4 h of isothermal curing was investigated in a high-temperature camera MTC-hightemp in a 25–1150 °C temperature range. It was evidenced that katoite is stable till 275 °C. At higher temperature (350 °C) katoite is fully transformed in to mayenite. It should be underlined that due to different CaO/Al_2O_3 molar ratio between katoite (3) and mayenite (1.72), reflection patterns of calcium oxide were identified in the products. It was determined that the crystallinity of mayenite increased by increasing temperature till 1150 °C.

References

1. R.M. Parreira et al. *Ceramics International*, Calcium aluminate cement-based compositions for biomaterial applications, 2016, 42, 11732–11738
2. L. Hermansson, *Journal of the Korean Ceramic Society*, A Review of Nanostructured Ca-aluminate Based Biomaterials within Odontology and Orthopedics, 2018, 55, 95–107
3. W.T. Barbosa et al. *Ceramics International,* New cement based on calcium and strontium aluminates for endodontics, 2019, 45, 19784-19792
4. K. Karim et al. *Journal of Wuhan University of Technology-Mater*, Low Temperature Synthesis of Nano Porous $12CaO{\cdot}7Al_2O_3$ Powder by Hydrothermal Method, 2016, 1201–1205.

Electrochemical Synthesis of Dendritic Gold Nanostructures and Application for the Development of Glucose Biosensor

L. Sakalauskiene[1], A. Popov[1], A. Kausaite-Minkstimiene[1], A. Ramanaviciene[1]

[1]NanoTechnas–Center of Nanotechnology and Materials Science, Faculty of Chemistry and Geosciences, Vilnius University Vilnius, Lithuania

e-mail: laura.sakalauskiene@chgf.vu.lt

ABSTRACT

An important task for modern medicine is achieving comprehensive and accurate diagnosis of diseases. The new medical diagnostic achievement – bioanalytical methods and biosensors could help to solve the analytical problems. Nanoscience and nanotechnology breakthroughs have a high impact on the different fields of science, including analytical and bioanalytical chemistry, medicine and pharmacy. Gold micro- and nano-structures have received considerable attention due to their attractive physical and chemical properties [1]. Immobilization of glucose oxidase (GOx) on the gold nanoparticles allows to improve stability and sensitivity of glucose biosensors. These biosensors exhibited a high selectivity and can be used for the glucose detection in the blood even in the presence of other electrochemically active substances. Additionally, gold nanoparticles are biocompatible, can ensure good enzymatic activity and higher GOx uploading on the same electrode surface using different immobilisation methods [2,3].

In this work the optimal conditions for electrochemical synthesis of dendritic gold nanostructures on the graphite rod electrode were determined. Different GOx immobilisation methods – adsorption and covalent immobilisation through self-assembled monolayer without and with cross-linking, were applied for the development of electrochemical glucose biosensor. All electrochemical measurements were performed with a computerized potentiostat/galvanostat PGSTAT 30/Autolab (EcoChemie, Netherlands) with GPES 4.9 using three-electrode system. Glucose biosensor based on GOx covalently immobilised on DGNs/GR electrode surface modified with 11-mercaptoundecanoic acid possesses better stability, higher sensitivity, and lower limit of detection.

Acknowledgment

This research was funded by a grant (No. S-LU-20-11) from the Research Council of Lithuania.

References

1. N. Li, P. Zhao, D. Astruc. *Angew. Chem. Int. Ed.,* Anisotropic gold nanoparticles: synthesis, properties, applications, and toxicity, 2014, 53, 1756-1789.
2. N. German, A. Ramanavicius, A. Ramanaviciene. *Sensor Actuat. B: Chem,* Electrochemical deposition of gold nanoparticles on graphite rod for glucose biosensing, 2014, 203, 25–34.
3. N. German, A. Kausaite-Minkstimiene, A. Ramanavicius, T. Semashko, R. Mikhailova, A. Ramanaviciene. *Electrochim. Acta,* The use of different glucose oxidases for the development of an amperometric reagentless glucose biosensor based on gold nanoparticles covered by polypyrrole, 2015, 169, 326-333.

Effect of Mn Doping on Hydrolysis of Low-Temperature Synthesized Metastable Alpha-Tricalcium Phosphate

L. Sinusaite*, A. Kareiva, A. Zarkov
Institute of Chemistry, Vilnius University, Naugarduko St. 24, LT-03225 Vilnius, Lithuania
e-mail: lauryna.sinusaite@chgf.vu.lt

ABSTRACT

Calcium phosphates (CPs) are the main constituents of human hard tissues like bone and teeth. They are getting a lot of attention in medicine and dentistry as bone regenerating materials because of their positive *in vivo* responses like biocompatibility, bioactivity, osteoconductivity and relatively low cost [1]. α-Tricalcium phosphate ($Ca_3(PO_4)_2$, α-TCP) belongs to biomaterials and used in regenerative medicine in cement form due to its excellent resorbability and osteoconductivity. The solubility of α-TCP is intermediate between orthophosphates, however α-TCP hydrolyze to calcium deficient hydroxyapatite ($Ca_{10-x}(PO_4)_{6-x}(HPO_4)_x(OH)_{2-x}$, CDHA), which is similar to bone hydroxyapatite [2].

It is well known that partial substitution by other bioactive ions into the CP lattice can influence not only structural changes and morphology, but also important biological properties like bioactivity, biocompatibility, solubility and kinetics of ion release [3]. Manganese has proven to be important element in promoting various vital processes such as metabolism and formation of bones. Research has also showed that Mn^{2+} enhances the ligand binding affinity on integrin, activates cell adhesion and increases osteoblast adhesion [4, 5].

In this study, effect of Mn doping on hydrolysis rate of low-temperature synthesized metastable α-TCP was investigated. Pristine and α-TCP powders containing 0.5 and 1 mol% of Mn^{2+} ions were synthesized by wet co-precipitation process. The crystal structure of synthesized compounds were evaluated by X-ray diffraction (XRD) analysis and Fourier-transform infrared spectroscopy (FTIR). Morphology of the initial and after fully hydrolyzed products was investigated using scanning electron microscopy (SEM). Chemical composition of the initial and after fully hydrolyzed products were analyzed by inductively coupled plasma optical emission spectrometry (ICP-OES).

It was demonstrated that presence of Mn^{2+} ions significantly retards hydrolysis of α-TCP. Pristine, 0.5 and 1 mol% Mn doped α-TCP fully hydrolyzed with a conversion to CDHA in 10 h, 20 h and 35 h, respectively. The results of elemental analysis confirmed that chemical composition of starting and fully hydrolyzed powders was identical, indicating that there is no selective ion release during hydrolysis process.

Acknowledgements
This project has received funding from European Social Fund (project No 09.3.3-LMT-K-712-19-0069) under grant agreement with the Research Council of Lithuania (LMTLT).

References

1. G. Fernandez de Grado et al. J. Tissue Eng., Bone substitutes: a review of their characteristics, clinical use, and perspectives for large bone defect healing, 2018, 9, 1-18.
2. R.G. Carrodeguas et al. Acta Biomater., α-Tricalcium phosphate: synthesis, properties and biomedical applications, 2011, 7(10), 3536-3546.
3. Laskus et al. Int. J. Mol. Sci., Ionic Substitutions in Non-Apatitic Calcium Phosphates, 2017, 18, 2542.
4. T. Wu et al. *Mater. Sci. Eng. C,* Improving osteogenesis of calcium phosphate bone cement by incorporating with manganese doped b-tricalcium phosphate, 2020, 109, 110481.
5. P.M.C. Torres et al., *J. Inorg. Biochem.*, Effects of Mn-doping on the structure and biological properties of β-tricalcium phosphate, 2014, 136, 57-66.

Sol-Gel and Molten Salt Synthesis of Novel $Y_{3-2x}Ca_{2x}Ta_xAl_{5-X}O_{12}$ Garnet Structure Phosphors

M. Skruodiene[1]*, R. Juodvalkyte[2], G. Inkrataite[2], A. Sarakovskis[1], R. Skaudzius[2]
[1] *Institute of Solid State Physics, University of Latvia, Riga LV-1063, Latvia*
[2] *Institute of Chemistry and Geosciences, Vilnius University, Naugarduko 24, 03225, Vilnius, Lithuania*
e-mail: monika.skruodiene@cfi.lu.lv

ABSTRACT

There is a strong demand for the development of new inorganic luminescent materials which nowadays shows tremendous progress through physics, engineering, chemistry, biology and medicine. The growing need for LEDs and laser development by the human society demands environmentally friendly synthesis techniques, safe use and fabrication of low-cost novel multifunctional materials. One of the most suitable ways to solve this demand is to search for novel structure garnets and ceramics for versatile applications with controllable broad color tuning and improvement of quantum yield, thermal and radiation stability. The incorporation of garnet structure compounds into the glass ceramics is a good alternative for the conventional LEDs and laser diodes due to their potentially low manufacturing costs, high efficiency and ease of processing [1-3].

Yttrium aluminum garnet $Y_3Al_5O_{12}$ (YAG) doped with trivalent rare-earth ions shows optical, thermal and physical properties comparable to single-crystal rods, and currently is used in a wide variety of applications. The YAG ceramics is easier to fashion into shapes ideal for newly designed laser devices, and it can be less expensive to fabricate in large quantities. As is generally recognized that the lasing performance of single crystals is restricted. From the spectroscopic point of view, poly-crystalline transparent ceramics can substitute a single lasing crystal with extending capabilities. The increased compositional versatility of transparent ceramics enables tailoring improved laser materials. However, the optical properties of transparent ceramics strongly depend on their microstructure, which is a direct consequence of sintering [4-6].

In this research, two methods of synthesis are compared. Sol-Gel synthesis, is the most exploited method for the synthesis of metal oxides. This method is based on the hydrolysis, condensation, and polymerization reactions of metal precursors. Molten Salt synthesis, the synthesis of metal oxides, which involves the use of molten salt as the medium for preparing complex oxides from their constituent materials [7,8].

References

1. B. P. de Sousa, L. M. Marcondes et al. *Materials Chemistry and Physics,* Phosphate glasses with high tantalum oxide contents: Thermal, structural and optical properties, 2020, 239, 121996.
2. L. M. Marcondes, S. H. Santagneli et al. *Journal of Alloys and Compounds,* High tantalum oxide content in Eu^{3+}-doped phosphate glass and glass-ceramics for photonic applications, 2020, 842, 155853.
3. Y. Tratsiak, Y. Bokshits et al, *Optical Materials*, $Y_2CaAlGe(AlO_4)_3$:Ce and $Y_2MgAlGe(AlO_4)_3$:Ce garnet phosphors for white LEDs, 2017, 67, 108–112.
4. Y. Tratsiak, Y. Bokshits et al, *Radiation Measurements,* Garnet-based complex substituted glass ceramic materials, 2019, 122, 97–100.
5. S. Hu, C. Lu et al,, *Ceramics International,* Transparent YAG:Ce ceramics for WLEDs with high CRI: Ce^{3+} concentration and sample thickness effects, 2016, 42. 6, 6935-6941.
6. M. Karabulut, E. Melnik et al, *Journal of non-Crystalline Solids*, Mechanical and Structural Properties of Phosphate Glass, 2001, 288, 8-17.
7. G. Blasse, B. C. Grabmaier, *Luminescent materials. Springer, Berlin, Heidelberg,* A general introduction to luminescent materials, 1994, 1-9.
8. D. E. Bugaris, H.-C. zur Loye, *Angewandte Reviews,* Materials Discovery by Flux Crystal Growth: Quaternary and Higher Order Oxides, 2012, 51, 3780 – 3811.

Microstructure and Corrosion Properties of Plasma Sprayed Al_2O_3 and Al_2O_3-TiO_2 Coatings

A. Šuopys[1] *, L. Marcinauskas[1], E. Griškonis[2], R. Kėželis[1], R. Uscila[1], M. Aikas[1]
[1]Lithuanian Energy Institute, Plasma Processing Laboratory, 3 Breslaujos, Kaunas LT44403, Lithuania
[2]Kaunas University of Technology, Department of Physical and Inorganic Chemistry
e-mail: airingas.suopys@lei.lt

ABSTRACT

Al_2O_3 is one of the most highly used bio ceramics due to its abundance, low cost and inherently low levels of reactivity compared with other materials such as polymers and metals as well as surface reactive or resorbable ceramics. In a human body, they are expected to be non-toxic, non-allergenic, and non-carcinogenic for a life-time, which leads to a corresponding range of engineering design philosophies for medical application [1]. It is possible to enhance desired qualities by using alumina as a basis for composite materials. Addition of titania is known to increase corrosion resistance and reduce porosity of the coating [2,3]. Plasma-spraying technique is currently used commercially to produce ceramic coatings on metallic implants [4].

In this research atmospheric plasma spraying (APS) was employed to deposit Al_2O_3, Al_2O_3-3%TiO_2, and Al_2O_3-13%TiO_2 coatings on the steel substrate. Ceramic coatings were formed by direct current plasma torch at atmospheric pressure using air-hydrogen plasma. Microstructural analysis of the as-sprayed coatings was carried out using scanning electron microscopy (SEM). Elemental analysis of the coatings was performed using energy-dispersive X-ray spectroscopy (EDS), and phase composition was analyzed using X-ray diffraction. The corrosion behaviors of the coatings were performed using potentiostat in 0.5M NaCl solution for 96 hours. The surface microstructure, elemental composition and phase composition of the coatings was re-examined after the corrosion tests. Results indicated that coatings had only insignificant changes in surface morphology - no defects or delamination were found after chemical resistance tests. More pronounced changes were observed in elemental composition, where due to appearance of sodium and chlorine, the percentage of aluminum on the surface was reduced up to 10%. The XRD results indicated that γ-Al_2O_3 phase was the dominant phase in all coatings. Corrosion tests demonstrated that Al_2O_3-13%TiO_2 coating exhibit the best anti-corrosion properties and showed the highest phase stability.

References

1. S.F. Hulbert, J.C. Bokros et al. *High Tech Ceramics,* Ceramics in clinical investigations: Past, present and future, 1987, 189-213.
2. J. Sheng-kai, Z. Yong et al. *Transactions of Nonferrous Metals Society of China,* Effect of TiO2 content on properties of Al2O3 thermal barrier coatings by plasma spraying, 2015, 25, 175-183
3. T. Sreekumar Rajesh, R. Venkata Rao. *Materials today: proceedings,* Experimental Investigation and Parameter Optimization of Al2O3-40%TiO2 Atmospheric Plasma Spray Coating on SS316 Steel Substrate, 2018, 5, 5012-5020.
4. S. Yilmaz, M. Ipek et al. *Vacuum,* The effect of bond coat on mechanical properties of plasma-sprayed Al_2O_3 and Al_2O_3-13wt%TiO_2 coatings on AISI 316L stainless steel, 2005, 77, 315-321.

Comparison of Two Different Healing Abutment Cleaning Protocols

S. Zukauskas[1,2,3], E. Svazas[1], T. Linkevicius[1,2], M. Misevicius[4]
[1]Vilnius University, Faculty of Medicine, Institute of Dentistry
[2]Vilnius Research group
[3]Vilnius Implantology Center
[4]Vilnius University, Faculty of Chemistry and Geosciences
e-mail: svazas.ernestas@gmail.com

ABSTRACT

Background: In clinical dentistry practice used and sterilized healing abutments are more common than new ones. The main reason for this phenomen – economic considerations (in order to minimize prime cost of the surgical procedure) [1]. It is thought, that used and sterilized healing abutments can not guarantee totally clean surface and can lead to crest bone stability failure around implants [2].

Aim/Hypothesis: Analyze and compare different healing abutment washing protocols by detecting contamination after sterilization.

Materials and Methods: The research was conducted in Vilnius University Institute of Dentistry. In total 60 new identical healing caps were observed by using scanning electron microscope (SEM) at Vilnius University, Faculty of Chemistry and Geosciences.

1) Control group - 20 unused healing abutments observation.

2) Test 1 group - 20 healing abutments used only once and sterilized by using cleaning protocol No.1

3) Test 2 group - 20 healing abutments used only once and sterilized by using cleaning protocol No.2

Cleaning protocol No.1 includes healing abutment disinfection with „EndoStar" in ultrasonic bath, cleaning with distilled water and steam autoclave.

Cleaning protocol No.2 includes healing abutment disinfection with „EndoStar" in ultrasonic bath, cleaning with distilled water, 17% EDTA solution in ultrasonic bath, cleaning with distilled water again and steam autoclave.

„EndoStar'' consists of: 5% alkyldimetylammoniumethosulfate, 1% polyhexamethylenbiguanidhydrochlorid, 1,8% cocospropylenguanidiniumacetat.

Results: In total – 60 healing abutments were observed. The most contaminated healing abutments were found in group No.2 (5,34± 1,72). New healing abutments did not have any carbon contamination (0,00± 00). Using washing protocol with EDTA 17% solution (group No.3) carbon decontamination was slightly better than in group No.2 (4,86± 1,29), but statistically significant difference was not found ($p>0,05$).

Conclusion and Clinical implications: All healing abutments, which were used and sterilized by different washing protocols, are more contaminated by carbon element than new ones. Washing protocol with EDTA 17% solution is slightly better than traditional washing method and should be used practically. Mechanical damages can be observed on the used healing abutment's surface, which can be good niche to deposit contaminants. More clinical researches should be done, in order to evaluate what quantity of carbon contamination is significant for implant osseointegration, biologic width formation and crestal bone stability.

References:

1. Bidra, A.S., Kejriwal, S. and Bhuse, K. (2020), Should Healing Abutments and Cover Screws for Dental Implants be Reused? A Systematic Review. Journal of Prosthodontics, 29: 42-48. doi:10.1111/jopr.13106
2. Vezeau PJ, Koorbusch GF, Draughn RA, Keller JC. Effects of multiple sterilization on surface characteristics and in vitro biologic responses to titanium. J Oral Maxillofac Surg. 1996 Jun;54(6):738-46

Synthesis of $NaYF_4$ Nano/Micro Particles by Microwave-Assisted Solvothermal Method

Lukas Šerpytis[1], Simas Šakirzanovas[1]

[1] *Institute of Chemistry, Faculty of Chemistry and Geosciences, Vilnius University, Naugarduko 24, LT-03225 Vilnius, Lithuania*

lukas.serpytis@chgf.stud.vu.lt

ABSTRACT

In recent years, rare-earth doped photoluminescence nanocrystals have attracted much interest due to fascinating optical properties including sharp emission lines, large Stokes shift and long fluorescence lifetime [1- 2]. The doped photoluminescence materials have a wide spectrum of applications in different fields such as new generation displays, LED, solid-state lasers and bioimaging [1-3]. The choice of a suitable host matrix is crucial step in designing efficient rare-earth doped photoluminescent materials. Among various rare-earth hosts, fluorides are selected due to close lattice match for dopant ions, low phonon energy, high quantum efficiency and good thermal stability [4-5]. $NaYF_4$ nanoparticles are considered as an excellent host matrix for doping with various optically active lanthanide ions [2]. Because of previously mentioned benefits $NaYF_4$ nano/micro particles were synthesized via one pot microwave-assisted solvothermal synthesis in ethylene glycol.

α-$NaYF_4$ phase – nano spheres and β-$NaYF_4$ phase nano/micro hexagonal prisms with good monodispersity have been successfully obtained employing a microwave-assisted solvothermal synthesis route. In this work we systematically investigate effects of various synthesis parameters including capping agent concentration, temperature, synthesis time, pH, Na^+/Y^{3+} ions ratio and reaction mixture concentration on synthesized phase purity, particles size and morphology. Synthesized $NaYF_4$ have been characterized by X-ray diffraction (XRD) and scanning electron microscopy (SEM). The results showed that this synthesis route is a promising modern synthesis method which does not require expensive precursors, has a relatively short synthesis time (up to an hour) and allows strict control of synthesis conditions.

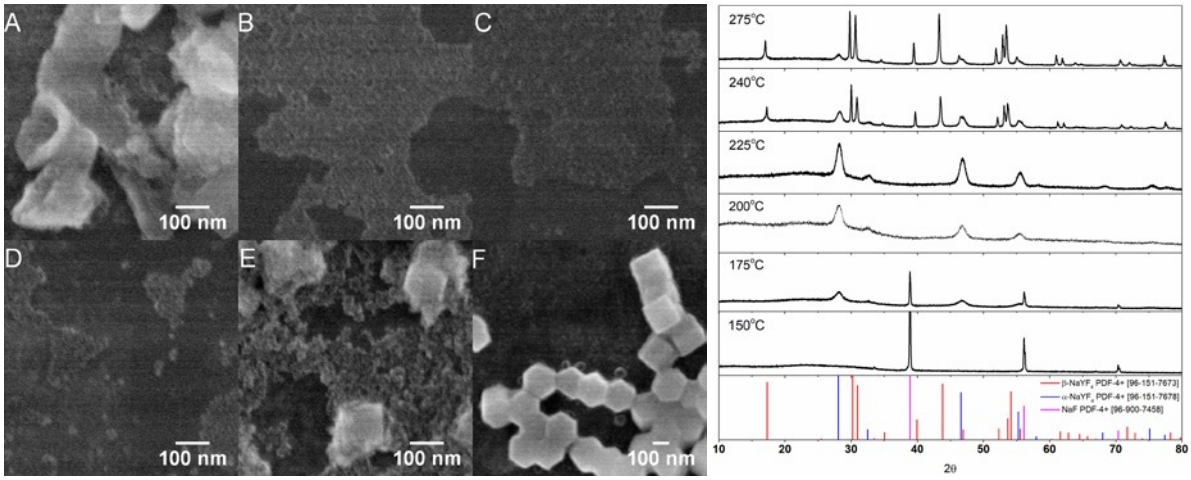

Fig. 1. Synthesized $NaYF_4$ nano/micro particles SEM micrographs and XRD diffractograms after microwave synthesis in different temperatures: A – 150°C; B – 175°C; C – 200°C; D – 225°C; E – 240°C; F – 275°C.

References

1. M. Baghbanzadeh, L. Carbone, P.D. Cozzoli, C.O. Kappe, Microwave-Assisted Synthesis of Colloidal Inorganic Nanocrystals, Angew. Chemie Int. Ed. 50 (2011) 11312–11359. https://doi.org/10.1002/anie.201101274.
2. Z. Wang, R. Cao, L. Meng, Microwave-Assisted Synthesis of Small Doped NaGdF Nanocrystals for PL / CT / MR Multimodal Imaging, SM Gr up SM J. Clin. Med. Imaging. 3 (2017) 1–6.
3. S. Liu, G. De, Y. Xu, X. Wang, Y. Liu, C. Cheng, J. Wang, Size, phase-controlled synthesis, the nucleation and growth mechanisms of NaYF4:Yb/Er nanocrystals, J. Rare Earths. 36 (2018) 1060–1066. https://doi.org/10.1016/j.jre.2018.01.025.
4. Y. Jiao, Y. Pu, J.X. Wang, D. Wang, J.F. Chen, Process Intensified Synthesis of Rare-Earth Doped β-NaYF4 Nanorods toward Gram-Scale Production, Ind. Eng. Chem. Res. 58 (2019) 22306–22314. https://doi.org/10.1021/acs.iecr.9b05412.

Nanosilica as the Inorganic Filler for Dental Composites Obtained by Photopolymerization

M. Topa[1]*, J. Ortyl[1,2]
[1]*Faculty of Chemical Engineering and Technology, Cracow University of Technology, Cracow, Poland*
[2]*Photo HiTech Ltd., Bobrzyńskiego 14, 30-348 Cracow, Poland*
e-mail: monika.topa@doktorant.pk.edu.pl

ABSTRACT

Photopolymerization is increasingly popular in the production of new generation dental composites due to the fact that it provides several advantages, e.g. ambient operation, solvent free formulations, and low energy consumption. Dental composites obtained by photopolymerization consist of two basic components: an organic matrix and an inorganic filler. Inorganic filler is primarily responsible for increasing the mechanical strength of the composition. The content of the inorganic filler in the dental composites can reach up to 90% [1,2].

In this work, Bisphenol A-glycidyl methacrylate (BisGMA from Sigma Aldrich) and triethylene glycol dimethacrylate (TEGDMA form Sigma Aldrich) in the weight ratio 7:3 were applied as a model monomer for free-radical photopolymerization for dental application. Camphorquinone (CQ form Sigma Aldrich) and ethyl 4-(dimethylamino)benzoate (EDB from Sigma Aldrich) as photoinitiators systems were selected for the study and the nanosilica in different concentration was applied as inorganic filler. Nanosilica has been investigated for increasing the mechanical strength of composite resins. The influence of the concentration of the nanosilica on the obtained conversions was studied using real time-FT-IR and Photo-DSC method. Depending on the amount of nanosilica, different properties of dental composites were obtained (Figure 1).

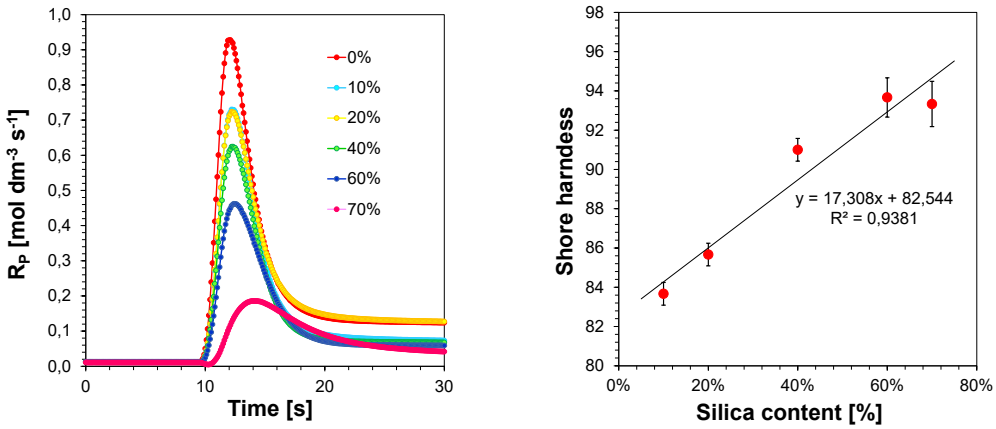

Fig. 1. Dependence Rp on time for composite using the CQ/EDB initiating systems with different amount of silica (on the left) and dependence of shora hardness on silica content in dental composites using the CQ/EDB initiating systems (on the right).

Acknowledgments
This work was financed by the Polish Ministry of Science and Higher Education from budget funds for science in the years 2018–2022 as a research project no. 0052/DIA/2018/47 under the "Diamond Grant" program.

References

1.J. W. Stansbury, *Journal of Esthetic and Restorative Dentistry*, Curing Dental Resins and Composites by Photopolymerization, 2000, 12(6), 300–308.
2.M. Topa, J. Ortyl, *Materials*, Moving Towards a Finer Way of Light-Cured Resin-Based Restorative Dental Materials: Recent Advances in Photoinitiating Systems Based on Iodonium Salts, 2020, 13, 4093.

Sol–Gel Synthesis of $Mg_{2-X}M_x/Al_1$ (M = Ca, Sr, Ba) Layered Double Hydroxides

Ligita Valeikiene[1]*, Marina Roshchina[2], Inga Grigoraviciute-Puroniene[1], Vladimir Prozorovich[2], Aleksej Zarkov[1], Andrei Ivanets[2], Aivaras Kareiva[1]

[1]Institute of Chemistry of Faculty of Chemistry and Geosciences of Vilnius University, Naugarduko Str. 24, LT-03225,Vilnius, Lithuania

[2]Institute of General and Inorganic Chemistry of National Academy of Sciences of Belarus, Surganova Str. 9/1, 220072 Minsk, Belarus;

ligita.valeikiene@chgf.vu.lt

ABSTRACT

Layered double hydroxides ($[M^{2+}_{1-x}M^{3+}_x(OH)_2]^{x+}(A^{y-})_{x/y}\cdot zH_2O$, where M^{2+} and M^{3+} are divalent and trivalent metal cations, respectively, and A^{y-} is a intercalated anion, LDHs) are widely used in catalysis, in ion-exchange processes, as catalyst support precursors, adsorbents, anticorrosion inhibitors, anion exchangers, flame retardants, polymer stabilizers, and in pharmaceutical applications, optics, in separation science and photochemistry [1, 2]. In this synthetic approach, the synthesized Mg–Al–O precursor gels were converted to the mixed metal oxides (MMO) by heating the gels at 650 °C. The LDHs were fabricated by the reconstruction of MMO in deionized water at 80 °C. The synthesized materials were characterized using X-ray powder diffraction (XRD) analysis and scanning electron microscopy (SEM). Nitrogen adsorption by the Brunauer, Emmett, and Teller (BET) and Barrett, Joyner, and Halenda (BJH) methods were used to determine the surface area and pore diameter of differently synthesized alkaline earth metal substituted MMO compounds. It was demonstrated for the first time that the microstructure of reconstructed MMO from sol–gel derived LDHs showed a “memory effect”.

This work was supported by a Research grant N°CAMAT (No. S-LB-19-2) from the Research Council of Lithuania and Belarusian Republican Found for Fundamental Research (No. 19LITG-007).

References

1. Smalenskaite, M.M. Kaba et al. *Materials,* Sol-gel synthesis and characterization of coatings of Mg-Al layered double hydroxides (LDHs), 2019,12, 736
2. D. Sokol, K.Klemkaite-Ramanauske et al. *Materials Science,* Reconstruction Effects on Surface Properties of Co/Mg/Al Layered Double Hydroxide, 2017, 23, 144-149

Application of Transition Metals Hexacyanoferrates in Optical Sensing of Hydrogen Peroxide

P. Virbickas[1], G. Kavaliauskaitė[1], A. Valiūnienė[1]
[1]Faculty of Chemistry and Geosciences of Vilnius University, Naugarduko str. 24, LT-03225 Vilnius, Lithuania
e-mail: povilas.virbickas@chgf.vu.lt

ABSTRACT

Application of transition metals hexacyanoferrates in electrochemical sensing of hydrogen peroxide is well known due to their ability to catalyse redox reactions of H_2O_2. However, among all transition metals hexacyanoferrates only Fe (II) hexacyanoferrate (FeHCF) and Co (II) hexacyanoferrate (CoHCF) can chemically react with H_2O_2 and be applied in optical sensing of H_2O_2 [1, 2, 3].

In this study comparison of physicochemical properties of FeHCF and CoHCF is presented in order to highlight their differences and possibilities to apply them for optical sensing of H_2O_2. Electrochemical investigations [1] indicated that the reduced form of FeHCF (Fe(II) hexacyanoferrate(II), $FeHCF_{red}$) exhibits an electrocatalytic activity towards reduction of H_2O_2, while FeHCF in oxidised state (Fe(III) hexacyanoferrate(III), $FeHCF_{ox}$) is reported to catalyse the electrooxidation of H_2O_2. Later investigation proved [2, 4, 5] that FeHCF in reduced form ($FeHCF_{red}$) can be also applied in formation of optical H_2O_2 sensors. The possibility of $FeHCF_{red}$ to be used in optical detection of hydrogen peroxide is based on H_2O_2-caused oxidation of $FeHCF_{red}$ (Eq. 1), which is accompanied with the change in $FeHCF_{red}$ colour from transparent to deep blue.

$$K^+Fe^{2+}[Fe^{2+}(CN^-)_6] \rightarrow K^+Fe^{3+}[Fe^{2+}(CN^-)_6] + K^+ + e^- \quad (1)$$

Cobalt(II) hexacyanoferrate(III) (CoHCF) is another transition metal hexacyanoferrate which can chemically react with H_2O_2 and it can also catalyse the electrochemical oxidation of H_2O_2 [3]. During the chemical reaction with H_2O_2, CoHCF changes its redox state from initial oxidized state ($CoHCF_{ox}$) into reduced state ($CoHCF_{red}$) (Eq. 2) and this transformation of CoHCF redox state is accompanied with the color change from the initial purple-brown color ($CoHCF_{ox}$) to the final olive-brown color ($CoHCF_{red}$) [3]. The intensity of this conversion can be evaluated through the measurements of optical absorption and eventually be used for quantification of hydrogen peroxide concentration in sample.

$$K^+Co^{2+}[Fe^{3+}(CN^-)_6] + K^+ + e^- \rightarrow K^+Co^{2+}[Fe^{2+}(CN^-)_6] \quad (2)$$

These two transition metal hexacyanoferrates, which can be applied in optical sensing of H_2O_2, exhibit significant differences in their analytical characteristics. $FeHCF_{red}$-based sensing of hydrogen peroxide enables to detect H_2O_2 concentration in micromolar range [5] (1 µM – 100 µM) of linearly detectable H_2O_2 concentrations, while CoHCF-based H_2O_2 sensor is reported [3] to detect H_2O_2 concentration in millimolar range (1.5 mM – 20 mM). Therefore, considering what hydrogen peroxide concentrations will be determined, an appropriate metal hexacyanoferrate ($FeHCF_{red}$ or CoHCF) should be involved in the construction of optical H_2O_2 sensor. Moreover, concentration of oxygen and other oxidant in sensor's working solution should also be considered, since $FeHCF_{red}$ can lose a part of its selectivity to H_2O_2 due to the impact of oxygen [2, 3], while CoHCF demonstrates the excellent resistance to the impact of oxygen [3].

References

1. K. Itaya, N. Shoji, I. Uchida. *Journal of the American Chemical Society*, Catalysis of the Reduction of Molecular Oxygen to Water at Prussian Blue Modified Electrodes, 1984, 106, 3423-3429.
2. P. Virbickas, A. Valiūnienė et al. *Journal of The Electrochemical Society*, Prussian White-Based Optical Glucose Biosensor, 2019, 166, B927–B932.
3. P. Virbickas, G. Kavaliauskaitė et al. *Electrochimica Acta*, Cobalt hexacyanoferrate based optical sensor for continuous optical sensing of hydrogen peroxide, 2020, 362, 137202.
4. R. Koncki, T. Lenarczuk, S. Glab. Analytica Chimica Acta, Optical sensing schemes for Prussian Blue/Prussian White film system, 2000, 424, 27–35.
5. K. Koren, P.Ø. Jensen, M. Kühl. *Analyst*, Development of a Rechargeable Optical Hydrogen Peroxide Sensor – Sensor Design and Biological Application, 14, 141.

Aqueous Sol-Gel Synthesis and Characterization of Apatite-Type Materials

A. Žalga*, A. Diktanaitė, G. Gaidamavičienė
Department of Applied Chemistry, Institute of Chemistry, Faculty of Chemistry and Geosciences, Vilnius University, Naugarduko Str. 24, 03225 Vilnius, Lithuania
e-mail: arturas.zalga@chf.vu.lt

ABSTRACT

Metal phosphates, which have a structure of apatite crystals, have received much attention because of their use in medicine and biotechnologies. These compounds correspond the general formula of $A_{10}(PO_4)_6X_2$, wherein A is either a divalent (Ca^{2+}, Sr^{2+}, Ba^{2+}) cation, or a combination of mono- and trivalent cation, and X, which corresponds to a monovalent anion (OH^-, Cl^-, Br^-, F^-). In addition, it is essential to note that apatite-type materials have different functional properties, such as biocompatibility, catalytic activity, ionic conductivity, which usually results from cation and/or anion exchange in the initial apatite matrix [1]. In order to apply such kind of materials for medical purposes, it is important to prepare the final compound with desirable shape, size, surface morphology and high phase purity of the obtained particles. Moreover, the used synthesis method also should be environmentally friendly, which possesses low cost and high efficiency. An aqueous sol-gel synthesis technique by using tartaric acid as a chelating agent that interacts as a ligand at the molecular level with the reaction mixture during both dissolution in water and sol-gel formation fulfils all requirements which enable to forecast the properties of obtained materials. In this work, we demonstrated that this method is suitable for the synthesis of hydroxyapatite, which crystallization started before the temperature of 500 ºC. The thermal analysis of the as-prepared gel precursor revealed a possible mechanism of the decomposition of volatile intermediates and crystallization of the final ceramic. Besides, the X-ray diffraction clearly showed the crystalline composition of the initial gel precursor and its transformation into the hydroxyapatite at elevated temperatures. Meanwhile, the scanning electron microscopy showed the surface morphology of heat-treated samples, which is typical for ceramic materials obtained using this tartaric acid-assisted synthesis technique.

References

1.M. Pogosova, A. Eliseev, et al., Synthesis, structure, luminescence, and color features of the Eu-and Cu-doped calcium apatite, *Dyes and Pigments* 141 (2017) 209-216.

Vesicle Immobilisation on Titanium Foil Nanopores

E. Zolubas[1*], E. Skinderytė[1], A. Valiūnienė[1]
[1] Faculty of Chemistry and Geosciences, Vilnius University, Naugarduko str. 24, Vilnius, Lithuania
[*]e-mail: eimantas.zolubas@chgf.stud.vu.lt

ABSTRACT

As a result of their outstanding properties, like flexibility, high tensile strength, resistance to body fluid effects, great biocompatibility, and ability to withstand high corrosion, titanium (Ti) and titanium alloys are one of the most utilized implant materials for biomedical applications [1]. However there are problems that may arise in titanium-based implants, like the generation of titanium and titanium alloy particles and ion deposition into surrounding tissues due to the corrosion and implant wear, resulting in bone loss due to inflammatory reactions, which can contribute to osseointegration failure [2-3]. To reduce inflammation antimicrobial peptide such as GL13K can be used by immobilizing it on Ti implant surface. This peptide regulates macrophages' polarisation and the expression of inflammatory and anti-inflammatory effects thus promoting the process of bone regeneration and osseointegration [4]. The goal of this study was - to attatch vesicles, on the surface of nanoporous Ti and to evaluate qualaty of this process. For this, surface characteristics were interpreted using contact angle measurements and atomic force microscopy (AFM). Should it be successful this method could be aplied for vesicle attatchment with immobilised anti-inflammatory peptides which in turn could be used to make implants with better osseointegraton and longevity.

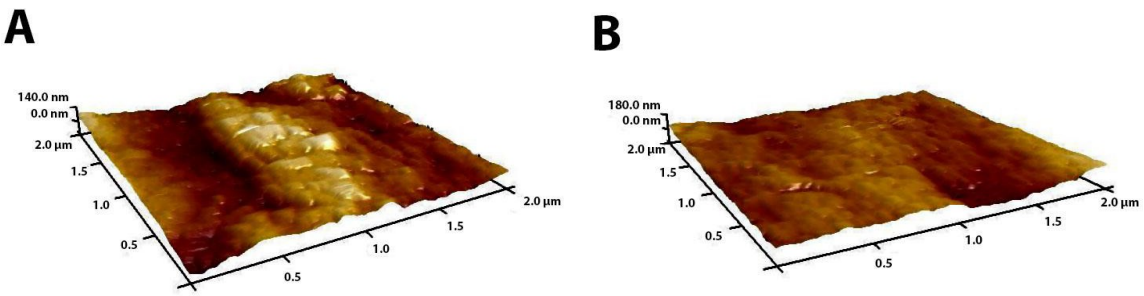

Fig. 1. Morphology of titanium nanopore surfaces observed using atomic force microscopy: (A) - before vesicle attachments, Rq =44.5 nm and (B) - after vesicle attachment on titanium surface functionalised with pyridine, Rq = 33.0 nm.

References

1. P. Roy, S. Berger and P. Schmuki *Angewandte Chemie Int. Ed.,* TiO_2 Nanotubes: Synthesis and Applications, 2011, 50, 2904-2939.
2. D. Olmedo, M.M. Fernandez, M.B. Guglielmotti, R.L. Cabrini. *Implant Dentistry*. Macrophages related to dental implant failure. 2003, 12, 75–80.
3. T. Fretwurst, K. Nelson, D.P. Tarnow, H.L. Wang, W.V. Giannobile. *Journal of Dental Research*. Is metal particle release associated with peri-implant bone destruction? An emerging concept 2018, 97, 259–265.
4. X. Chen, L. Zhou, D. Wu, W. Huang, Y. Lin, B. Zhou, J. Chen. *BioMed research international.* The Effects of Titanium Surfaces Modified with an Antimicrobial Peptide GL13K by Silanization on Polarization, Anti-Inflammatory, and Proinflammatory Properties of Macrophages 2020, 1-9.

Index of Authors

U

V

Z

Ž

Vilnius University Press
9 Saulėtekio Av., Building III, LT-01513 Vilnius
info@leidykla.vu.lt, www.leidykla.vu.lt